

DESIGN OF SWITCHING SCHEMES FOR VOLTAGE SOURCE INVERTER

DISSERTATION
SUBMITTED IN PARTIAL FULFILLMENT OF THE REQUIREMENTS
FOR THE AWARD OF THE DEGREE
OF

MASTER OF TECHNOLOGY
IN
POWER SYSTEM

Submitted by:

Ankit Yadav

Roll No. 2K12/PSY/03

Under the supervision of

DR. MADAN MOHAN TRIPATHI



DEPARTMENT OF ELECTRICAL ENGINEERING

DELHI TECHNOLOGICAL UNIVERSITY

(Formerly Delhi College of Engineering)

Bawana Road, Delhi-110042

2014

DEPARTMENT OF ELECTRICAL ENGINEERING

DELHI TECHNOLOGICAL UNIVERSITY

(Formerly Delhi College of Engineering)

Bawana Road, Delhi-110042

CERTIFICATE

I, ANKIT YADAV, Roll No. 2K12PSY03 student of M. Tech. (POWER SYSTEM), hereby declare that the dissertation/project titled “**Design of Switching Schemes for Voltage Source Inverter**” under the supervision of Dr. Madan Mohan Tripathi Delhi Technological University in partial fulfillment of the requirement for the award of the degree of Master of Technology has not been submitted elsewhere for the award of any Degree.

Place: Delhi

(ANKIT YADAV)

Date: 28.07.2014

DR. MADAN MOHAN TRIPATHI

(SUPERVISOR)

Associate Professor (DTU)

ACKNOWLEDGEMENT

I am highly grateful to the Department of Electrical Engineering, Delhi Technological University (DTU) for providing this opportunity to carry out the project work.

The constant guidance and encouragement received from Dr. M. M. TRIPATHI of Department of Electrical Engineering, DTU, has been of great help in carrying my present work and is acknowledged with reverential thanks.

I would like to express a deep sense of gratitude and thanks profusely to Dr. VISHAL VERMA, for their kind suggestion related to S-function. Without the wise counsel and able guidance, it would have been impossible to complete the project in this manner. I would like to express my thankfulness to PROF. MADHUSHUDAN SINGH and Dr. DHEERAJ JOSHI for providing the laboratory and other facilities to carryout the project work. Again, the help rendered by DR. M. M. TRIPATHI, for the literature, and for experimentation is greatly acknowledged.

Finally, I would like to expresses gratitude to other faculty members of Electrical Engineering Department, DTU for their intellectual support throughout the course of this work.

ANKIT YADAV

2K12/PSY/03

M. Tech. (Power System)

Delhi Technological University

ABSTRACT

DC-AC Inverters are key components in various industrial applications that include power supplies, motor drive systems and power systems. Now-a-days dc-ac inverters (both 1-phase & 3-phase) are finding more attention in renewable energy systems also. These inverters are big source of harmonics, which leads to various other problems like heating of instruments, faulty operation of protection devices etc. The harmonics generated by inverter can be controlled and minimise by controlling the switching of the device. Several approaches has been made already to deal with this problem like as carrier based PWM (pulse width modulation), selected harmonic elimination, Random PWM etc.

Although the methods named above have been succeeded in improving the quality of power by reducing the harmonics but the problem is still not solved completely, so it still required attention. The Proposed project work is to design new switching schemes for single phase H-bridge Voltage Source DC – AC inverter. The motive of new switching technique is to further improve the quality of output by reducing total harmonic distortion. Two switching scheme are proposed for the project work. One is “modified hysteresis switching scheme” and another one is “wavelet modulation techniques”. Both schemes are considered for voltage source inverter.

Modified hysteresis switching scheme as well as wavelet based modulation technique would be studied, analysed and applied for switching of single phase and three phase voltage source inverters to produce significantly improved fundamental components and low harmonic contents. The inverter along with its switching technique would be simulated using MATLAB software and results would be analysed.

CONTENTS

Certificate	i
Acknowledgement	ii
Abstract	iii
Contents	iv
List of Figures	vii
List of Tables	xii
Abbreviations	xiii
CHAPTER 1 INTRODUCTION	01
1.1. Modified Hysteresis Switching Scheme	04
1.2. Wavelet	04
CHAPTER 2 LITERATURE SURVEY	06
2.1. Basic Concepts of Converter	07
2.1.1. AC – DC Converter	07
2.1.2. DC –AC Converter (Inverter)	08
2.1.3. Firing Angle	08
2.1.4. Drawback of Power Electronics Devices	09
2.2. Existing Switching Schemes	13
2.2.1. Pulse Width Modulation	13
2.2.2. Selected Harmonic Elimination	15
2.2.3. Hysteresis Band Current Control	15
2.2.4. Other Switching Techniques	17
2.3. Basics of Wavelet	17
2.3.1. Wavelet	17
2.3.2. Wavelet Transform	19
CHAPTER 3 MODIFIED HYSTERESIS SWITCHING SCHEME FOR 1-PHASE VOLTAGE SOURCE INVERTER	23

3.1. Modified Hysteresis Switching Scheme	24
3.1.1. How it is Different from Existing Scheme	25
3.1.2. New Switching Scheme	25
3.1.3. Reference Signal	27
3.1.4. Problems and Modifications	28
3.2. Implementation	30
3.3. Testing, Results and Discussion	33
3.3.1. Linear load (R-L load)	34
3.3.2. Dynamic load (Motor load)	38
CHAPTER 4 MODIFIED HYSTERESIS SWITCHING SCHEME FOR 3-PHASE VOLTAGE SOURCE INVERTER	43
4.1. Modified Switching Scheme for 3-Phase Voltage Source Inverter	44
4.1.1. New Switching Strategy	44
4.1.2. Reference Signals	45
4.2. Implementation	46
4.3. Simulation Results	50
4.3.1. Linear load (R-L load)	50
4.3.2. Nonlinear load (Rectifier load)	57
CHAPTER 5 WAVELET MODULATION FOR 1-PHASE INVERTER	65
5.1 Modulation Overview	66
5.1.1. Reference Signal	66
5.1.2. Output Waveform	67
5.1.3. Sampling and Reconstruction	67
5.1.4. Flowchart	69
5.2 Wavelet Modulation	70
5.3 Modulation and Simulation	72
5.4 Result and Discussion	72
5.4.1. R – L Load	73
5.4.2. R load	79
CHAPTER 6 CONCLUSION	85

CHAPTER 7	FUTURE SCOPE	88
REFERENCES		90
PUBLICATIONS		94

LIST OF FIGURES

Sr. No.	Figure No.	Description	Page No.
1.	Figure 2.1 –	Simulation model of (a) 1-phase converter, (b) 3-phase converter, (c) 1-phase inverter, (d) 3-phase inverter.	11
2.	Figure 2.2 –	Simulation result of (a) 1-phase converter, (b) 3-phase converter, (c) 1-phase inverter, (d) 3-phase inverter (result of phase ‘a’ is shown).	13
3.	Figure 2.3 –	(a) Comparator for PWM, (b) Pulse generation using comparator.	14
4.	Figure 2.4 –	(a) Simulation model of single-phase PWM inverter, (b) output voltage and current waveform of 1-ph PWM inverter.	15
5.	Figure 2.5 –	Selected harmonic elimination for 3rd harmonic.	16
6.	Figure 2.6 –	Hysteresis band current control.	17
7.	Figure 2.7 –	(a) Haar Wavelet (b) Daubenchies wavelet family	19
8.	Figure 3.1 –	Single-phase H-bridge VS DC – AC inverter model.	
9.	Figure 3.2 –	Block diagram for new switching scheme.	24
10.	Figure 3.3 –	(a) A conceptual plot for new switching scheme, (b) Plot for new switching scheme with practical data.	26
11.	Figure 3.4 –	Reference signal A.	26
12.	Figure 3.5 –	Error signal representation.	28
13.	Figure 3.6 –	Flowchart for modified switching scheme.	29
14.	Figure 3.7 –	Single-phase H-bridge VS DC–AC inverter test result (load voltage and load current waveform) for R-L load using PWM switching scheme.	32

15.	Figure 3.8 –	Single-phase H-bridge VS DC–AC inverter test result (load voltage and load current waveform) for R-L load using modified switching scheme.	36
16.	Figure 3.9 –	THD in load voltage waveform of single-phase H-bridge VS DC–AC with R-L load using (a) PWM (b) Modified switching scheme.	36
17.	Figure 3.10 –	THD in load current waveform of single-phase H-bridge VS DC–AC with R-L load using (a) PWM (b) Modified switching scheme.	38
18.	Figure 3.11 –	Single-phase H-bridge VS DC–AC inverter test result (load voltage and load current waveform) for motor load using PWM scheme.	40
19.	Figure 3.12 –	Single-phase H-bridge VS DC–AC inverter test result (load voltage and load current waveform) for motor load using modified switching scheme.	40
20.	Figure 3.13 –	THD in load voltage waveform of single-phase H-bridge VS DC–AC with motor load (a) PWM (b) modified-switching scheme.	41
21.	Figure 3.14 –	THD in load current waveform of single-phase H-bridge VS DC–AC with motor load (a) PWM (b) modified-switching scheme.	42
22.	Figure 4.1 –	Circuit diagram of three – phase voltage source inverter.	44
23.	Figure 4.2 –	Block diagram for modified switching scheme.	46
24.	Figure 4.3 –	Method of replacing time-interval with respective relation between references.	47
25.	Figure 4.4 –	Flowchart for new switching scheme for three-phase voltage source inverter.	49
26.	Figure 4.5 –	Three-phase VS DC–AC inverter output (load voltage and load current) waveform of R- Phase under linear loading using PWM scheme.	52
27.	Figure 4.6 –	Three-phase VS DC–AC inverter output (load voltage	53

and load current) waveforms under linear loading using modified switching scheme.

- | | | | |
|------------|---------------|--|----|
| 28. | Figure 4.7 – | THD in load voltage waveforms of three-phase VS DC–AC inverter with linear load using (a) PWM (b) modified switching scheme. | 54 |
| 29. | Figure 4.8 – | THD in load current waveforms of Three-phase VS DC–AC inverter with linear load using (a) PWM (b) modified switching scheme. | 54 |
| 30. | Figure 4.9 – | Three-phase VS DC–AC inverters output waveform under linear loading using PWM scheme. (a) load voltage R, Y and B-phase (b) load current R,Y and B phase. | 55 |
| 31. | Figure 4.10 – | Three-phase VS DC–AC inverter output waveforms under linear loading using modified switching scheme. (a) load voltage R, Y and B-phase (d) load current R,Y and B-phase. | 56 |
| 32. | Figure 4.11 – | Three-phase VS DC–AC inverter output (load voltage and load current) waveform of R- Phase under non-linear loading using PWM scheme. | 58 |
| 33. | Figure 4.12 – | Three-phase VS DC–AC inverter output (load voltage and load current) waveform of R- Phase under non-linear loading using modified scheme. | 59 |
| 34. | Figure 4.13 – | THD in load voltage waveforms of Three-phase VS DC–AC inverter with non-linear load (a) PWM (b) modified switching scheme. | 60 |
| 35. | Figure 4.14 – | THD in load current waveforms of Three-phase VS DC–AC inverter with non- linear load (a) PWM (b) modified switching scheme. | 61 |
| 36. | Figure 4.15 – | Three-phase VS DC–AC inverters output waveform under linear loading using PWM scheme. (a) Voltage of R, Y and B-phase (b) Current in R,Y and B-phase. | 62 |

37.	Figure 4.16 – Three-phase VS DC–AC inverters output waveform under non-linear loading using modified scheme. (a) Voltage of R, Y and B-phase (b) current R,Y and B-phase.	63
38.	Figure 4.17 – Load voltage and load current waveform for load resistance of rectifier when supplied from three-phase VS DC–AC inverter with PWM switching scheme.	64
39.	Figure 4.18 – Load voltage and load current waveform for load resistance of rectifier when supplied from three-phase VS DC–AC inverter with modified switching scheme.	64
40.	Figure 5.1 – An example to view the relation of output voltage and current (in PWM method).	67
41.	Figure 5.2 – Haar wavelet function	70
42.	Figure 5.3 – Haar scaling function	70
43.	Figure 5.4 – MATLAB model of single-phase H-bridge voltage source DC – AC inverter using IGBTs.	73
44.	Figure 5.5 – Single-phase H-bridge VS DC–AC inverter test result (load voltage and load current waveform) for R-L load using PWM switching scheme.	75
45.	Figure 5.6 – Single-phase H-bridge VS DC–AC inverter test result (load voltage and load current waveform) for R-L load using square pulse switching scheme.	76
46.	Figure 5.7 – Single-phase H-bridge VS DC–AC inverter test result (load voltage and load current waveform) for R-L load using wavelet switching scheme.	76
47.	Figure 5.8 – THD in load voltage waveform of single-phase H-bridge VS DC–AC with R-L load using (a) PWM (b) square pulse (c) wavelet switching scheme.	77
48.	Figure 5.9 – THD in load current waveform of single phase H-bridge VS DC–AC with R-L load using (a) PWM (b) square pulse (c) wavelet switching scheme.	78

49.	Figure 5.10 – Single-phase H-bridge VS DC–AC inverter test result (load voltage and load current waveform) for R load using PWM switching scheme.	80
50.	Figure 5.11 – Single-phase H-bridge VS DC–AC inverter test result (load voltage and load current waveform) for R load using square pulse switching scheme.	81
51.	Figure 5.12 – Single-phase H-bridge VS DC–AC inverter test result (load voltage and load current waveform) for R load using wavelet switching scheme.	81
52.	Figure 5.13 – THD in load voltage waveform of single-phase H-bridge VS DC–AC with R load using (a) PWM (b) square pulse (c) wavelet switching scheme.	82
53.	Figure 5.14 – THD in load current waveform of single-phase H-bridge VS DC–AC with R load using (a) PWM (b) square pulse (c) wavelet switching scheme.	83
54.	Figure 5.15 – Flowchart of wavelet modulation for single-phase inverter.	84

LIST OF TABLES

Sr. No.	Table No.	Tittle	Page No.
1.	Table 3.1 –	SIMULATION RESULTS FOR R – L LOAD (SINGLE PHASE)	35
2.	Table 3.2 –	SIMULATION RESULTS FOR DYNAMIC LOAD (SINGLE PHASE)	39
3.	Table 4.1 –	SIMULATION RESULTS FOR LINEAR LOAD (THREE-PHASE)	52
4.	Table 4.2 –	SIMULATION RESULTS FOR NON - LINEAR LOAD (THREE-PHASE)	58
5.	Table 5.1 –	SIMULATION RESULT FOR R-L LOAD (SINGLE- PHASE)	75
6.	Table 5.2 –	SIMULATION RESULT FOR R LOAD (SINGLE- PHASE)	80

ABBREVIATIONS

VS	Voltage Source
RMS	Root Mean Square
THD	Total Harmonic Distortion
IGBT	Insulated Gate Bipolar Transistor
PWM	Pulse Width Modulation
RPWM	Random PWM
SHE	Selected Harmonic Elimination
WM	Wavelet Modulation
MRA	Multi Resolution Analysis

CHAPTER 1

INTRODUCTION

CHAPTER 1

INTRODUCTION

The world's first power system was built at Godalming in England, in 1881 and in last 130 years, it has become the backbone of world's civilization, with enormous number of existing power system, where each individual system is having an ocean of generating units, loads, and other essential equipment. In current scenario, the world cannot dare to survive without electricity, as it was few centuries back.

In the beginning of power system network, the elements like as generating units, loads, transmission network were less in number, as well as they were less sensitive to the disturbances. So, the quality of power was not a big issue, as it is today. In today's era of technology the power network has expanded drastically and is full of electronic and power electronic devices which are highly sensitive to the disturbances in the system. In the same period need of more and more energy is leading us to look for various renewable sources to fulfill the energy requirements. These energy sources are operating in grid connected or off-grid mode. Power supply from these renewable resources are not pure sinusoidal and its conversion to sinusoid injects large amount of harmonics in the system and thus deteriorate the quality of power supply. Also now-a-days, reliability of power supply has become need of hour. Considering the above issues, the quality of the power supply has emerged as a serious concern in front of the engineers involved in power system technology.

Power electronic devices have shown their ability to control the power flow with greater flexibility and so, their use in power system is increasing day-by-day. With increasing number of power electronic devices to manage the expanding power system network, the study of controlling these devices requires the attention. All the power electronic devices being used now a days are dependent on the gate pulse & firing angle

α for any type of control, or we can say, only by controlling gate signal, we can control the behavior of our power electronic devices and thus the power system network.

The operation of these devices are controlled by gate signals and thus the output, harmonic, efficiency and other factors can be controlled by controlling gate signal. Poor switching schemes of these power electronic devices may result in degradation of the quality of power flowing on the wires and in to the systems. A proper switching strategy can give an efficient and better control over output of power electronics device leading to better quality of power. Several factors of operation that must be taken care while designing the switching strategy are as follows.

- a. RMS values of voltage and current
- b. Average and Peak value of voltage and current
- c. Total harmonic distortion (THD) waveforms
- d. Switching losses
- e. Practical implementation

The work on switching strategy of power electronic switching devices came in to existence with the birth of power electronics and has resulted in several options such as single pulse switching, pulse width modulation (PWM), random PWM (RPWM), selected harmonic elimination (SHE), delta modulation, hysteresis & variable band, optimal PWM. The reason behind development of all these methods is to minimize the switching losses and higher order harmonics because the power electronics devices are major source of these higher order harmonics. From all these methods, PWM has been widely accepted because of its simplicity and ability to solve the problem significantly. Although PWM has proven a better option, there is still a scope of improvement, as the problem is not eradicated completely. This has given a motivation for further research in the area of switching techniques for power electronic devices.

This project is dealing with the same gate pulses and switching schemes to improve the operation of the power electronic devices, as the efficiency and performance of existing switching methodologies are not sufficient to minimize the

level of harmonics injected in the system from the power electronics devices in current scenario. In this work new switching strategies have been proposed for power electronics switching devices. Two new switching schemes for controlling voltage source inverter namely, (i) modified hysteresis switching scheme and (ii) wavelet modulation technique have been proposed, designed and tested. The modified hysteresis switching scheme is modification of existing hysteresis band current control scheme, has been designed for single-phase as well as for three-phase voltage source inverter. However wavelet based switching scheme has been designed for single-phase inverter only.

1.1 Modified Hysteresis Switching Scheme

Current regulated modulations of voltage source inverter are in knowledge from very beginning of the inverter. Tolerance band control, fixed frequency control etc. fall in of this family. The proposed modified hysteresis switching scheme is also a current regulated modulation technique. It is modification of existing hysteresis band current control method. This technique uses the value of output current as feedback signal and the value of desired output current as the reference signal. These two signals contribute in defining the controlling actions to be taken and accordingly the gate pulses for the inverter get generated. Thus in the proposed strategy, the relation between values of the load current and reference signal is used for generating the gate pulses to the IGBT switches of the Inverter.

1.2 Wavelet

A wavelet is a wave-like oscillation with amplitude that begins at zero, increases and then decreases back to zero. It can typically be visualized as a “brief oscillation” like one might see recorded by seismograph or heart monitor. Generally, wavelets are purposefully crafted to have specific properties that make them useful for signal processing. Wavelets can be combined, using a “reverse, shift, multiply and sum” technique called convolution, with portions of unknown signal to exact information from the unknown signal. The development of wavelets can be linked to several separate trains of thought, starting with Haar's work in the early 20th century.

Later works by Dennis Gabor yielded Gabor atoms (1946), which, constructed similarly to wavelets, and applied to similar purposes. Notable contributions to wavelet theory can be attributed to Zweig's discovery of the continuous wavelet transform in 1975 (originally called the cochlear transform and discovered while studying the reaction of the ear to sound). Pierre Goupillaud, Grossmann and Morlet's formulation of what is now known as continuous wavelet transform (CWT) (1982), Jan-Olov Strömberg's early work on discrete wavelets (1983), Daubechies' orthogonal wavelets with compact support (1988), Mallat's multiresolution framework (1989), Akansu's Binomial QMF (1990), Nathalie Delprat's time-frequency interpretation of the CWT (1991), Newland's harmonic wavelet transform (1993) and many others since.

Wavelets also can be applied in field of power electronics, as in this project we are applying the wavelets for modulating the gate pulse of the inverter. The generation of gate pulses for power electronic devices and using them to generate the output waveform of current and voltage, is actually a kind of signal processing, where we desire to obtain a sinusoidal output waveform. That means, the methods of signal processing can be applied to the power electronic devices. We have several methods in practice for signal processing like as: Fourier transform, Laplace transform etc., but the common drawback of all existing methods is that, at a time, they can work with either frequency or time but wavelet transform deals with both simultaneously. In last few decades, wavelet has made its significant place in field of signal processing and thus draws our attention toward itself.

The performances of both the proposed schemes are very encouraging compared to existing switching schemes. These proposed schemes may be implemented into hardware and applied into the power system.

CHAPTER 2

LITERATURE SURVEY

CHAPTER 2

LITERATURE SURVEY

Since we are interested in design of new strategy to generate the gate pulses for improved operation of the power electronic devices, it becomes important to know and study the basic concepts of converter and the importance of gate pulses. We need to go through the existing switching scheme before we start designing new one.

2.1 Basic Concepts of Converter

As we have opted the study related to the switching strategy and to design a new strategies, so it becomes the need of hour to understand the working concept of commonly used power electronics devices, such as inverters and converters (both single-phase and three-phase). With this purpose, we have used few basic models using the available literatures on power electronics and have discussed them with respective simulation result, which have been obtained using SIMULINK facility of MATLAB [1]-[2].

2.1.1. AC – DC Converter

AC – DC converter (also known as controlled rectifier) is a thyristor based power electronics device for rectification purpose. The figure 2.1(a) and 2.1(b) shows the single-phase and three-phase converter devices and their respective simulation outputs is shown in figure 2.2(a) and 2.2(b). The simulation is performed with inductive load at firing angle of 30° for single-phase converter, while it is 20° in case of three-phase converter. The observation of output waveforms of the single and three-phase converter shows that the nature of output of the power electronic devices is dependent on the firing angle applied to the power electronics switches. Thus, the firing angle and

its control are directly responsible for the operation of the devices and quality of the output. Input to these converter is pure sinusoidal AC, while the output is controlled DC.

2.1.2. DC – AC Converter (Inverter)

In a similar fashion as AC – DC converter, DC – AC converter (inverter) can be designed. The important thing to notice is that, the design of inverter using thyristor is very complex, as thyristor requires commutation circuit, when being used for inverting purpose and at the same instant, the design of commutation circuit put more complexity as well as cost to the device. To avoid the unnecessary cost and complexity, inverters are designed using IGBT or GTO, as these devices demand no additional circuitry for commutation.

Single-phase, as well as three-phase inverter circuits have been designed for simulation purpose and are shown in figure 2.1(c) and 2.1(d) respectively. The simulation results of these circuits with inductive loading are also shown in figure 2.2(c) and 2.2(d) respectively. The input to these devices is a supply with constant DC voltage and output obtained is controlled AC. All the figures 2.1 (a), (b), (c) and (d) have blocks named as pulse, these block used as firing circuit of particular thyristor or IGBT.

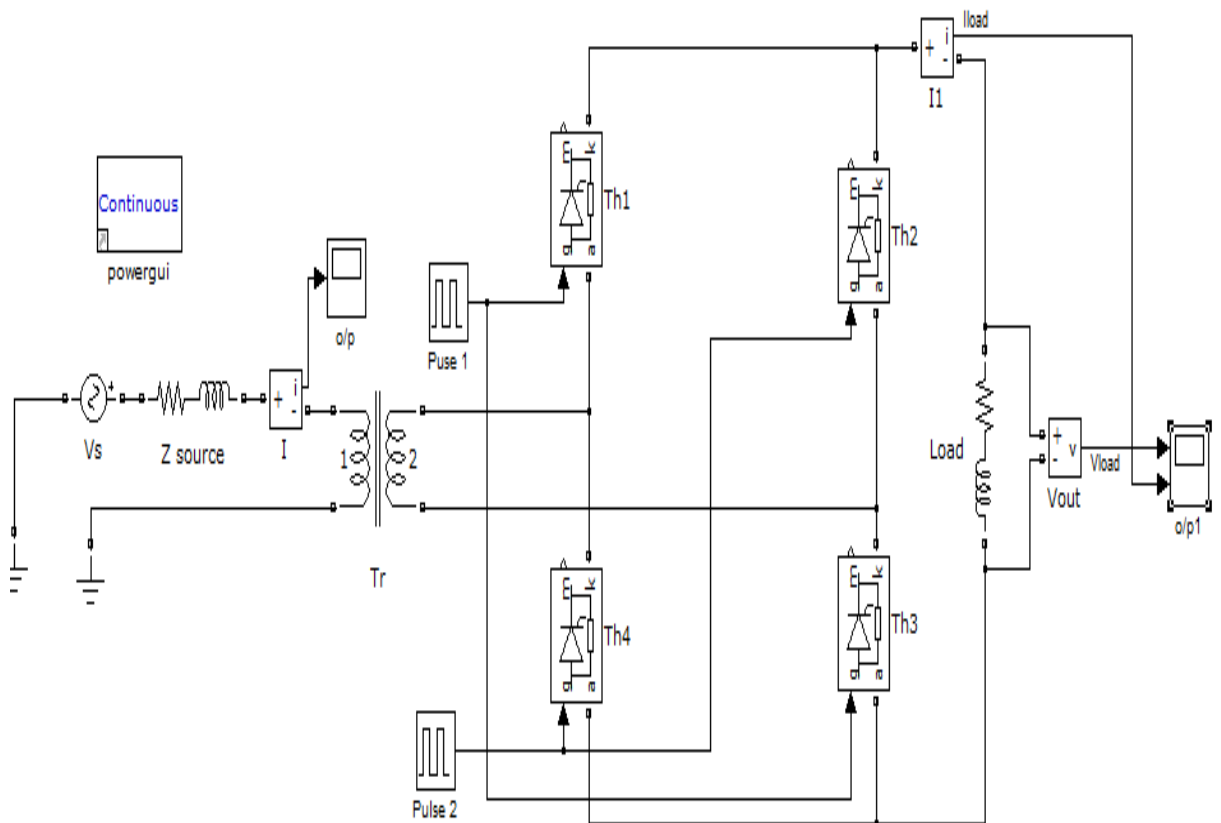
2.1.3. Firing Angle

Firing angle can be define as the angle at which the power electronics devices such as Thyristor, IGBT, GTO etc. are being turned on by gate pulse [3]-[4]. The complete operation, output and behaviour of the power electronic device is controlled by the controlling the firing angle of the device. Any variation in firing angle would cause direct impact over conduction angle and commutation angle of the device.

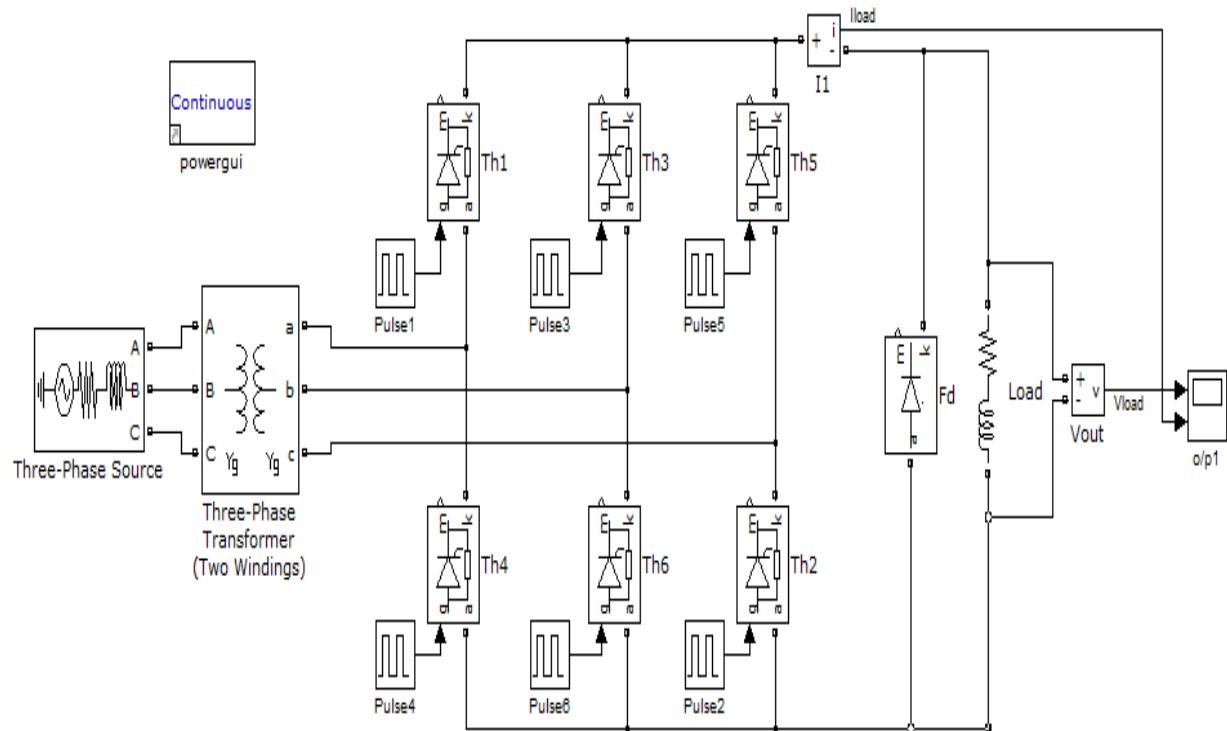
2.1.4. Drawback of Power Electronic Devices

Because of their wide range of controllability and applicability, power electronic devices have made the significant presence in power system network. These devices have resolve many important issues like as filtering harmonics due to loads, maintaining voltage profile, assuring maximum power transfer etc. and the application area of the power electronic devices is still growing. With the tremendous increment in the number of power electronic devices in the power system network, the impact of the devices also become the important concern.

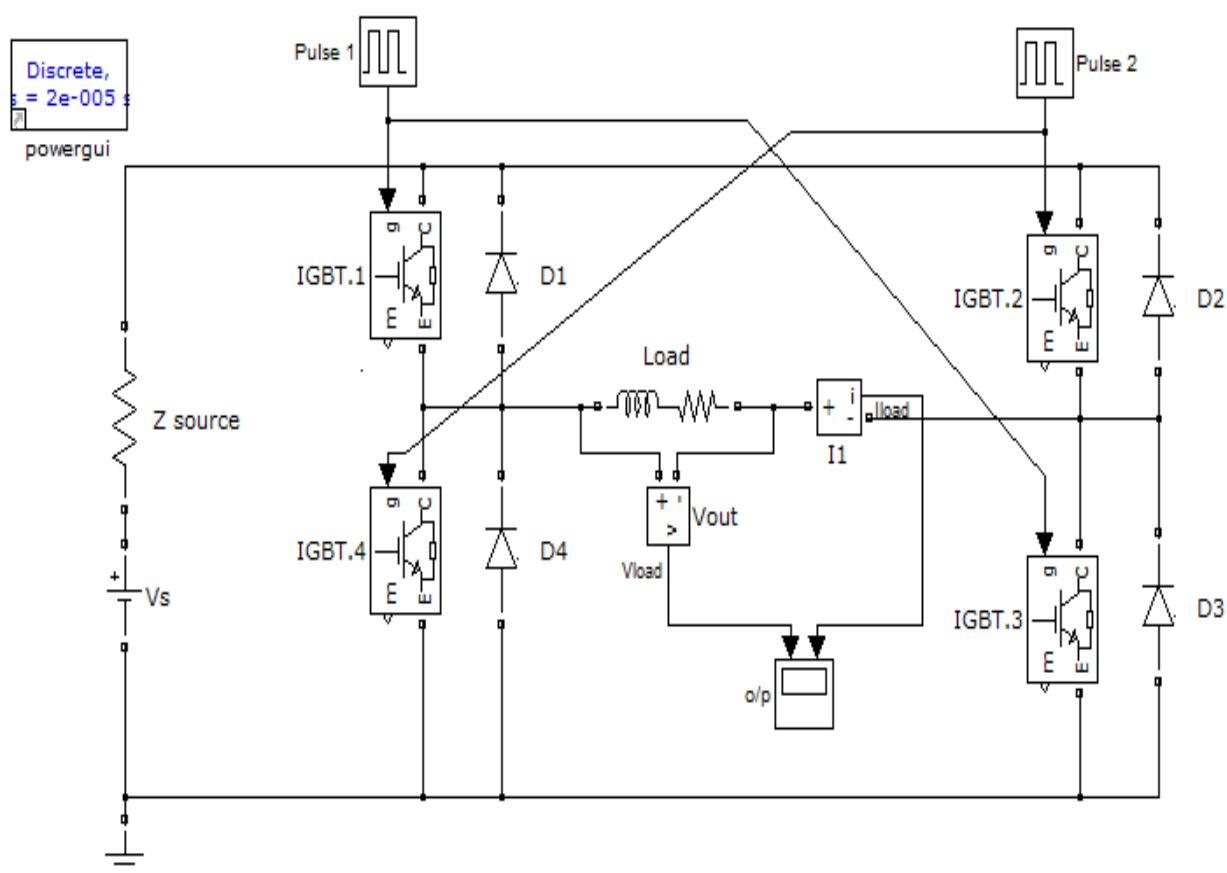
The power electronic devices are source of high frequency harmonics in power lines and causes high switching losses. Both the problems (harmonics and switching losses) depends on the switching strategy being used for the controlling the operation of the devices.



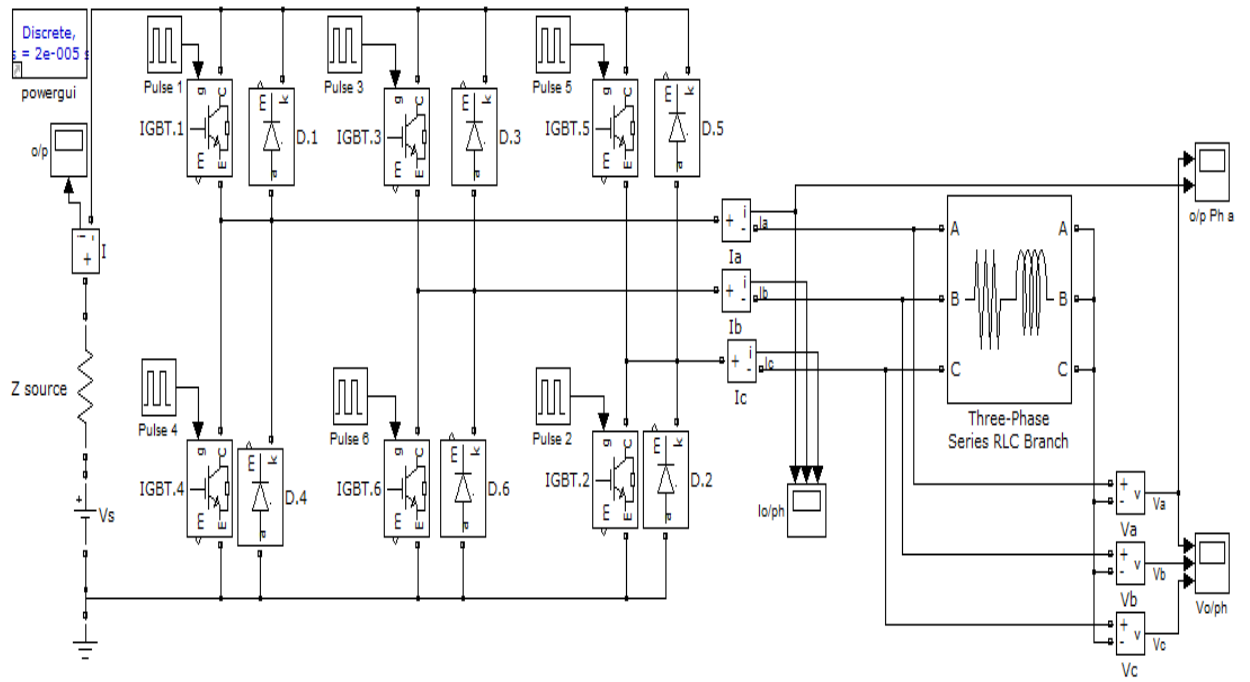
2.1 (a)



2.1 (b)

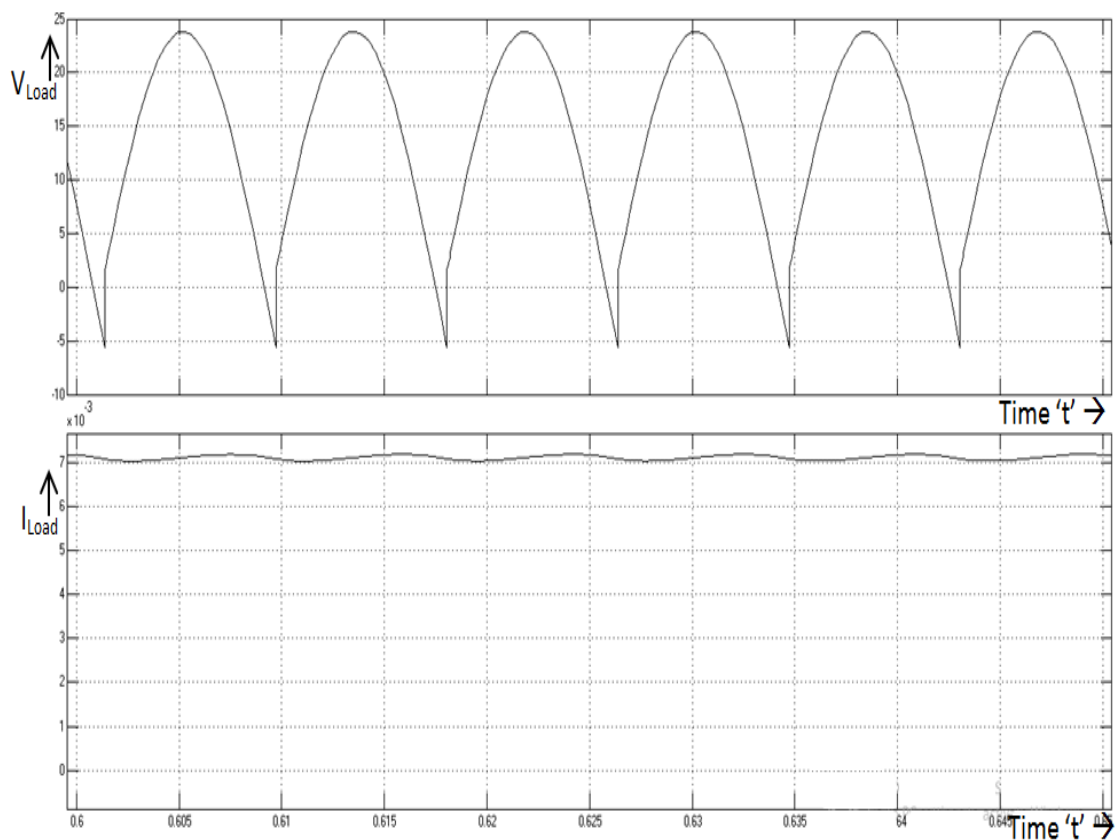


2.1 (c)

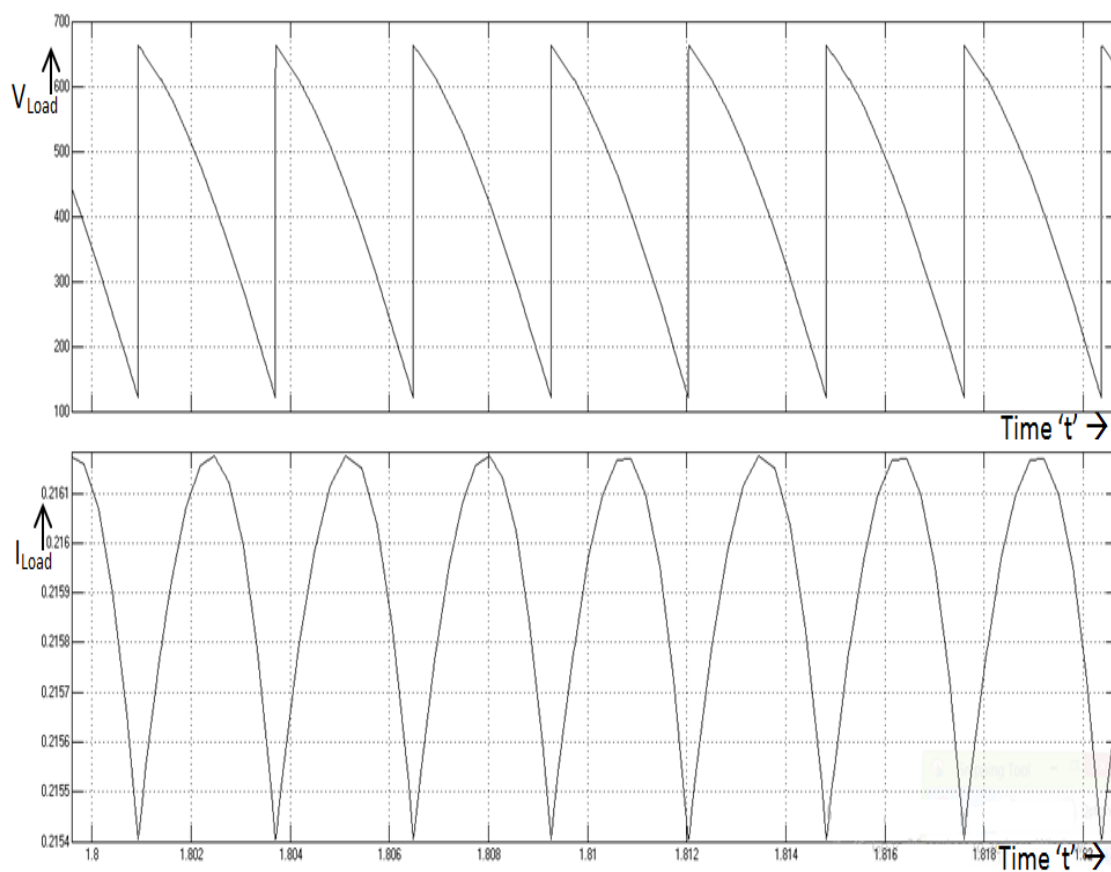


2.1 (d)

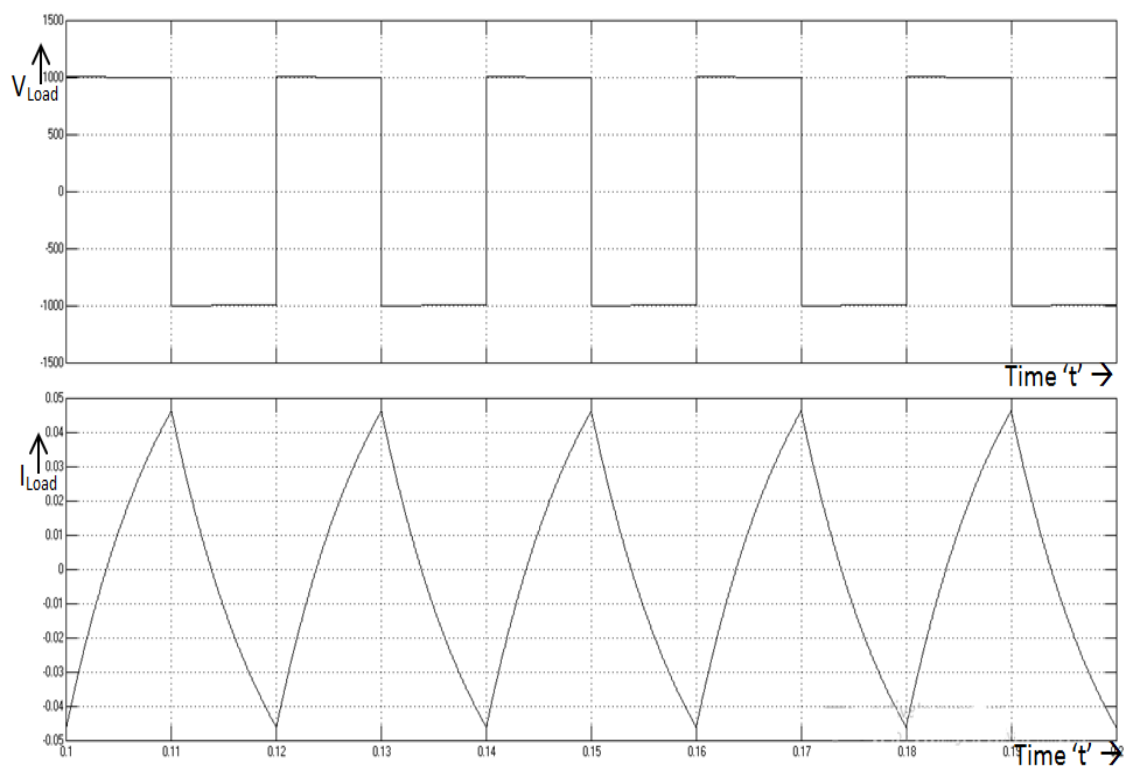
Figure 2.1 Simulation model of (a) 1-phase converter, (b) 3-phase converter, (c) 1-phase inverter, (d) 3-phase inverter.



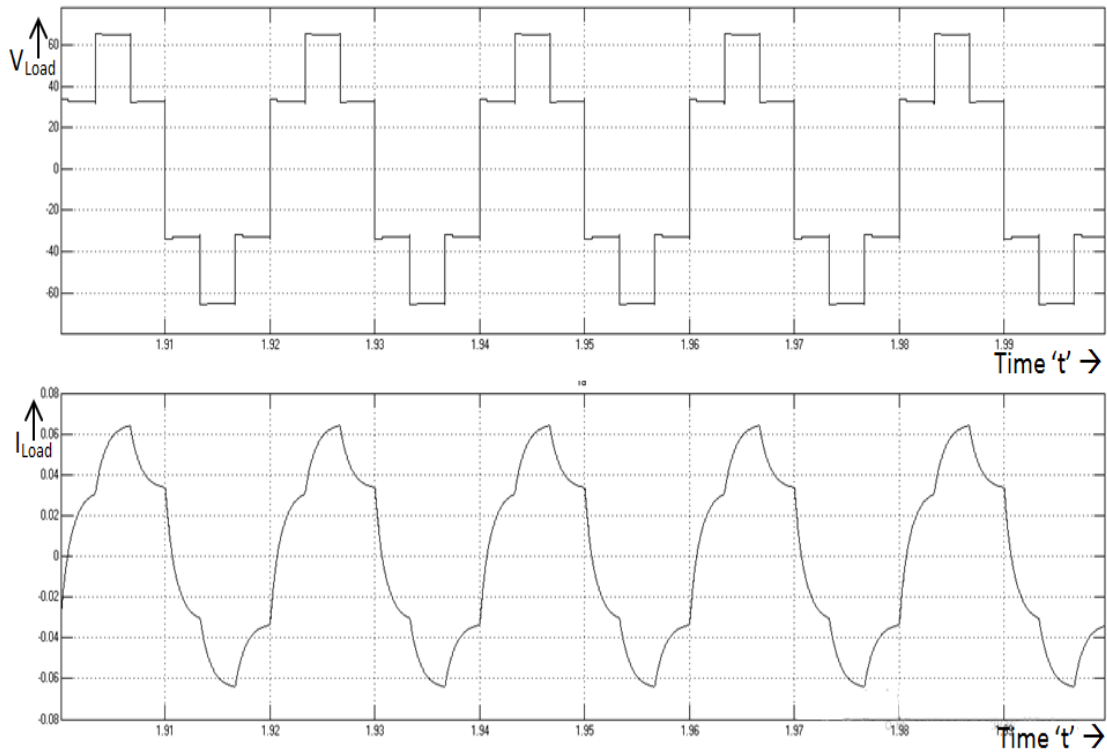
2.2 (a)



2.2 (b)



2.2 (c)



2.2 (d)

Figure 2.2 Simulation result of (a) 1-phase converter, (b) 3-phase converter, (c) 1-phase inverter, (d) 3-phase inverter (result of phase 'a' is shown). Waveforms shown are voltage and current waveform respectively for each figure. The Y- axis is either voltage or current while X- axis represents time 't'.

2.2 Exiting Switching Schemes

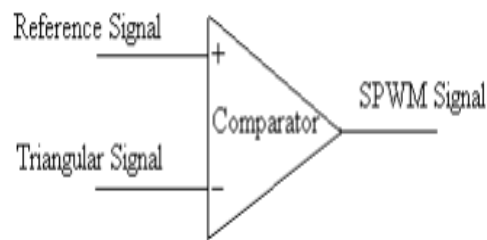
As discussed in first chapter, there are several strategies have been designed and developed over a period for generating the gate pulses. Few important switching strategies are as follows:-

2.2.1. Pulse Width Modulation

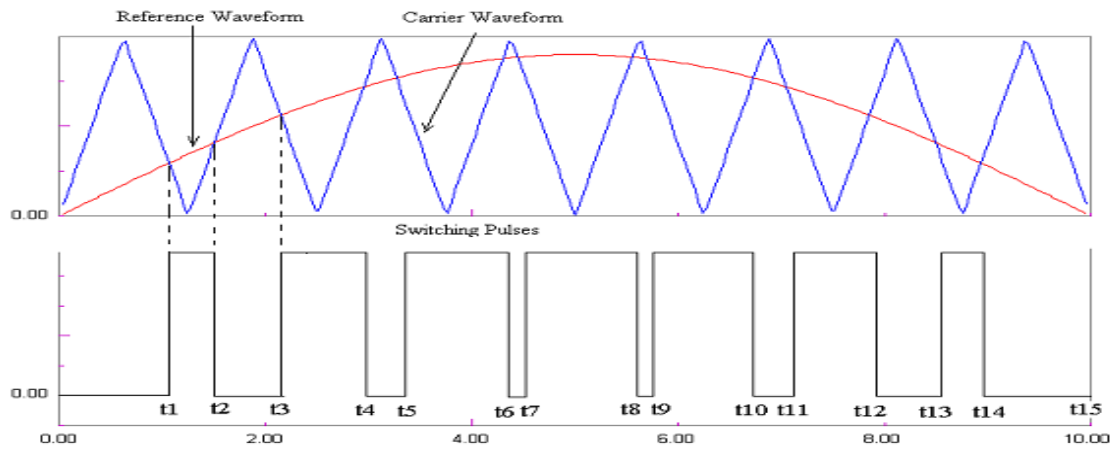
Pulse-width modulation (PWM) or pulse-duration modulation (PDM) is a modulation technique that controls the width of the pulse, formally the pulse duration, based on modulator signal information [5]-[7]. Although, this modulation technique can be used to encode information for transmission, its main use is to allow the control of

the power supplied to electrical devices, especially to inertial loads such as motors. The PWM switching frequency has to be much faster than what would affect the system.

The widely accepted PWM switching strategy for power electronic devices uses the basic concept of comparator, where two input ports of comparator are connected to reference signal (sin wave) and modulating signal (triangular wave) respectively, the comparator compares both the inputs and generate the output according to the logic. To understand this method one can refer to figure 2.3(a) & (b).



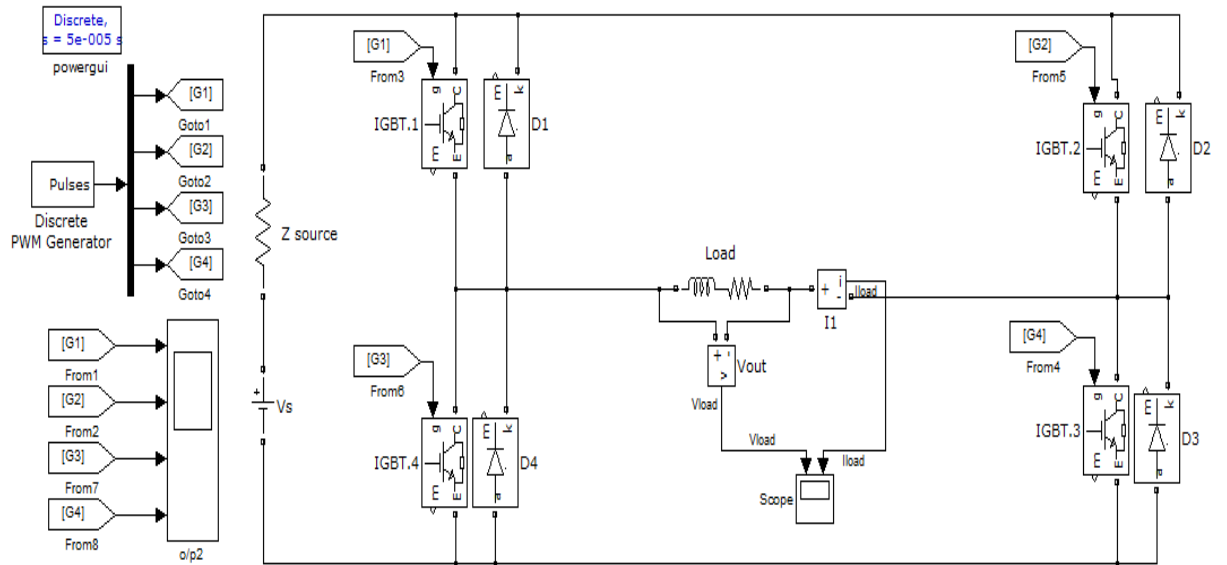
2.3 (a)



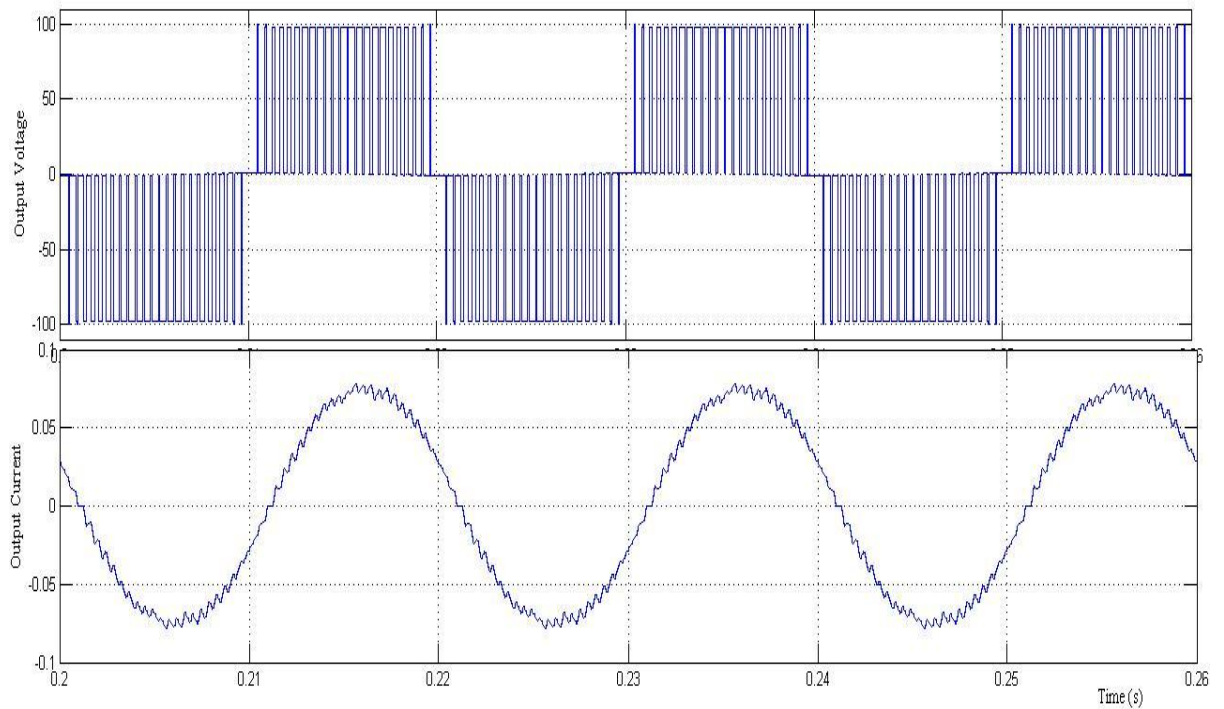
2.3 (b)

Figure 2.3 (a) Comparator for PWM, (b) Pulse generation using comparator.

With the purpose of understanding the application and impact of the PWM switching strategy, we used PWM generator block in Simulink as explained in figure 2.4(a) and perform the simulation with the triangular modulating signal at the frequency of 2 kHz to generate the output at 50 Hz. The final output is of 50 Hz is in figure 2.4(b).



2.4 (a)



2.4 (b)

Figure 2.4(a) Simulation model of single-phase PWM inverter, (b) output voltage and current waveform of 1-ph PWM inverter.

2.2.2. Selected Harmonic Elimination

Selected harmonic elimination targets over specified order of harmonic (e.g.-3rd 5th 7th etc.). For this purpose specified numbers of pulses with specified

pulse-width are applied to the gate terminal of the device. As mentioned in name, this method can be applied for specified order of harmonic only. We cannot apply this method for harmonics other than specified, which become the major drawback of this method and limits its application.

The condition must be satisfied for selected harmonic elimination is given as in (2.1): -

$$\delta k = \delta - \frac{2\pi}{n} \quad \text{for} \quad \frac{2\pi}{n} \leq \delta \leq \pi \quad (2.1)$$

Where ‘ δ ’ is pulse width and ‘ n ’ is the order of harmonic we want to eliminate.

A selected harmonic elimination method gives the following output waveform for the 3rd harmonic elimination. It should be noted that, with the third harmonic all other harmonics that are multiple of three (triplents, 3, 6, 9, 12, and so on) are also eliminated.

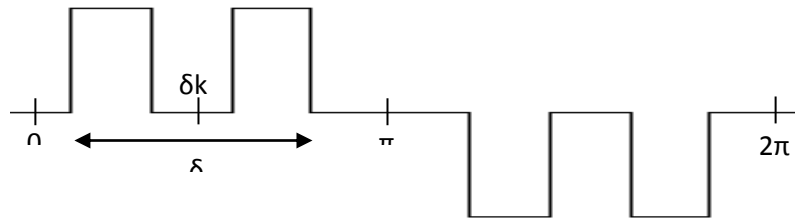


Figure 2.5 Selected harmonic elimination for 3rd harmonic.

2.2.3. Hysteresis Band Current Control

Hysteresis band current control could be explain as shown in with the figure 2.6. In hysteresis switching scheme, there is a reference and two bands (upper band and lower band) [8]. The controller compares the value of actual current with these band and turns on or off the switch pairs to generate the +V or –V at the output of inverter.

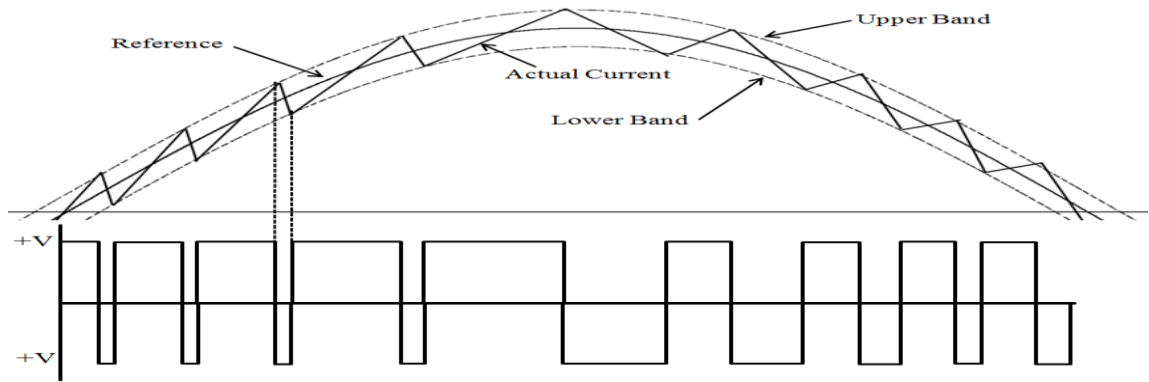


Figure 2.6 Hysteresis band current control

The hysteresis band concept shown here is bipolar switching scheme but it could be unipolar as well. The switching frequency depends upon how fast the current changes from upper limit to lower limit and vice-versa. This in turns depends upon the nature of load.

2.2.4. Other Switching Techniques

The importance of the suitable switching techniques can be understood by the fact that the list of the switching strategies doesn't stops here, there are many more techniques have been developed to tackle the issue. Random PWM (RPWM), optimal PWM, delta modulation, hysteresis control, variable band technique, hybrid PWM, phase shifted PWM, carrier-based PWM, multiple-carrier PWM, and tolerance band based PWM are the few name in the list of other switching strategies [13]-[21].

2.3 Basics of Wavelet

2.3.1. Wavelet

A wavelet is a wave-like oscillation with amplitude that begins at zero, increases, and then decreases back to zero. It can typically be visualized as a "brief oscillation" like one might see recorded by a seismograph or heart monitor [22].

The city of wavelet includes many families named Haar, Daubechies, Biorthogonal, Coiflets, Symlets, Morlet, Mexican Hat, Meyer and so on. The two major families are discussed in brief as follows.

2.3.1.1. Haar

Any discussion of wavelets begins with Haar wavelet, the first and simplest. Haar wavelet is discontinuous, and resembles a step function. It represents the same wavelet as Daubechies db1. A Haar wavelet is shown in figure 2.7 (a).

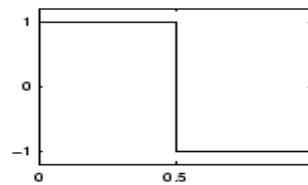


Figure 2.7 (a)

2.3.1.2. Daubechies

Ingrid Daubechies, one of the brightest stars in the world of wavelet research, invented what are called compactly supported orthonormal wavelets — thus making discrete wavelet analysis practicable.

The names of the Daubechies family wavelets are written dbN, where N is the order, and db the "surname" of the wavelet [22]. The db1 wavelet, as mentioned above, is the same as Haar wavelet. Wavelet functions of the next nine members of the family are shown below:

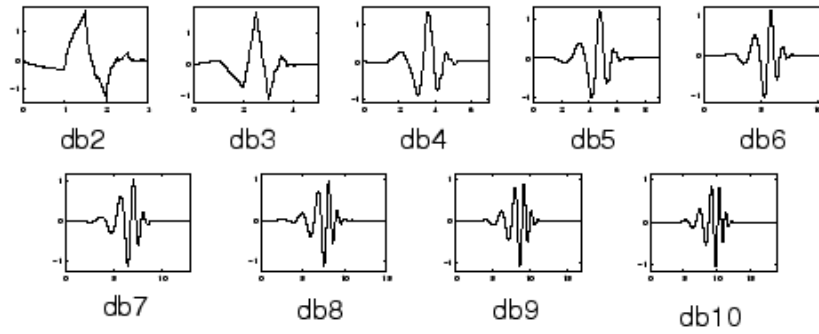


Figure 2.7 (b) Daubenchies wavelet family

2.3.2. Wavelet Transform

It is traditional to introduce the wavelet transform in the following way. The wavelet transform is similar to the short-time fourier transform, maps a function, $S(t)$, in to a two – dimensional domain (the time – scale plane) and is denoted by $Ws(a,b)$ given by:

$$\begin{aligned} Ws(a,b) &= \int_{-\alpha}^{+\alpha} S(t)h * \left(\frac{t-b}{a}\right) dt \\ &= \int_{-\alpha}^{+\alpha} S(t)hab*(t)dt \end{aligned} \quad (2.2)$$

Where $h(t)$ is in general called the mother wavelet, and the basis function of the transform, called daughter wavelet, are given by:

$$Hab(t) = \frac{1}{\sqrt{a}} h \left(\frac{t-b}{a} \right) \quad (2.3)$$

Equation 2.2 is also known as the expansion formula the forward transform or analysis; $hab(t)$ is a set of basis function obtained from the mother wavelet $h(t)$ by compression or dilation using scaling parameters ‘a’ and temporal translation using shift parameter ‘b’.

$$C = \int_{-\alpha}^{+\alpha} \left(\frac{|H(w)|^2}{w} \right) dw < \text{infinity} \quad (2.4)$$

Where C is constant.

Wavelets are localized wave and they extend not from $-\infty$ to $+\infty$ but only for finite time duration. We can thus think using $h(t)$ and its scaled daughter function as the basis for a new transform [23]-[25].

The most important point of wavelet is that the basis functions are obtained by scaling and shifting one particular function or by the manipulation of single function. In that sense, the wavelet transform is similar to a fourier transform, whose basis functions are obtained by manipulating a periodic function. Thus for periodic function the fourier analysis is ideal. However, with wavelet transform, we are not restricted to only periodic functions but any function, which satisfies its conditions. The implementation of a fourier transform using linear system involve a time – variant impulse response. In contrast, wavelet transform as defined can be implemented using time – invariant system. The components of wavelet transform are discussed below.

2.3.2.1. Multi resolution analysis (MRA)

Multi resolution analysis (MRA) can be considered the link between the harmonic analysis (i.e. time – frequency analysis) and discrete signal processing, and, in particular, discrete multi-rate filter banks using or quadrature mirror filters. MRA can be defined as analysis and synthesis of signal using wavelet basis function. Multi-resolution analysis is similar to sub-band decomposition; however, for this case, the time variable is continuous rather than discrete. On multi-resolution analysis the wavelet function is related to the impulse response of high pass filter, in a similar manner as in the sub-band case, a low-pass filter is also defined. The impulse response of this filter is the scaling function. It is defined from the mathematical standpoint as follows.

Given a sequence of embedded close subspaces i.e.

$$V_0 \subset V_1 \subset V_2 \subset V_3 \subset V_4 \dots \dots \dots \subset L^2(R) \quad (2.5)$$

The goal of multi-resolution is to choose these subspaces in a way that they encompasses the whole function space without any overlap or redundancy. The projection of the function gives finer result as the index j increases or the function resolved with sampling period $T = (1/2^j) * T_0$ where T_0 is the sampling period in V_0 [24].

2.3.2.2. Scaling Function

Wavelets are defined by the wavelet function $\psi(t)$ (i.e. the mother wavelet) and scaling function $\phi(t)$ (also called father wavelet) in the time domain [26],[27].

The wavelet function is in effect a band-pass filter and scaling it for each level halves its bandwidth. This creates the problem that in order to cover the entire spectrum, an infinite number of levels would be required. The scaling function filters the lowest level of the transform and ensures the entire spectrum is covered. We can construct an orthogonal basis for each space V_M by dilating and scaling a single function $\phi(t)$.

2.3.2.3. Sampling

Sampling is the reduction of a continuous signal to a discrete signal. In process of sampling, the values of the signal are recorded at specified interval. In case of wavelet, the interval for sampling is calculated by scaling function. The sampling process must satisfy the nyquist Sampling Rate given as $f_s > 2 * B$.

2.3.2.4. Reconstruction

Reconstruction is the method of obtaining the original signal from the sampled signal. In other words, one may say that generating a continuous signal from discrete signal. As in sampling, the scaling function defines the interval for the

sampling also in case of reconstruction the scaling function would be used for proper generation of original signal.

CHAPTER 3

MODIFIED HYSTERESIS SWITCHING SCHEME FOR 1- PHASE VOLTAGE SOURCE INVERTER

CHAPTER 3

MODIFIED HYSTERESIS SWITCHING SCHEME FOR 1-PHASE VOLTAGE SOURCE INVERTER

3.1 Modified Hysteresis Switching Scheme

The modified hysteresis switching scheme has been designed for single-phase H-bridge VS DC–AC inverter. A circuit model of single-phase H-bridge VS DC–AC inverter is shown in figure 3.1, which has been used throughout the process of designing and testing of new switching scheme. The inverter model has four IGBT switches S1, S2, S3, and S4. These IGBT switches are controlled via gate pulses provided through G1, G2, G3 and G4 respectively. Switching scheme is logic for the proper sequence, which is implemented through a programmable logic circuitry. The new switching scheme is discussed below.

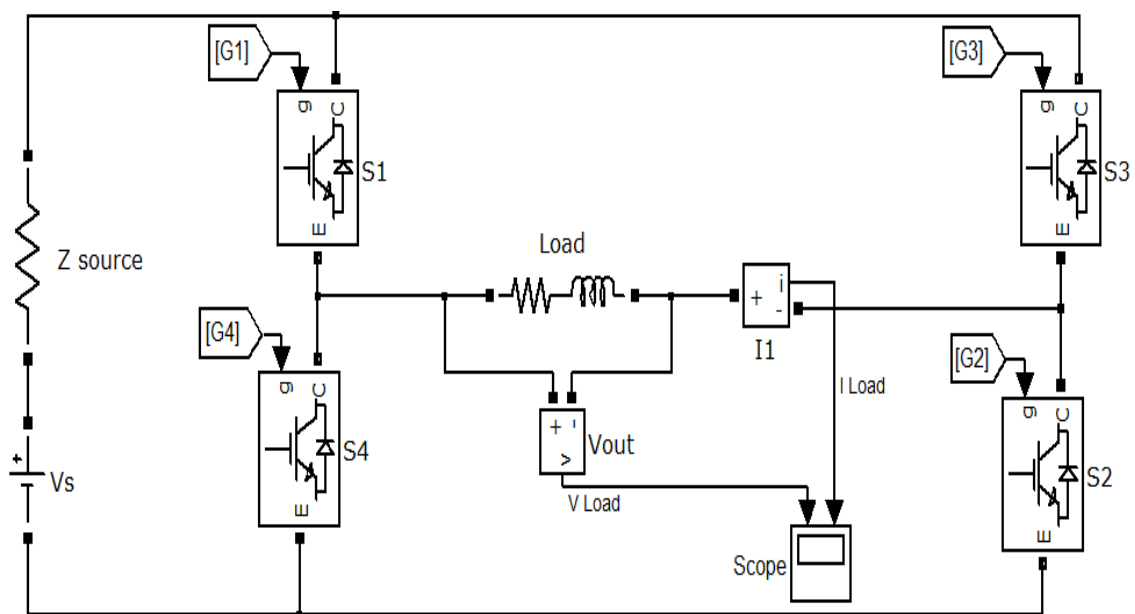


Figure 3.1 Single-phase H-bridge VS DC – AC inverter model.

3.1.1. How is it Different for Existing Scheme

The designed modified hysteresis scheme is modification of exiting hysteresis current control scheme. The new switching scheme differs from existing one in following term.

- I. No Band: - The new switching scheme is free from band concept when we apply it for three-phase system. Although, it is a hybrid of band and band less concept for single-phase system.
- II. Hybrid: - It is a hybrid of unipolar and bipolar unlike to existing schemes, as they are either unipolar and bipolar.
- III. Variable reference: - The reference in new scheme is of variable nature instead of being fixed in earlier schemes. The reference is derived from the load current itself.

All the above concepts and the switching scheme is discussed in detail in the following sections.

3.1.2. New Switching Scheme

The block diagram of new switching scheme is shown in figure 3.2. In new switching scheme the readings of output current in ammeter is taken as feedback. Thus, the feedback signal is a copy of load current. This feedback signal can be named as signal B. The reference signal for the new switching scheme is a sinusoidal signal, define as in (3.1).

$$A = A_{\max} \sin(\omega t) \quad (3.1)$$

Where A_{\max} is the maximum value of reference signal A. The reference signal in this switching scheme is actually a copy of desired sinusoidal load current. During the process of generating the gate pulses, the switching circuit compares feedback signal B with respect to the sinusoidal reference signal A. Figure 3.3 (a) shows a conceptual diagram the of new switching scheme for positive cycle. When

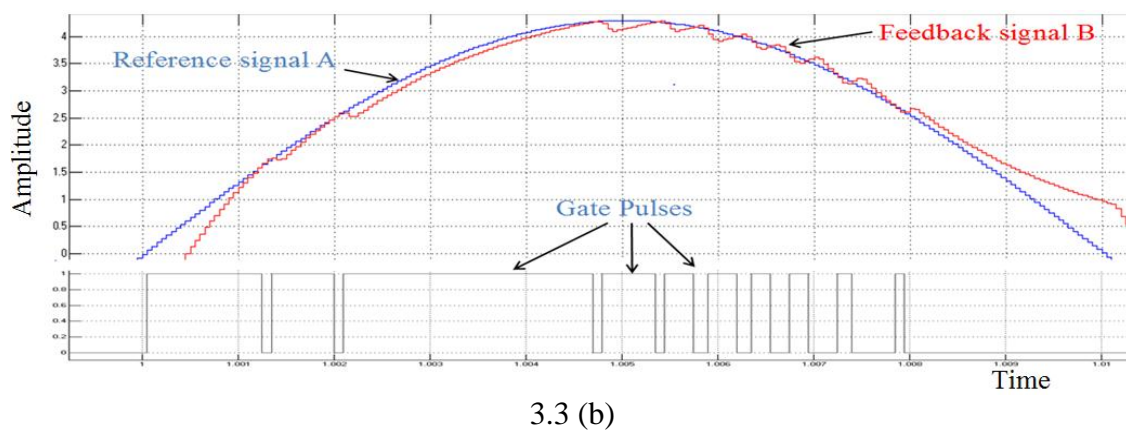
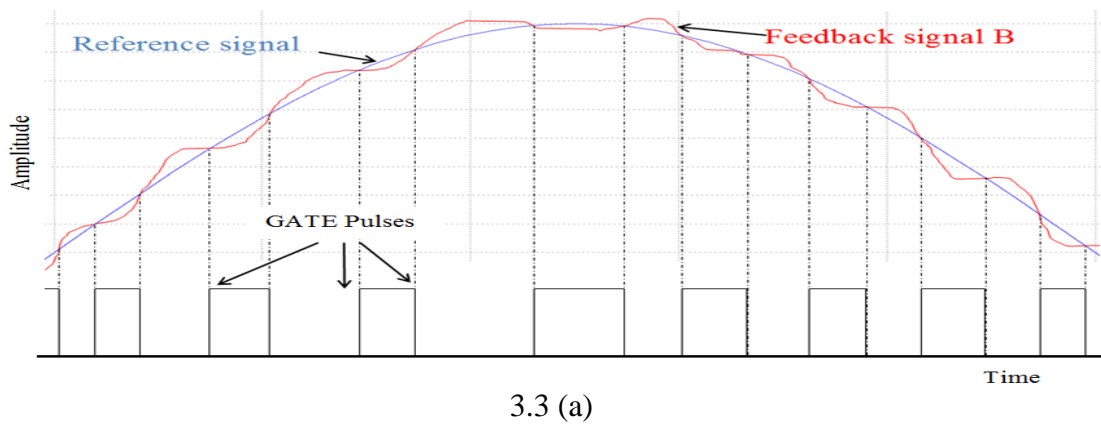
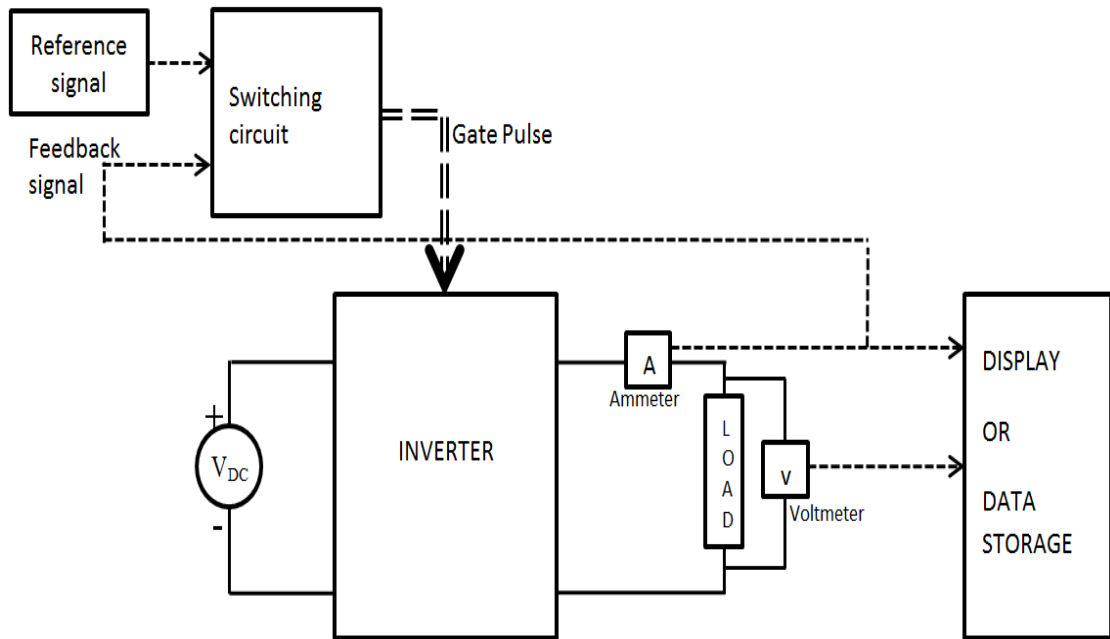


Figure 3.3 (a) A conceptual plot for new switching scheme, (b) Plot for new switching scheme with practical data.

the feedback signal B is less than the reference signal A, the switching circuit generates ON pulse to the switch S1 and S2. This ON pulse brings the switches S1 and S2 in conducting mode and as soon as switches S1 and S2 comes in conducting mode the load current and thus the feedback signal starts increasing. As the load current and thus the feedback signal B attains higher value than the reference signal A, the switching circuit generates OFF pulse for switches S1 and S2. This OFF pulse blocks the conduction mode of switches S1 and S2. This decreases the value of load current (and feedback signal) to the level of reference or even lower than that. A similar process is being followed for the negative cycle also. Switches S1 and S2 operate during positive cycle and switches S3 and S4 operates during negative cycle of output current. A plot showing actual feedback, reference and gate signals are shown in figure 3.3(b).

3.1.3. Reference Signal

The reference signal plays an important role in any switching scheme. The complete process of switching (or pulse modulation) depends on the selected reference signal. As discussed earlier, the reference signal for new switching scheme is a sinusoidal signal defined in (3.1). The uniqueness of the new strategy lies in its reference signals. Instead of having a fixed reference signal and scaling the modulating signal to that range the, a new concept of variable reference signal has been introduced. This reduces the calculation and eliminates the circuitry to scale the modulating signal. This reference signal is a copy of desired load current and the load current depends on load, so, may not have same value for all kind of load. So, the reference signal also may not be same for all kind of application. The value of amplitude of desired load current and thus reference signal will vary from load to load.

Considering the above facts the value of A_{\max} has been kept variable and thus the reference signal has been defined in two parts.

- I. Initial reference signal
- II. Updated reference signal

Initial reference signal is defined with a small constant value of amplitude as in (3.2a). Here a_{\max} is constant value and is less than A_{\max} .

$$A = a_{\max} \sin(\omega t) \quad (3.2a)$$

This initial reference signal is required to initiate the switching process. As soon as the switching process begins and inverter starts delivering power to the load, the reference signal must be updated according to the load demand, until its amplitude reaches to maximum value A_{\max} as shown in figure 3.4. The updating of reference signal follows the equation (3.2b).

$$a_{\max} = b_{\max} \quad (3.2b)$$

Where b_{\max} is the maximum amplitude of the feedback signal in the ongoing cycle.

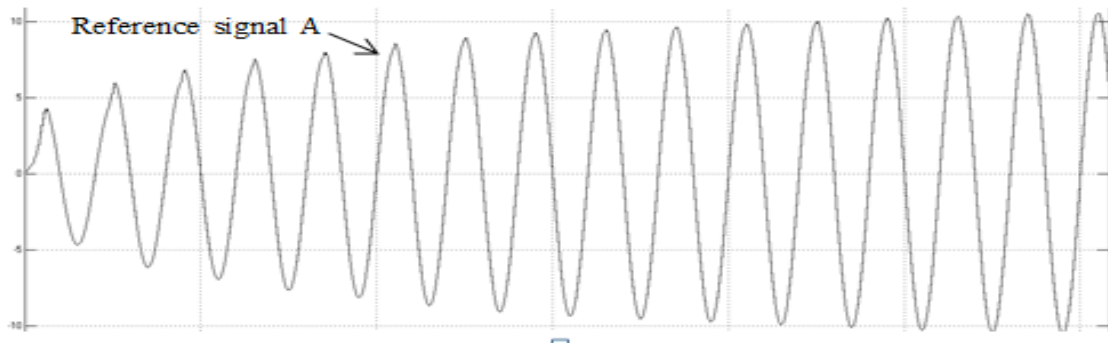


Figure 3.4 Reference signal A.

3.1.4. Problems and Modification

The defined switching scheme has a problem also. Figure 3.3 (b) shows that in the second half of positive cycle when the gate pulse is OFF even though the feedback signal (load current) of the inverter is not following the reference signal. Load current is higher than the reference current during this period and just switching off the switches S1 and S2 is not sufficient enough to decrease the value of feedback signal (load current) to the level of reference signal. This problem arises because of inductive nature of the load. The inductive property of load causes the storage of energy during the first half of positive cycle when the load current is increasing and during second

half of the cycle, it behaves as a current source and causes the excess value of load current.

The solution of this problem has been driven from the concept of hysteresis control (or modulation) scheme for inverters. Similar to the tolerance band of hysteresis current control, the concept of error band has been introduced to tackle the above problem. By recording, the difference between reference signal and feedback signal one can obtain the error signal. If we observe the error signal shown in figure 3.5, then we can analyze that the error between the reference signal and feedback signal is almost in a fixed limit except the specific period of second half of positive or negative cycle. The inductive effect of load is causing trouble during this period.

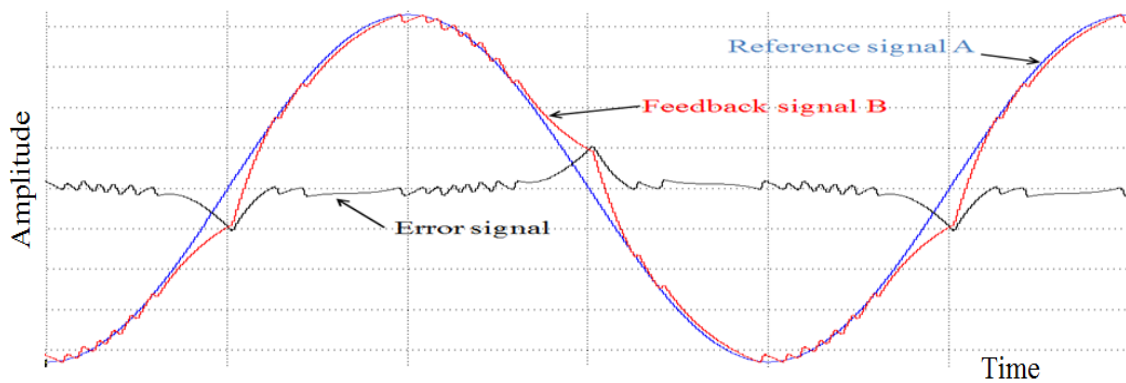


Figure 3.5 Error signal representation.

As the error signal is almost in fixed limit except the specific period, we can define an error band as a band of fixed limit for the error signal. Furthermore, two new terminologies have been introduced.

A. Positive error

Positive error is the error between reference signal and feedback signal during positive cycle.

B. Negative error

Similar to positive error, negative error is the error between reference signal and feedback signal during negative cycle.

Using the above concept of error band and positive and negative error, an additional switching scheme has been defined. Switching circuit compares the error with the error band and accordingly generates gate pulses. During the positive cycle when the positive error becomes more than the error band the switching circuit generates ON pulse for switches S3 and S4. This establishes a negative voltage across the load with respect to existing voltage and tries to establish a current in opposite direction and so the excess energy gets balanced. A similar logic is applied to the negative cycle also. Switches S3 and S4 get operated during positive cycle and S1 and S2 during negative cycle.

It must be noted that this modification of error band is applied for very short duration of time in respect of time-period of one cycle of current. During this period, the switching becomes bipolar and is unipolar for the rest of operation. Now this error band based switching scheme is applied to the inverter along with the previously defined new switching scheme.

3.2 Implementation

Designed switching scheme is implemented using the S-function block of SIMULINK facility of MATLAB R 2011b. A program has been written to realize the modified switching scheme. Simulation and testing for the modified switching scheme is performed on the model of single-phase VS DC–AC inverter shown in figure 3.1. The flowchart of the complete switching scheme is shown in figure 3.6.

The power electronic switches of inverter are controlled by gate pulses. The output of the switching circuit is applied to the gate terminal of these switches. The gate terminals are named as G1, G2, G3 and G4 for switches S1, S2, S3 and S4 respectively.

Logic '1' on gate terminal of any switch represent ON pulse for respective switch and similarly logic '0' represents the OFF pulse. The error band is represented by E_b in the description and flowchart below. The step by step description of the modified switching scheme is as follows.

Step 1) Initialize the switching circuit.

Step 2) Define the basic parameter such as frequency (f_m) time period (T_m), sampling time (T_s) and set time $t=0$;

Step 3) Define initial reference current as in (3.2)

$$A = a_{\max} \sin(\omega t) \quad (3.2)$$

Step 4) Evaluate positive (+ve) error and negative (-ve) error.

$$+ve \text{ error} = A - B \text{ (During +ve cycle)} \quad (3.3)$$

$$-ve \text{ error} = B - A \text{ (During -ve cycle)} \quad (3.4)$$

Step 5) If $t \geq \frac{T_m}{2}$; then go to step 6. Otherwise go to step 9.

Step 6) If $A > B$; then $G1 = G2 = 1$ and $G3 = G4 = 0$. Otherwise go to step 7.

Step 7) If +ve error $> E_b$; then $G1 = G2 = 0$ and $G3 = G4 = 1$. Otherwise $G1 = G2 = G3 = G4 = 0$.

Step 8) Go to step 11.

Step 9) If $B > A$; then $G1 = G2 = 0$ and $G3 = G4 = 1$. Otherwise go to step 10.

Step 10) If -ve error $> E_b$; then $G1 = G2 = 1$ and $G3 = G4 = 0$. Otherwise $G1 = G2 = G3 = G4 = 0$

Step 11) Check the amplitude of reference signal, does it require update?

Step 12) Update the value of reference current if required, otherwise leave this step

Step 13) If $t \geq T_m$; then reset the value of t . otherwise leave this step.

Step 14) Go to step 4.

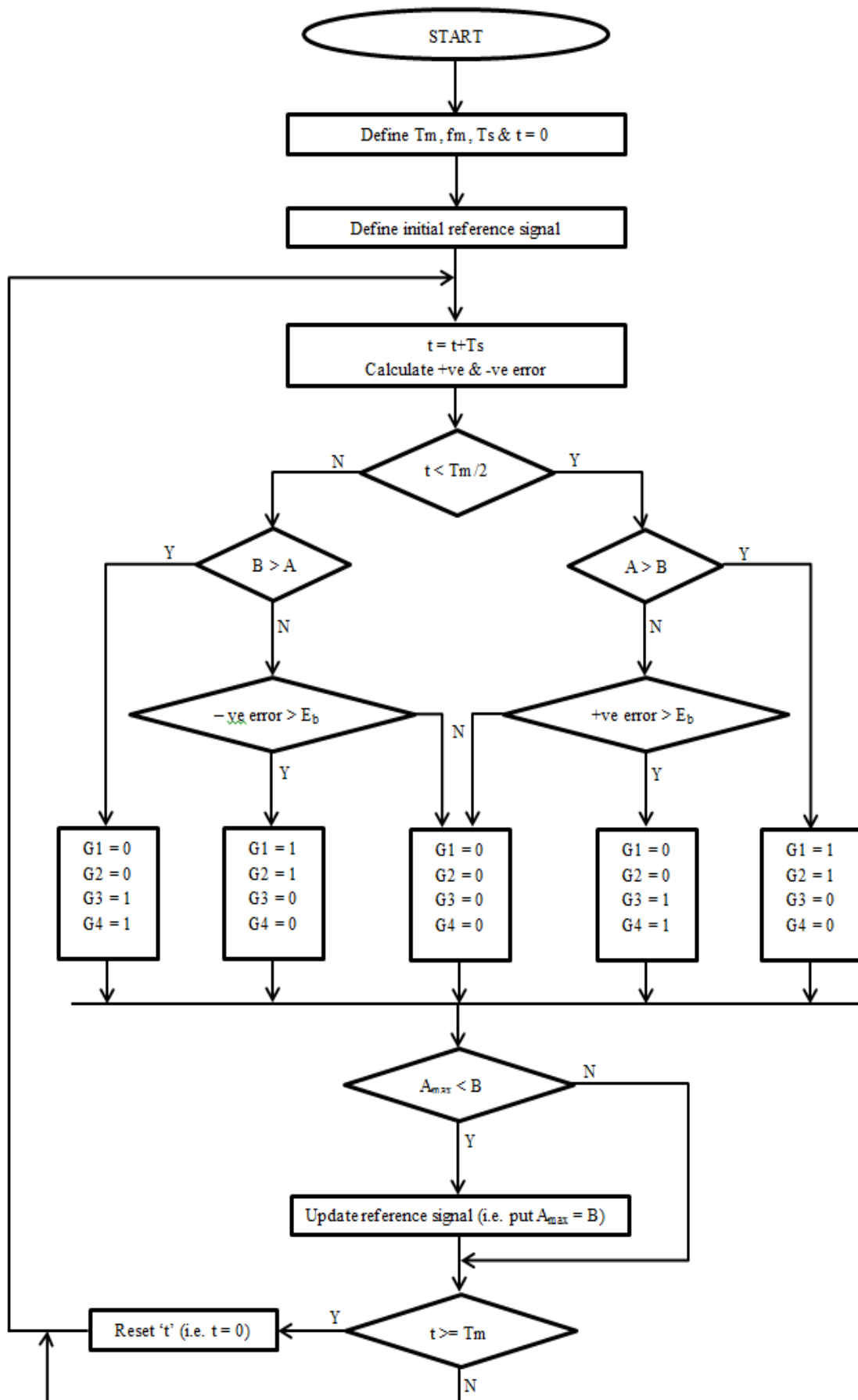


Figure 3.6 Flowchart for modified switching scheme.

When this switching scheme is applied to motor or any other load withdrawing relatively large load current in the beginning than the load current during steady state operation, then system faces a problem with reference signal that the large current in the beginning set a reference with relatively large amplitude than required during the steady state operation. This causes improper operation of system.

This issue is solved by employing the reset logic for reference signal once the current requirement reduced to its normal steady state condition. This reset instruction requires 10 to 20 cycles only, depending on the difference between the initial and updated reference signal and it improves the outcome significantly. Another way to solve this problem is to put a reset logic, which checks the reference signal in each cycle.

3.3 Testing, Results and Discussion

Simulation and testing has been performed for the designed modified switching scheme on the model of voltage source inverter is shown in figure 3.1. The simulation has been carried out for linear as well as dynamic loading condition. An R–L load is used for linear loading condition while for dynamic loading condition a main and auxiliary winding type motor is used. Simulation is also performed for the PWM switching scheme under same loading condition. The results from PWM as well as modified switching schemes are used for the comparative analysis. The voltage and current waveforms obtained under various loading condition with both switching scheme are presented in following section. The THD graphs of voltage and current are also presented for analysis. A comparative study also can be made by data available in table 3.1 and 3.2

The simulation is performed for the load current of 50 Hz at output terminal. All the waveforms presented in the paper are recorded under steady state condition. The various loading condition and other parameter for simulation is as follows.

- I. Source voltage (V_s) = 200 V
- II. Source impedance (Z_s) = 0.1 Ω
- III. Modulation index for PWM = 0.8
- IV. Modulation frequency for PWM = 1.2 KHz
- V. R–L load = 15+ j9.425 Ω
- VI. Motor loads (main and auxiliary winding motor)
 - a) Volt-ampere (VA) = 0.25 * 746 watt
 - b) Voltage rating = 220 V
 - c) Resistance (pu)
 - # main winding stator = 0.0311 Ω
 - # main winding rotor = 0.0635 Ω
 - # auxiliary winding stator = 0.110 Ω
 - d) Inductance (pu)
 - # main winding stator = 0.429 H
 - # main winding rotor = 0.0325 H
 - # auxiliary winding stator = 0.0493 H
 - # main winding mutual inductance= 1.0296 H

3.3.1. Linear load (R –L load)

The waveform of voltage and current for R–L load obtained using PWM scheme is shown in figure 3.7 and the voltage and current waveform obtained from modified switching scheme is shown in figure 3.8. The THD graphs for voltage and current is in figure 3.9 and 3.10 respectively. The simulation results obtained for given R–L load for new scheme and PWM are presented in table 3.1. By observing the waveforms and the result in table 3.1, a comparative analysis has been done.

The RMS and peak value of voltage from modified switching scheme is 127.1 V and 179.8 V respectively in respect of 112.8 V and 159.5 V respectively from PWM scheme. Similarly in case of current the new switching scheme results in 7.177 A RMS value and 10.15 A as peak value while the PWM scheme provide result with 6.367 A as RMS value and 9.004 A as peak value of current. The modified switching scheme has given better result than the PWM scheme. The RMS and peak value of

voltage and current for the modified switching scheme is more than that for PWM scheme. The THD (total harmonic distortion) has also shown the improvement in case modified switching scheme over the PWM scheme. THD in load current for modified switching scheme is 2.25% and same for PWM is 3.12%. Thus the harmonic content in load current is less in new defined scheme. The THD for voltage is 38.25% for modified switching scheme in comparison of 77.06% of PWM scheme. Similar to case of load current the harmonics content in load voltage is lesser in results obtained from modified scheme than the results obtained from PWM scheme. The analysis of outcome of both schemes signifies that the modified switching scheme gives better result than the PWM scheme in terms of RMS, peak as well as THD value of voltage and current for the given load and operating condition. The observation of RMS and peak values of current, voltage, the values of THDs and their waveforms suggest that the modified scheme is better than the PWM scheme under given operating conditions.

TABLE 3.1

SIMULATION RESULTS FOR R – L LOAD (SINGLE PHASE)

Load Type	Parameters	PWM	Modified Switching
R-L Load	Vrms	112.8 V	127.1 V
	Irms	6.367 A	7.177 A
	Vpeak	159.5 V	179.8 V
	Ipeak	9.004 A	10.15 A
	V THD	77.06%	38.25%
	I THD	3.12%	2.25%

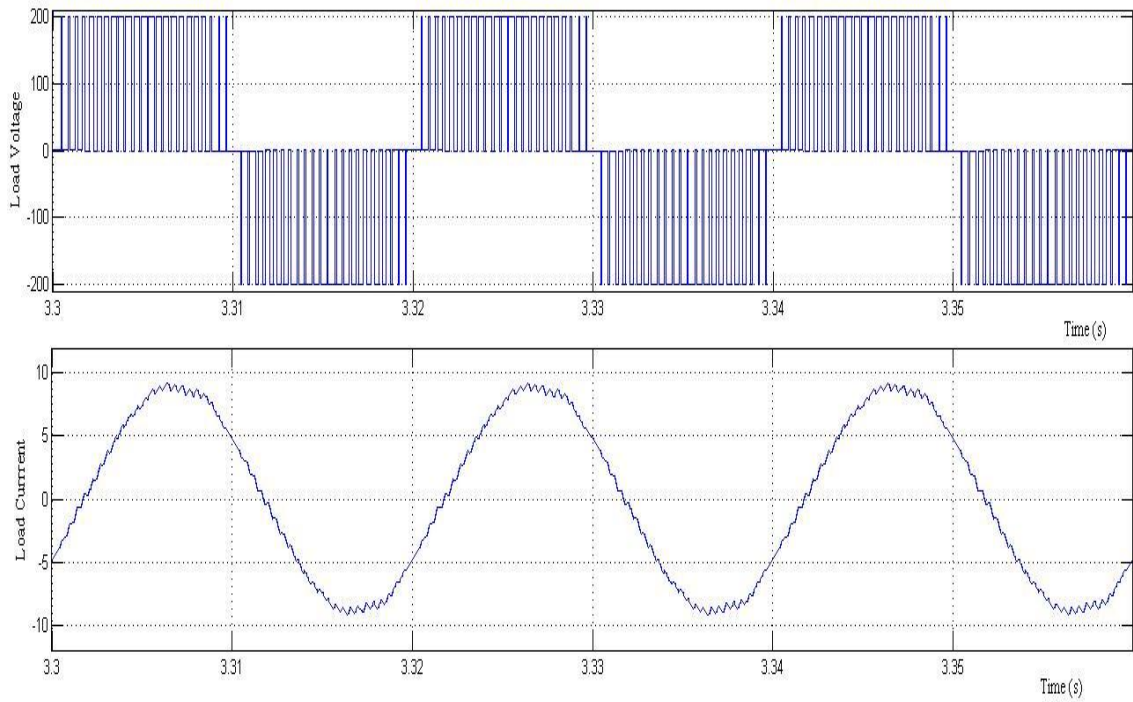


Figure 3.7 Single-phase H-bridge VS DC-AC inverter test result (load voltage and load current waveform) for R-L load using PWM switching scheme.

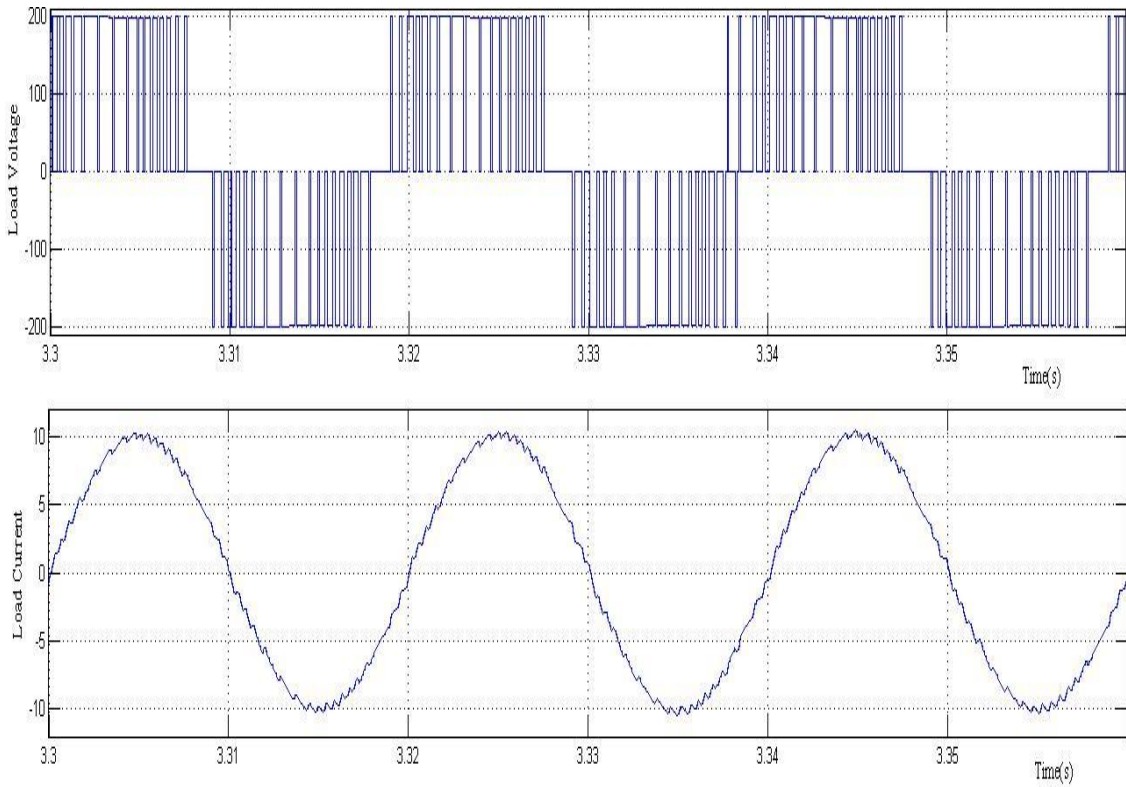
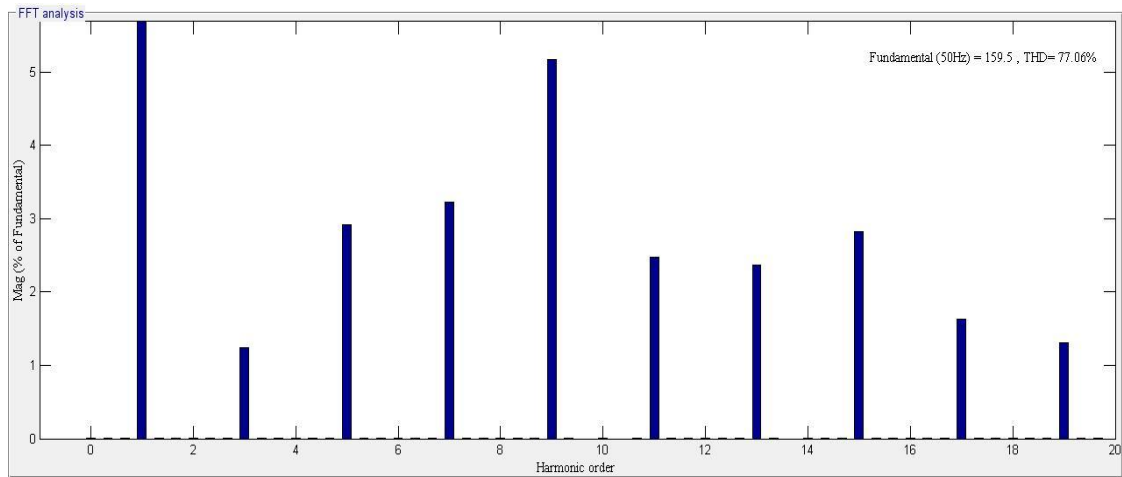
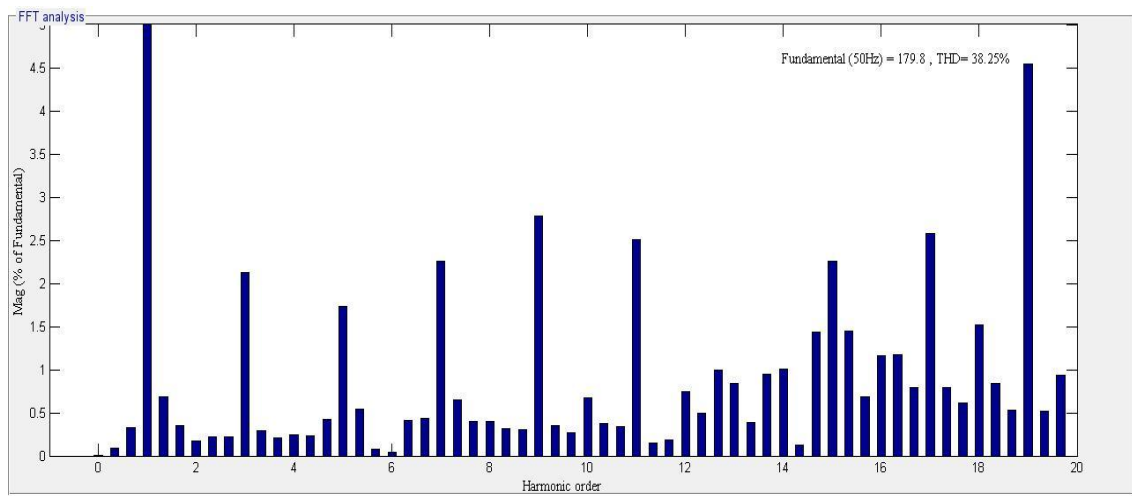


Figure 3.8 Single-phase H-bridge VS DC-AC inverter test result (load voltage and load current waveform) for R-L load using modified switching scheme.

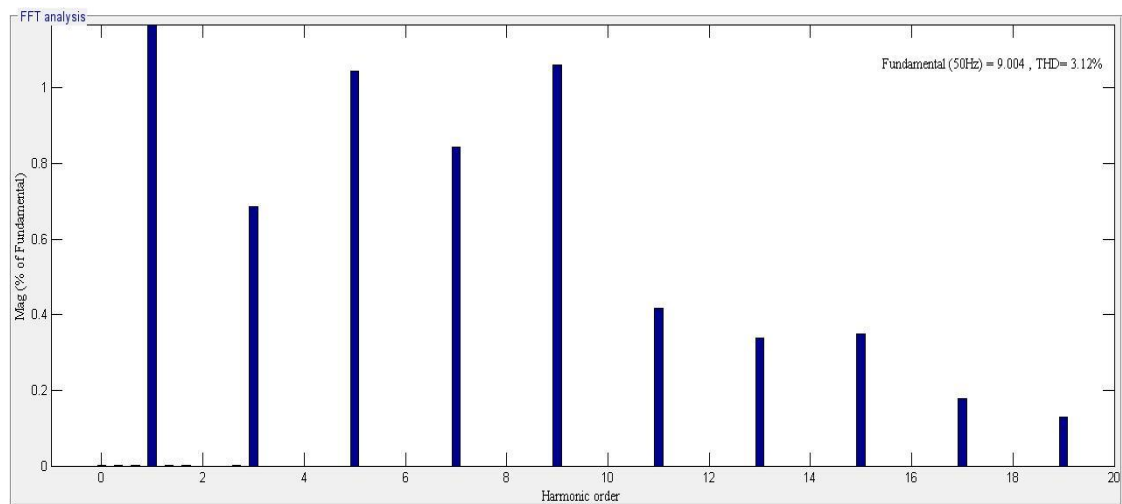


3.9 (a)



3.9 (b)

Figure 3.9 THD in load voltage waveform of single-phase H-bridge VS DC-AC with R-L load using (a) PWM (b) modified switching scheme.



3.10 (a)

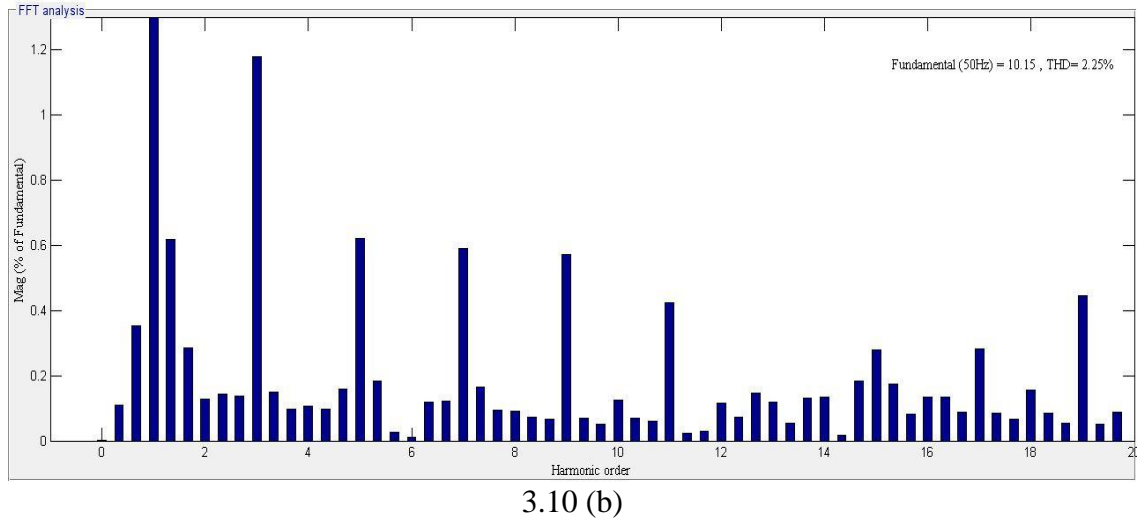


Figure 3.10 THD in load current waveform of single-phase H-bridge VS DC–AC with R-L load using (a) PWM (b) modified switching scheme.

3.3.2. Dynamic load (Motor load)

The simulation has been performed for motor load also under the previously defined loading conditions. The operating condition and other parameters have been kept identical for both the scheme under simulation. The motor used as load is a main and auxiliary winding type motor which specification is described above. The motor has been operated with constant torque of unity during simulation. The voltage and current waveforms obtained by applying PWM scheme is shown in figure 3.11 and waveform obtained using modified switching scheme are shown in figure 3.12. The THD graphs from both schemes are presented in 3.13 and 3.14 respectively for voltage and current. The comparative results of simulation of both the schemes are in table 3.2.

Similar to the case of R–L load, for motor load also, the modified scheme provides higher RMS and peak value of voltage as well as of current, than the values obtained from PWM scheme. The RMS and peak value of voltage from PWM is 109 V and 154 V respectively while the same from modified scheme is 151.7 V and 214.5 V respectively. The new switching scheme provides result with 4.852 A RMS value and 6.862 A peak value of current and same from PWM is 3.062 A and 4.339 A respectively.

The THD in load current is 5.03% for modified scheme which shows improvement over 6.26% of PWM scheme. The 46.33% THD in voltage from modified switching scheme is also a significant improvement with respect to 77.01% THD from PWM scheme. The amount of the harmonic distortion is reduced significantly in voltage as well as current when the inverter is operated with new scheme than the PWM scheme. The reduced value of THD implies lesser amount of harmonics in system and so thus better quality of output power.

The comparative analysis of voltage waveform for both switching schemes shows that new switching scheme requires very less amount of switching than the PWM scheme. This can be consider as an additional advantage of modified switching scheme over PWM. Similar to linear loading condition the observation of RMS and peak values of current, voltage, the values of THDs and their waveforms suggest that the modified scheme is better than the PWM scheme under given operating conditions.

TABLE 3.2

SIMULATION RESULTS FOR MOTOR LOAD (SINGLE PHASE)

Load Type	Parameters	PWM	Modified Switching
Motor	Vrms	109 V	151.7 V
	Irms	3.068 A	4.852 A
	Vpeak	154 V	214.5 V
	Ipeak	4.339 A	6.826 A
	V THD	77.01%	46.33%
	I THD	6.26%	5.03%

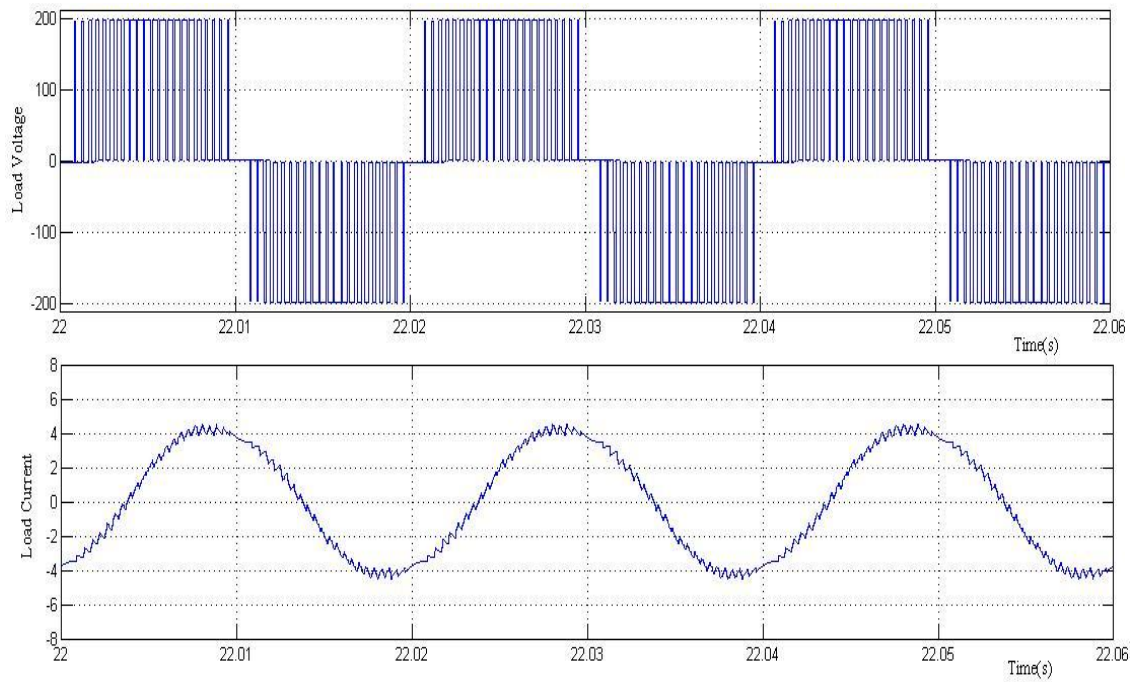


Figure 3.11 Single-phase H-bridge VS DC-AC inverter test result (load voltage and load current waveform) for motor load using PWM scheme.

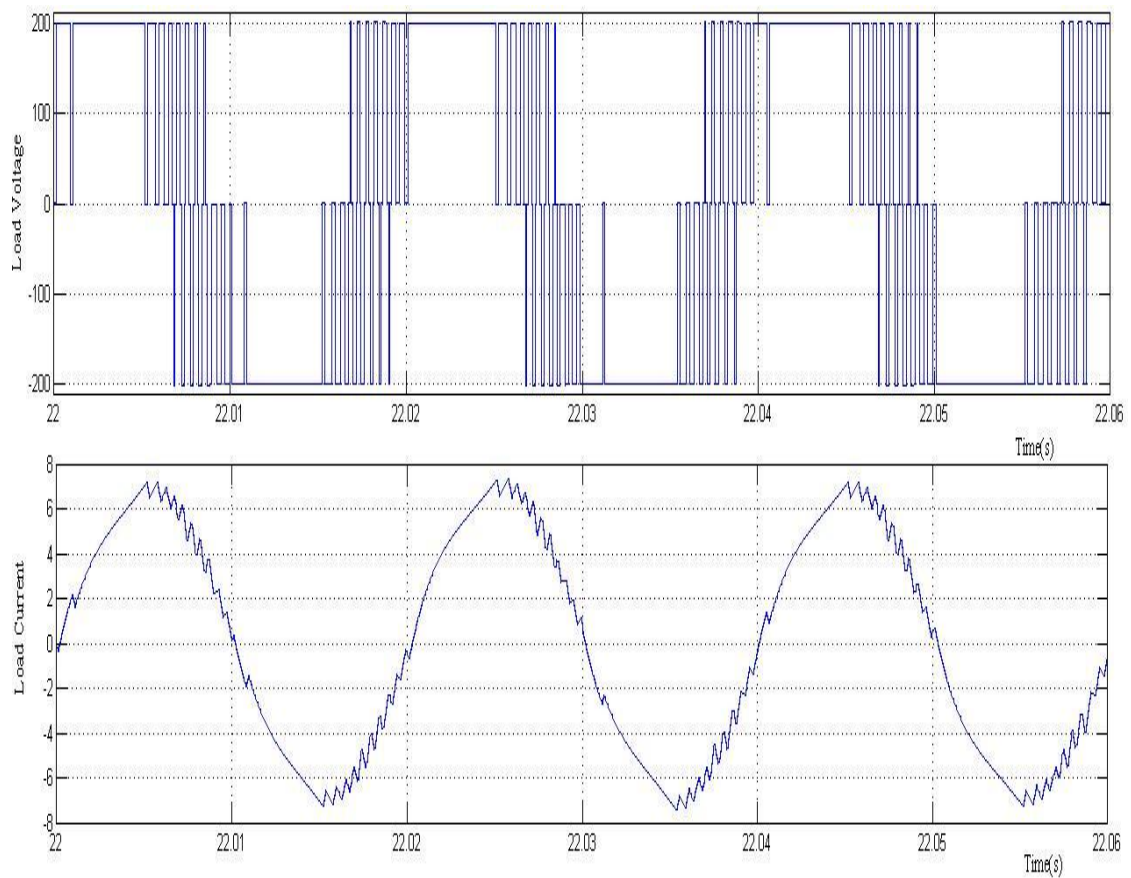
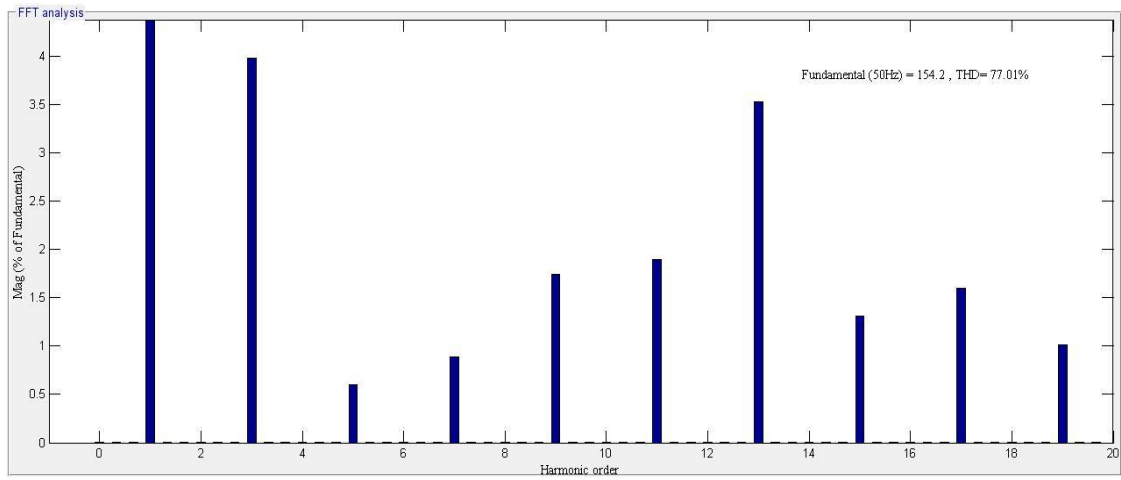
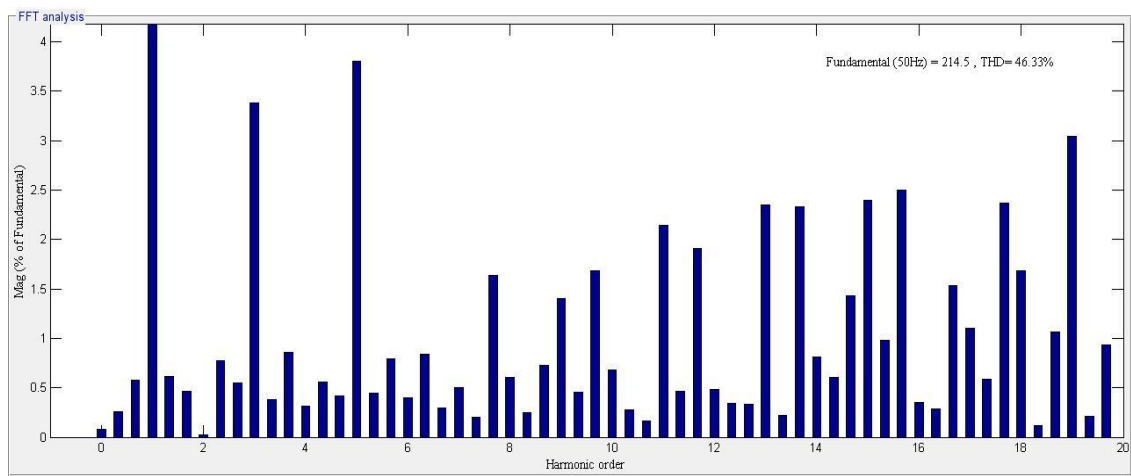


Figure 3.12 Single-phase H-bridge VS DC-AC inverter test result (load voltage and load current waveform) for motor load using modified switching scheme.

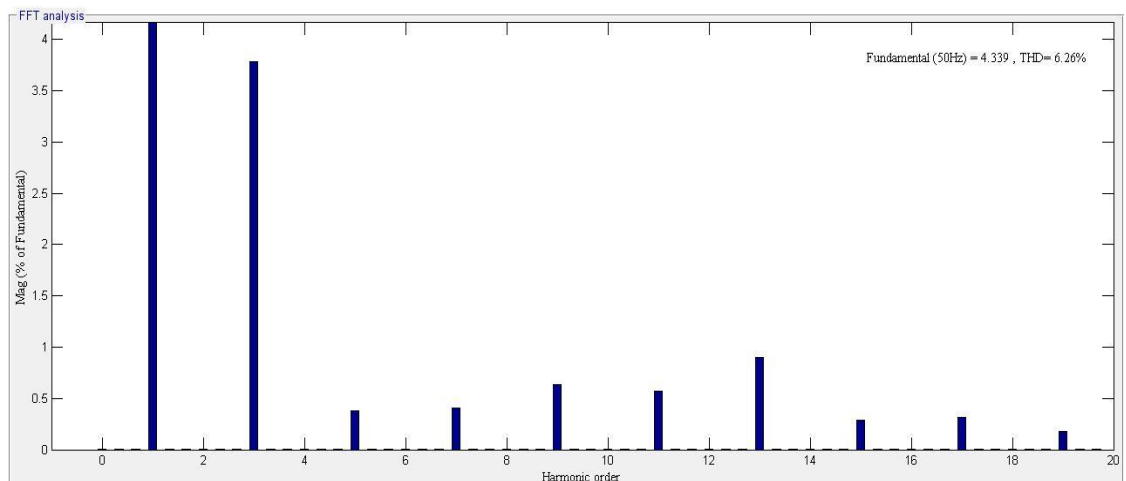


3.13 (a)

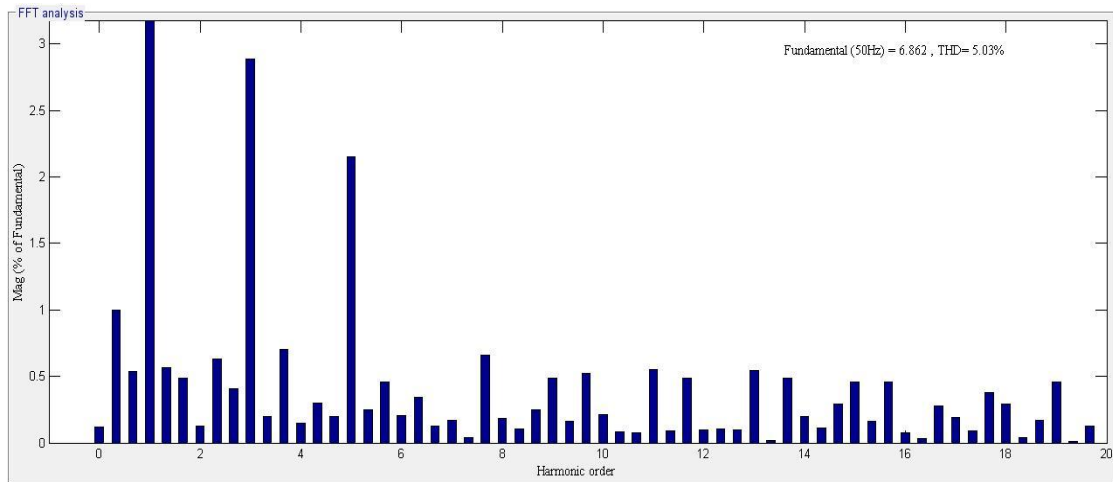


3.13 (b)

Figure 3.13 THD in load voltage waveform of single-phase H-bridge VS DC–AC with motor load (a) PWM (b) modified-switching scheme.



3.14 (a)



3.14 (b)

Figure 3.14 THD in load current waveform of single-phase H-bridge VS DC–AC with motor load (a) PWM (b) modified-switching scheme.

CHAPTER 4

MODIFIED HYSTERESIS SWITCHING SCHEME FOR 3- PHASE VOLTAGE SOURCE INVERTER

CHAPTER 4

MODIFIED HYSTERESIS SWITCHING SCHEME FOR 3-PHASE VOLTAGE SOURCE INVERTER

4.1 Modified Hysteresis Switching Scheme for 3-Phase Inverter

The proposed switching scheme has been designed for three-phase voltage source inverter. The circuit diagram of three-phase inverter is shown in Figure 4.1. It contains three legs, each with two switches. All the designing and testing has been performed using the same circuit diagram. The IGBT has been selected to be used as power electronics switch. The switches S1 to S6 are provided with gate signal through G1 to G6 respectively. These pulses follow the applied switching scheme and control the inverter accordingly. The new scheme is discussed below in detail.

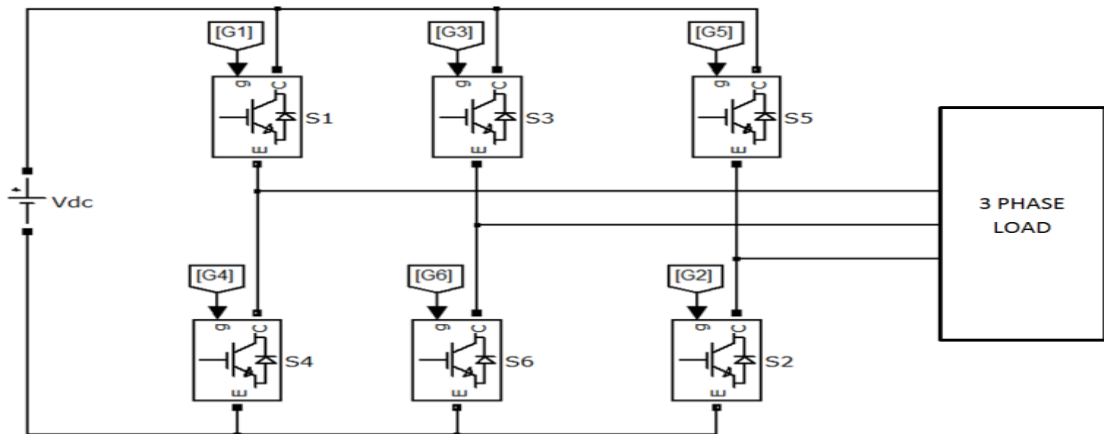


Figure 4.1 Circuit diagram of three – phase voltage source inverter.

4.4.1. New Switching Strategy

The block diagram of the new switching scheme for three-phase inverter shown in figure 4.2 is a modification of same scheme used for single-phase system discussed in chapter 3. The value of load currents are measured through ammeter and then their values are passed to switching circuit as feedback. Thus the feedback signals

are images of original load current waveforms. The reference signals for this scheme is sinusoidal signal defined as in (4.1).

$$R_a = R_{a_{\max}} \sin(\omega t) \quad (4.1(a))$$

$$Y_a = Y_{a_{\max}} \sin(\omega t - \omega T_m/3) \quad (4.1(b))$$

$$B_a = B_{a_{\max}} \sin(\omega t - \omega T_m/3) \quad (4.1(c))$$

Where R_a , Y_a , B_a are reference signals for R, Y, B phases respectively. R_{\max} , Y_{\max} , and B_{\max} are the maximum amplitude of reference signals respectively.

All the three reference signals are images of the desired load current in the respective phases. The feedback signal also can be named as R_b , Y_b and B_b respectively. Generating switching pulses for the three-phase inverter follows the same concept as single-phase inverter in chapter 3.

4.4.2. Reference Signals

The reference signal for three-phase system is similar to single-phase system. The only difference is that in three-phase system we have three reference signal i.e reference for each phase instead of single reference as in single-phase. The each reference signal includes two parts as explained in chapter 3.

- I. Initial reference signals
- II. Updated reference signal

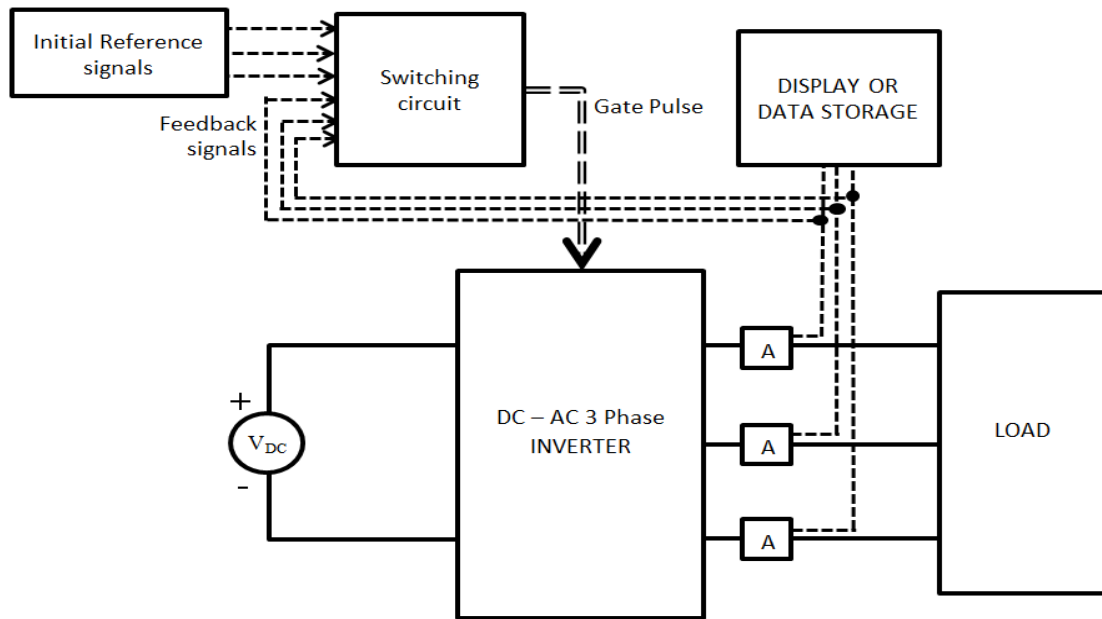


Figure 4.2 Block diagram for modified switching scheme.

4.2 Implementation

S-Function block of SIMULINK facility of MATLAB R2011b has been used for designing the switching logic. The program for switching logic has been written and then converted in MATLAB executable files. The simulation and testing has been performed using the three-phase voltage source inverter model shown in figure 4.1. The flowchart for the scheme is shown in figure 4.4.

The reference signal for all three phase is shown in figure 4.3. The figure shows the reference signal for time-period 'T'. The time-period 'T' can be sub divided in six equal parts $T/6$ as shown in figure. During the interval between t_0 and t_1 the reference R_a is more than reference Y_a , reference Y_a is less than reference B_a and reference B_a is more than or equal to reference R_a . A similar comparison can be observed for other time intervals. Using this comparison the logic of switching is defined in such a way that, it can be applied to obtain output current of any value of frequency, without much change in programming. Instead of defining logic of switching in terms of time interval, the respective value of all the three references has been used for it. The same has been used in designing the flow chart of programming.

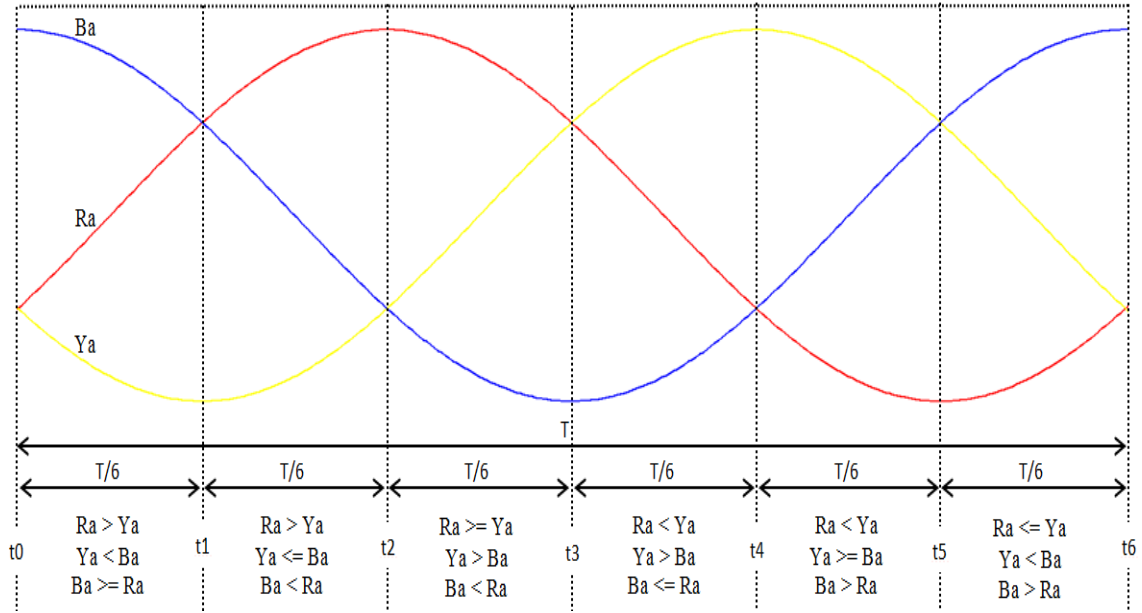


Figure 4.3 Method of replacing time-interval with respective relation between references.

The IGBT switches are controlled through the gate pulses generated from the switching circuitry. The ON pulses are represented by logic '1' and similarly OFF pulses by logic '0'. The description of the switching scheme is as follows.

- Step 1) Initialize the circuit.
- Step 2) Define parameters T_m (time-period), T_s (sampling time), t (set time) etc.
- Step 3) Define initial reference signals as in (1).
- Step 4) If $(Ra > Ya) \&\& (Ya < Ba) \&\& (Ba \geq Ra)$; then to step 5. Else jump to step 9.
- Step 5) If $(Ra > Rb)$; then $G1 = 1$ & $G4 = 0$. Else $G1 = 0$ & $G4 = 0$.
- Step 6) If $(Ya < Yb)$; then $G3 = 0$ & $G6 = 1$. Else $G3 = 0$ & $G6 = 0$.
- Step 7) If $(Ba > Bb)$; then $G5 = 1$ & $G2 = 0$. Else $G5 = 0$ & $G2 = 1$.
- Step 8) Jump to step 34.
- Step 9) If $(Ra > Ya) \&\& (Ya \leq Ba) \&\& (Ba < Ra)$; then to step 10. Else jump to step 14.
- Step 10) If $(Ra > Rb)$; then $G1 = 1$ & $G4 = 0$. Else $G1 = 0$ & $G4 = 0$.
- Step 11) If $(Ya < Yb)$; then $G3 = 0$ & $G6 = 1$. Else $G3 = 1$ & $G6 = 0$.
- Step 12) If $(Ba < Bb)$; then $G5 = 0$ & $G2 = 1$. Else $G5 = 0$ & $G2 = 0$.

- Step 13) Jump to step 34.
- Step 14) If($Ra \geq Ya$)&&(Ya > Ba)&&(Ba < Ra); then to step 15. Else jump to step 19.
- Step 15) If($Ra > Rb$); then $G1 = 1$ & $G4 = 0$. Else $G1 = 0$ & $G4 = 1$.
- Step 16) If($Ya > Yb$); then $G3 = 0$ & $G6 = 1$. Else $G3 = 1$ & $G6 = 0$.
- Step 17) If($Ba < Bb$); then $G5 = 0$ & $G2 = 1$. Else $G5 = 0$ & $G2 = 0$.
- Step 18) Jump to step 34.
- Step 19) If($Ra < Ya$)&&(Ya > Ba)&&(Ba \leq Ra); then to step 20. Else jump to step 24.
- Step 20) If($Ra < Rb$); then $G1 = 0$ & $G4 = 1$. Else $G1 = 0$ & $G4 = 0$.
- Step 21) If($Ya > Yb$); then $G3 = 1$ & $G6 = 0$. Else $G3 = 0$ & $G6 = 0$.
- Step 22) If($Ba < Bb$); then $G5 = 0$ & $G2 = 1$. Else $G5 = 1$ & $G2 = 0$.
- Step 23) Jump to step 34.
- Step 24) If($Ra < Ya$)&&(Ya \geq Ba)&&(Ba > Ra); then to step 25. Else jump to step 29.
- Step 25) If($Ra < Rb$); then $G1 = 0$ & $G4 = 1$. Else $G1 = 0$ & $G4 = 0$.
- Step 26) If($Ya > Yb$); then $G3 = 1$ & $G6 = 0$. Else $G3 = 0$ & $G6 = 1$.
- Step 27) If($Ba > Bb$); then $G5 = 1$ & $G2 = 0$. Else $G5 = 0$ & $G2 = 0$.
- Step 28) Jump to step 34.
- Step 29) If($Ra \leq Ya$)&&(Ya < Ba)&&(Ba > Ra); then to step 30. Else jump to step 34.
- Step 30) If($Ra < Rb$); then $G1 = 0$ & $G4 = 1$. Else $G1 = 1$ & $G4 = 0$.
- Step 31) If($Ya < Yb$); then $G3 = 0$ & $G6 = 1$. Else $G3 = 0$ & $G6 = 0$.
- Step 32) If($Ba > Bb$); then $G5 = 1$ & $G2 = 0$. Else $G5 = 0$ & $G2 = 0$.
- Step 33) Jump to step 34.
- Step 34) Update the reference signal
- Step 35) Calculate $t = t + T_s$.
- Step 36) If ($t \geq T_m$) ; then reset 't'. Else go to 36.
- Step 37) Jump to 4.

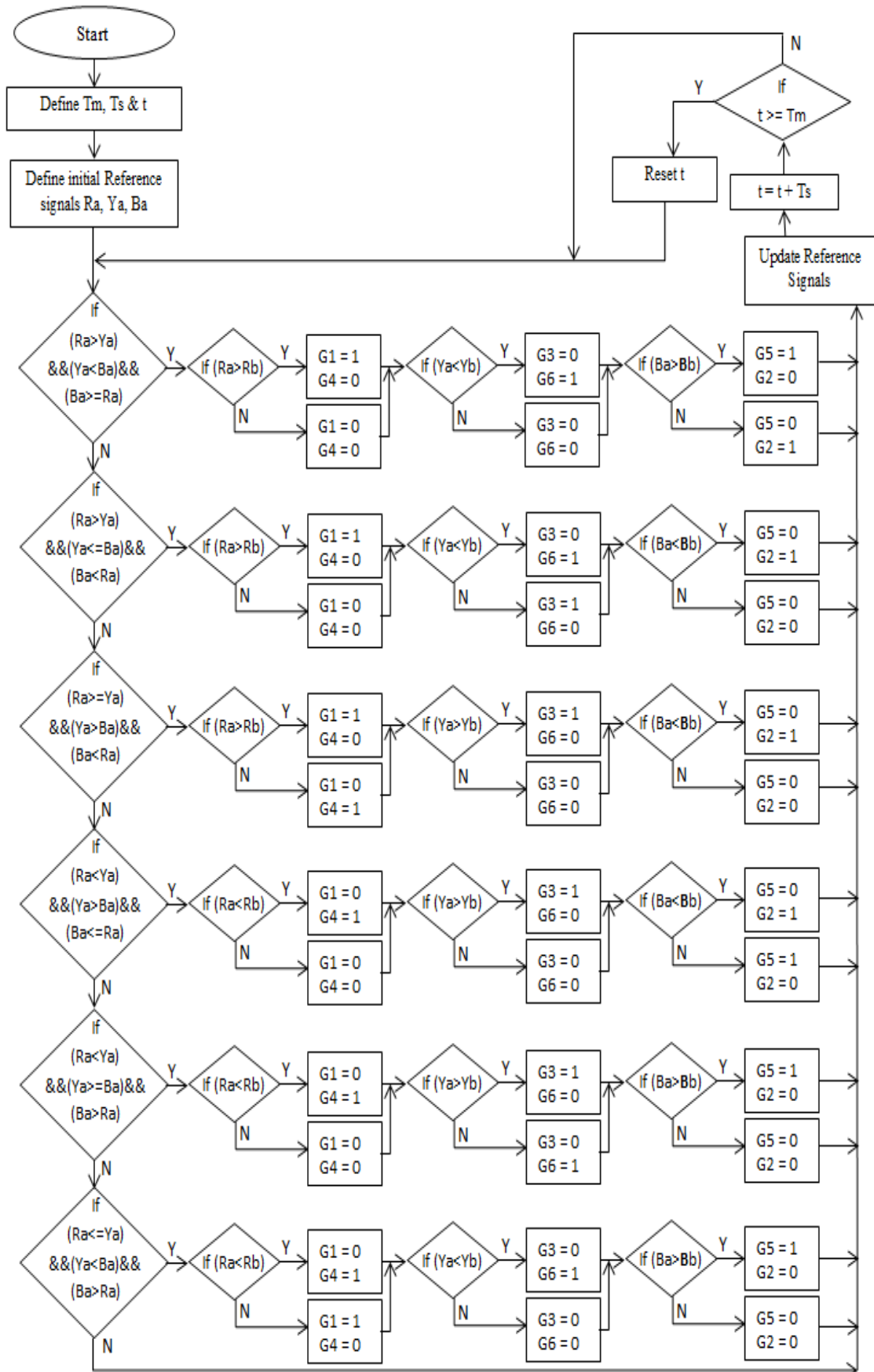


Figure 4.4 Flowchart for new switching scheme for three-phase voltage source inverter.

4.3 Simulation Results

Simulation and the testing have been performed on the three-phase voltage source inverter as shown in figure 4.1. Linear as well as nonlinear loading conditions have been used for testing of the designed scheme. The linear loading has been realized through R-L load while rectifier has been used for nonlinear loading condition. Along with designed switching scheme, PWM has also been tested and the results of both schemes have been compared for analytical study.

The simulation has been performed under the balanced loading condition for the output current of 50 Hz. The results and waveforms presented in the paper are recorded under the steady state condition. The various parameters and loading conditions are as follows:

- I. Source voltage (V_{dc}) = 700 V
- II. Source impedance (Z_{dc}) = 0.1 Ω
- III. Modulation index for PWM = 0.8
- IV. Modulation frequency for PWM = 1.2 KHz
- V. R–L load = 10+ j23.5619 Ω
- VI. Rectifier load
 - a) Resistance = 15 Ω
 - b) Capacitance = 100 μ f

4.3.1. Linear load

The Simulation and testing has been performed and observations have been made for all the three phases of the output. The above described loading condition has been used for simulation with both the scheme keeping all other operating conditions identical. The waveforms of voltage and current for all three phases are presented in figure 4.9 and 4.10 for PWM and modified switching scheme respectively. Since the model is operating under the balanced condition, so result and waveforms for R-phase only are used for comparative analysis. Waveforms of voltage and current for R-phase of three-phase voltage source inverter using PWM scheme and modified switching

scheme is shown in figure 4.5 and figure 4.6 respectively. Figure 4.7 and figure 4.8 presents THD in voltage and current respectively for PWM scheme as well as modified switching scheme. The result of simulation and testing of both schemes using linear load is in table 4.1.

We can observe that the new switching scheme has performed better than its counterpart PWM scheme under linear loading condition. The DC side voltage source is set as 700 V. The RMS value of output voltage for R-phase obtained from new scheme is 289.9 V, which is significantly, much more than 197.9 V, that obtained using PWM scheme. The peak voltage from PWM scheme is found to be 279.9 V which is much lesser than the 410 V from modified switching scheme. Also the value of RMS current 8.786 A, obtained from new switching scheme is more than 6.00 A RMS current value obtained from PWM scheme. Similarly, 12.42 A as peak value of current from modified scheme is respectively a large value than 8.49 A as peak value from PWM scheme.

The new scheme also presents a significant improvement in THD in voltage as well as in current. The THD in voltage obtained from PWM is 91.60% while same using new proposed switching scheme is 31.32%. Similarly, THD in output current obtained from PWM is 2.73% and same for new proposed switching scheme is 1.00%. We can observe from the waveform of THDs that the difference in the values of THD is mainly because of the difference in DC component present in output. The DC component is more when the inverter is operated with PWM scheme. In case of proposed scheme the DC components in voltage and current are 0.08102V and 0.02939 A respectively while in case of PWM the DC components in voltage and current are 7.388 V and 0.7458 A respectively.

The observation of RMS and peak values of current, voltage, the values of THDs and their waveforms shows the superiority of newly designed modified scheme over the PWM scheme under given operating conditions.

TABLE 4.1

SIMULATION RESULTS FOR LINEAR LOAD (THREE-PHASE)

Load Type	Parameters	PWM	Modified Switching
Linear Load	Vrms	197.9	289.9
	Irms	6.004	8.786
	Vpeak	279.9	410
	Ipeak	8.49	12.42
	V THD	91.60%	31.32%
	I THD	2.73%	1.00%
	DC component in Voltage	7.388	0.08102
	DC component in Current	0.7458	0.02939

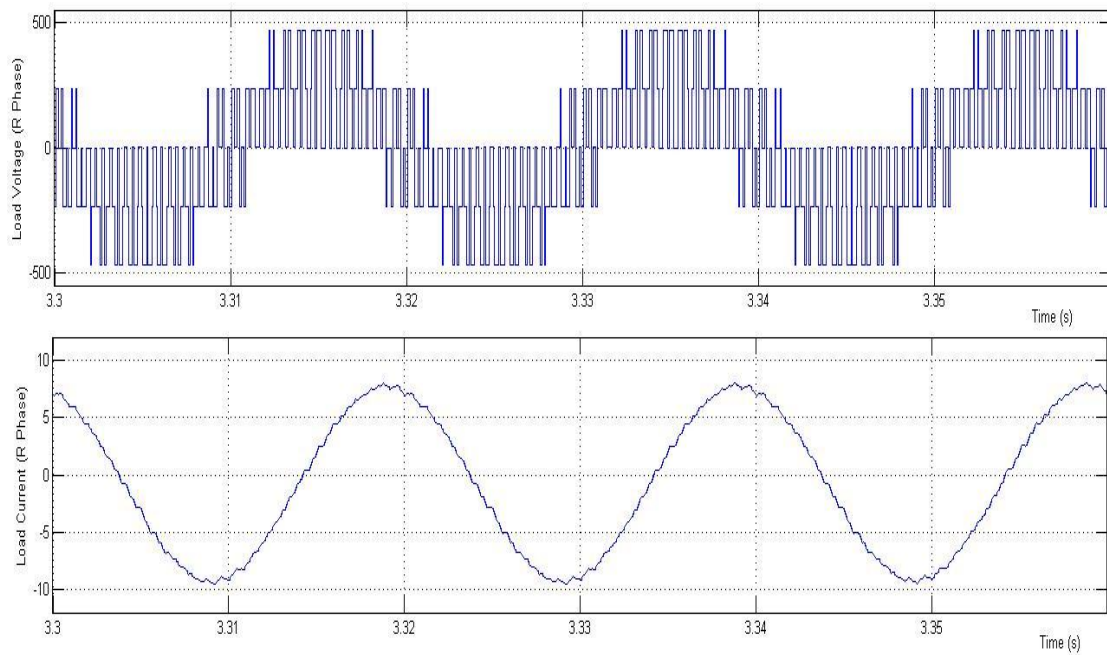


Figure 4.5 Three-phase VS DC–AC inverter output (load voltage and load current) waveform of R- Phase under linear loading using PWM scheme.

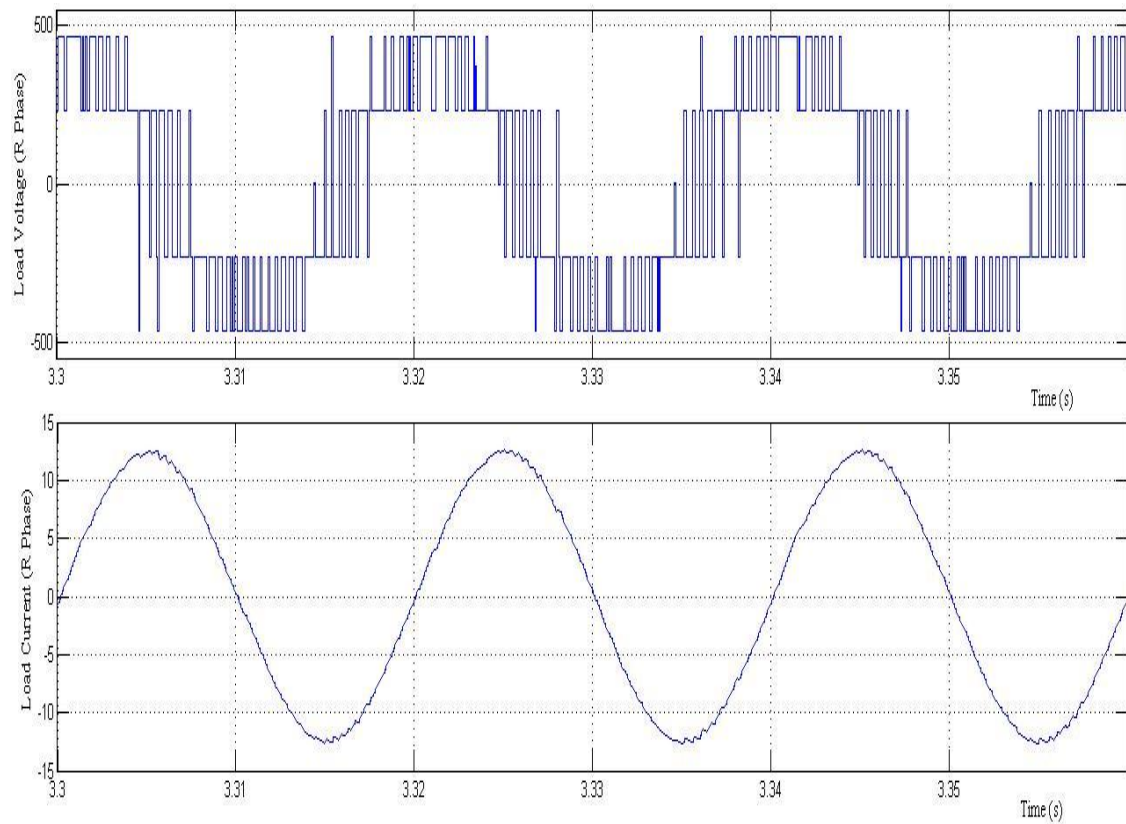
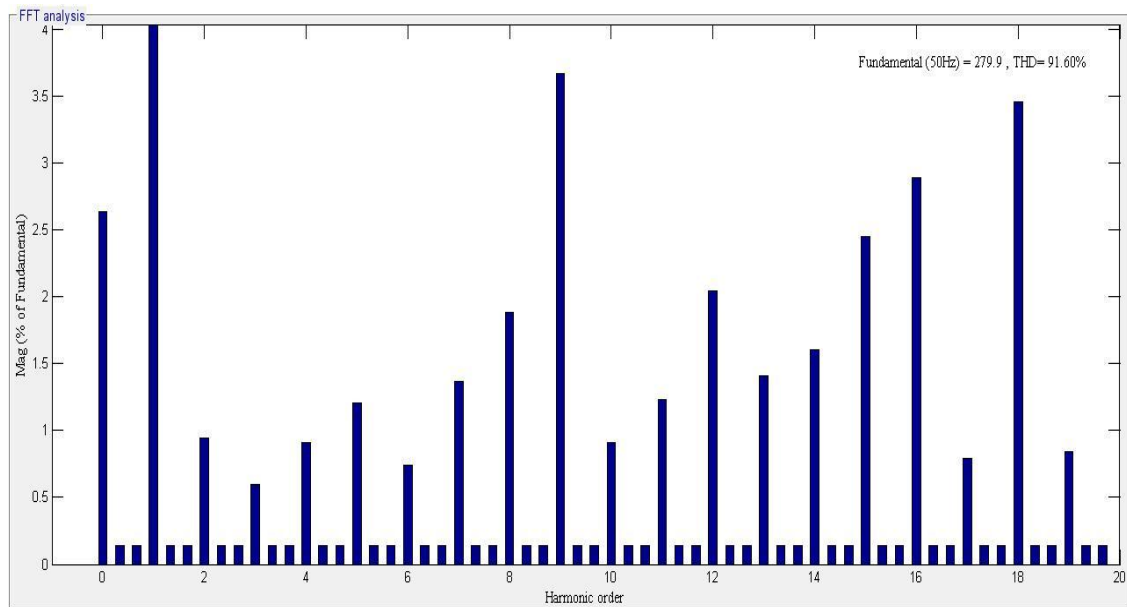
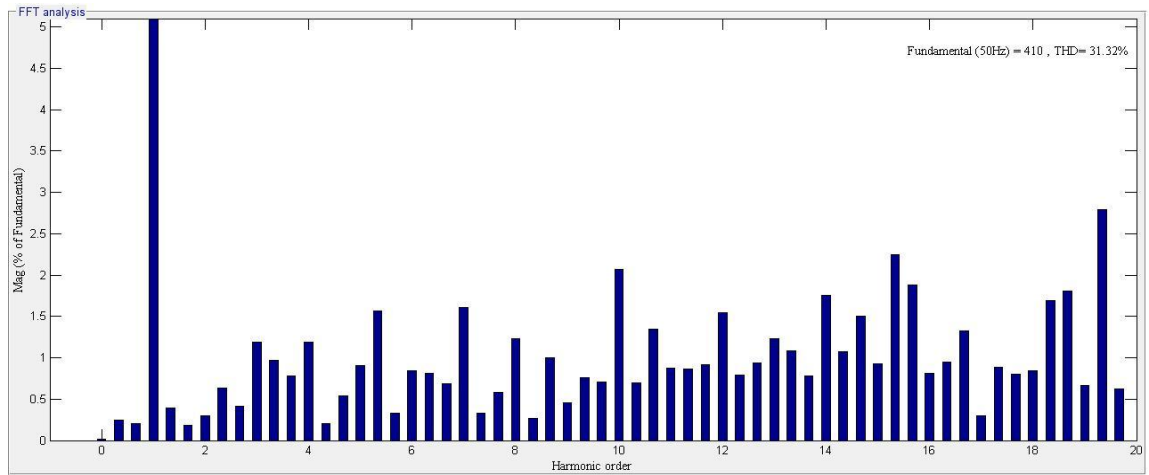


Figure 4.6 Three-phase VS DC–AC inverter output (load voltage and load current) waveforms under linear loading using modified switching scheme.

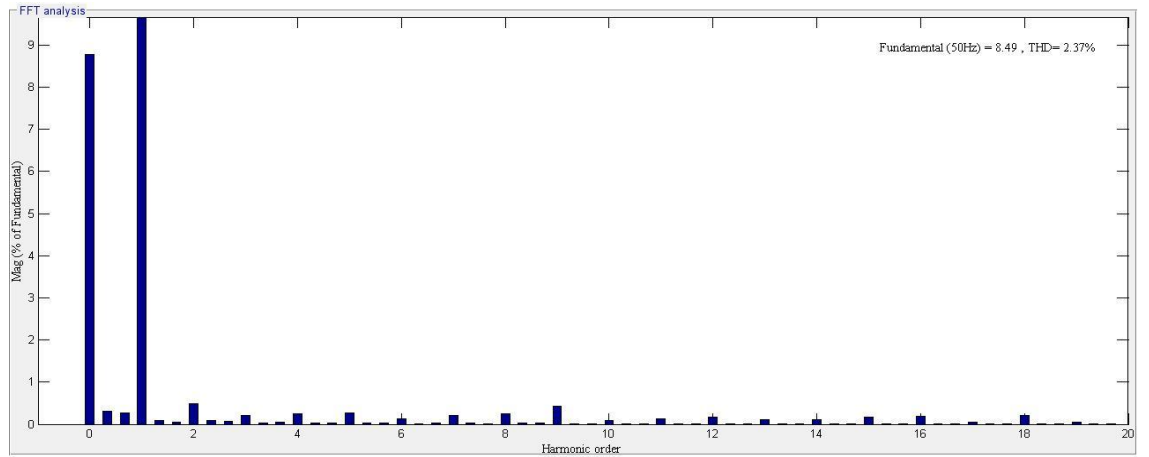


4.7 (a)

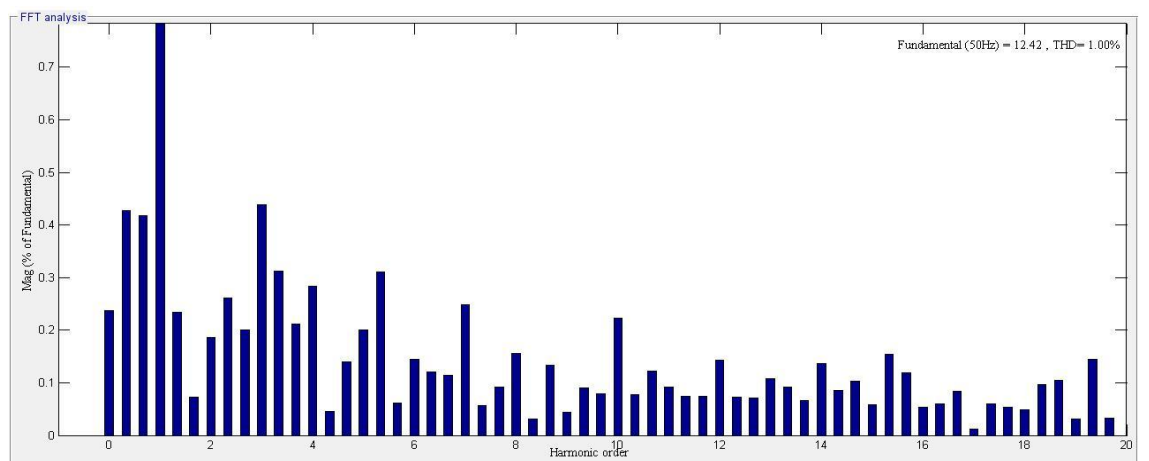


4.7 (b)

Figure 4.7 THD in load voltage waveforms of three-phase VS DC–AC inverter with linear load using (a) PWM (b) modified switching scheme.

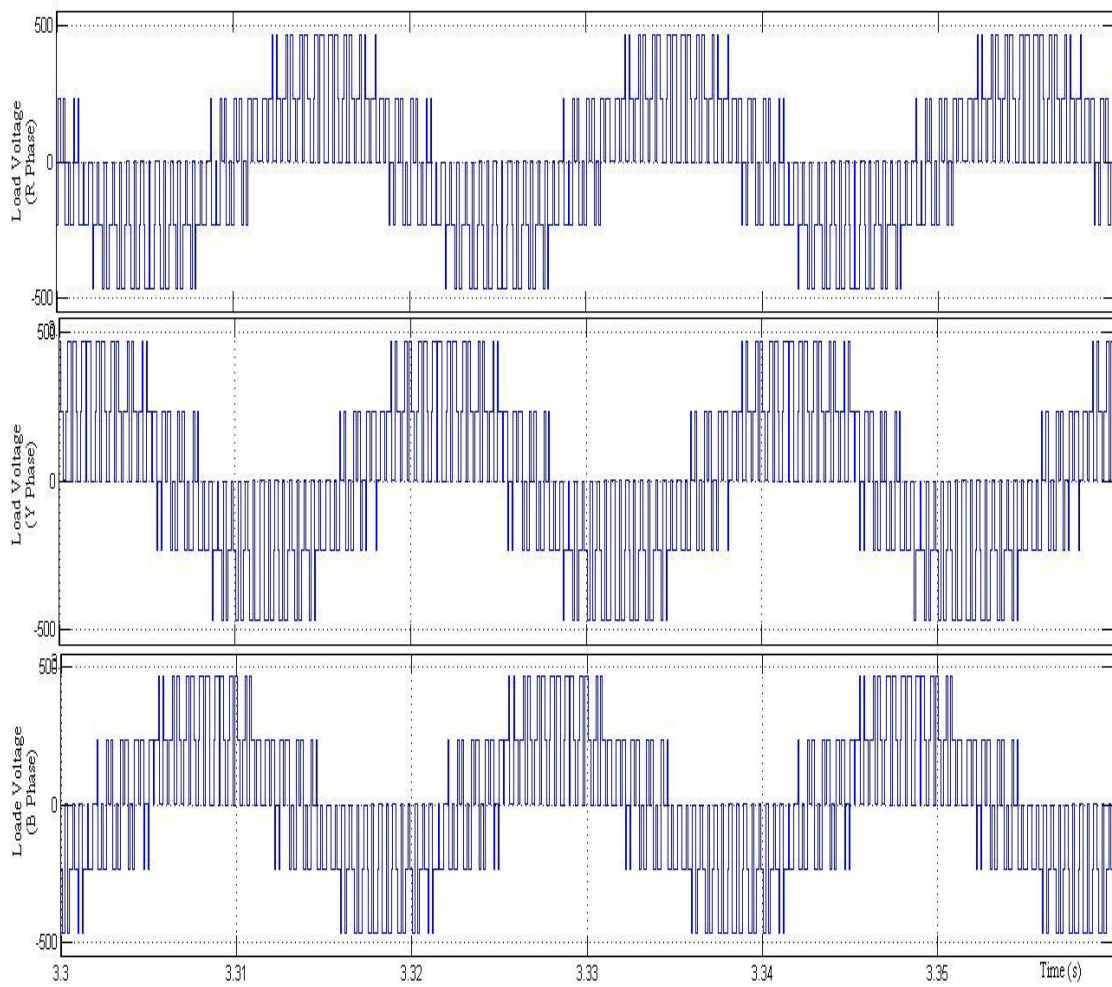


4.8 (a)

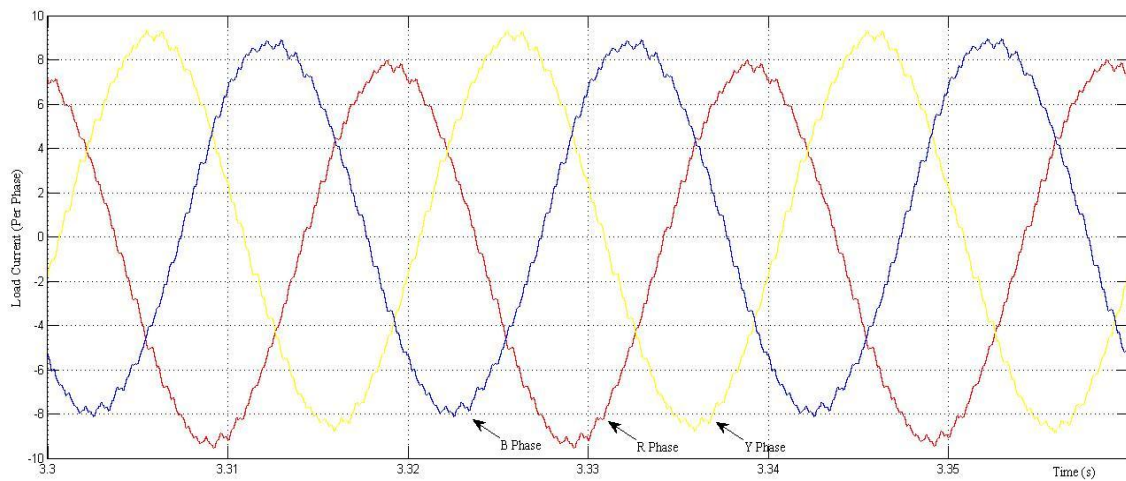


4.8 (b)

Figure 4.8 THD in load current waveforms of Three-phase VS DC–AC inverter with linear load using (a) PWM (b) modified switching scheme.

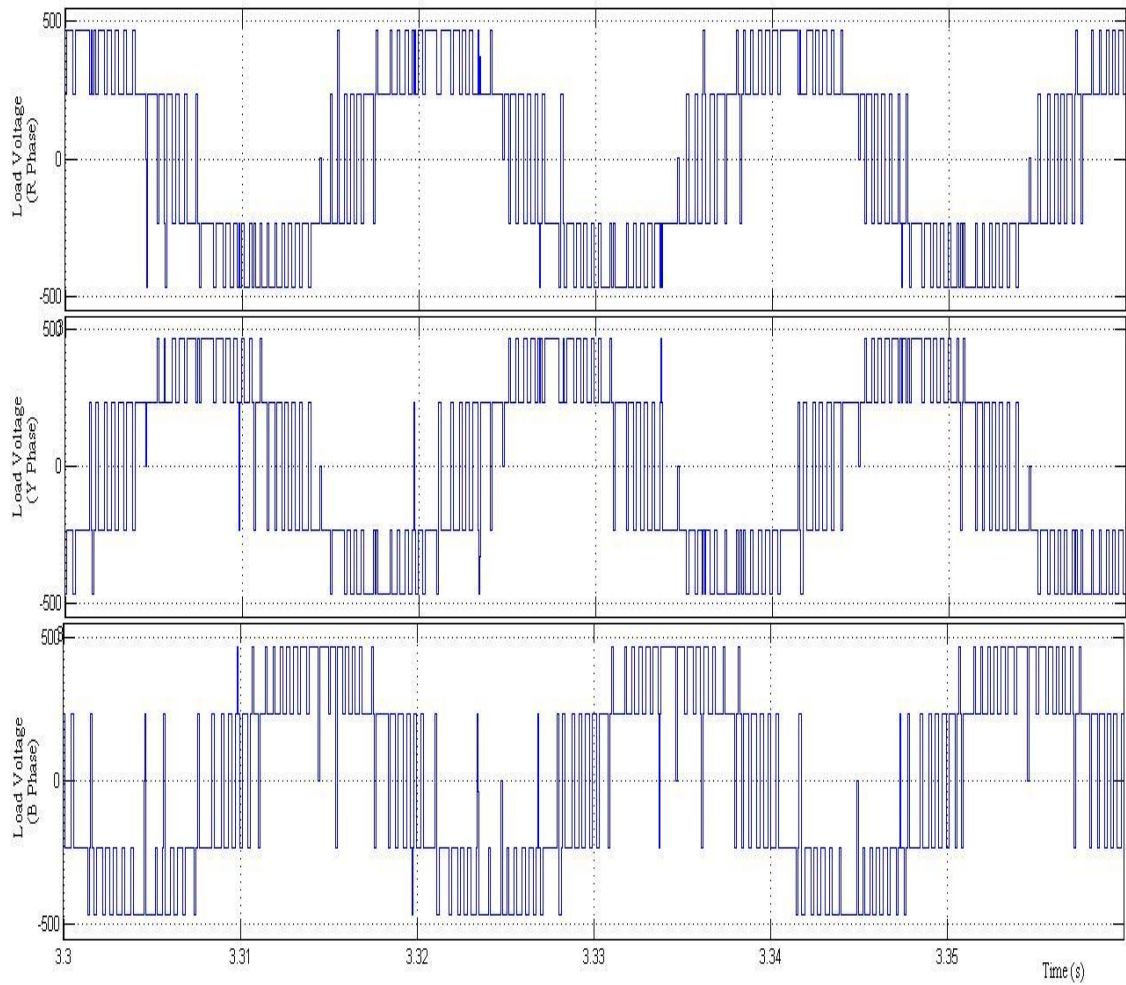


4.9 (a)

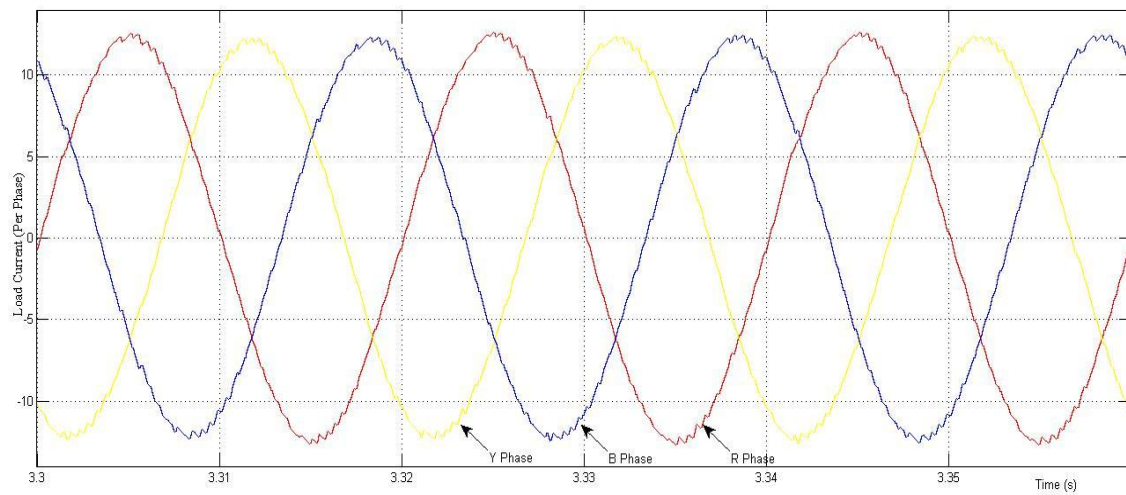


4.9 (b)

Figure 4.9 Three-phase VS DC-AC inverters output waveform under linear loading using PWM scheme. (a) load voltage R, Y and B-phase (b) load current R,Y and B phase.



4.10 (a)



4.10 (b)

Figure 4.10 Three-phase VS DC–AC inverter output waveforms under linear loading using modified switching scheme. (a) load voltage R, Y and B-phase (d) load current R,Y and B-phase.

4.3.2. Nonlinear load

Nonlinear loading conditions for simulation and testing has been realized using rectifier with pure resistive load with capacitor in parallel. Output waveforms of voltage and current for all the three-phase are shown in figure 4.15 and figure 4.16 for PWM and modified switching scheme respectively. Similar to the case of linear loading here also all the comparative analysis is performed over R- phase only. So, with this purpose the waveforms of voltage and current is presented in figure 4.11 for PWM scheme and same for modified scheme is in figure 4.12. THD in voltage and current waveforms are shown in figure 4.13 and figure 4.14. The result of all simulation results are shown in table 4.3. All these results are of output voltage and current at the output terminal of inverter considering the whole rectifier as load. The current and voltage across the resistive load is also presented in figure 4.17 and 4.18 for PWM and modified switching scheme.

Similar to linear load all the testing has been performed under the balanced three-phase condition. The DC voltage source for the testing and simulation is taken as 700 V. The rectifier load has been connected to the inverter through and inductive coil. The values have been monitored between the output port of inverter and inductive coil. The results presented in the paper are for R-phase only.

In this case also the RMS and peak as well as THD values of output voltage and current obtained from newly designed switching scheme show significant improvement over PWM scheme. RMS value of voltage is 212 V in new proposed scheme as compared to 196.7 V obtained from PWM scheme. Similar to RMS value the peak value of the voltage from modified scheme shows significant improvement over its counterpart. The peak value from modified scheme is 299.9 V in respect of same as 278.2 V from PWM scheme. The RMS value of current is 11.45 A for new proposed scheme which is significantly more than 11.12 A obtained from PWM scheme. 16.2 A as the peak value of current is shows an improvement over 15.73A from PWM scheme. THD in voltage waveform are 59.14% and 92.50% for new scheme and PWM scheme respectively. THDs in current waveform are 4.02% and 2.15% from PWM and modified scheme respectively. Similar to case of linear loading, we can observe from

the waveform of THDs that the difference in the values of THD is mainly because of the difference in DC component present in output. Here also the DC component is more when the inverter is operated with PWM scheme. The new switching strategy also shows significant improvement in terms of DC component in voltage and current. The DC component in voltage and current are 5.832V and 0.9474A for PWM scheme respectively. The same is 0.5593V and 0.0314 in voltage and current waveforms obtained from modified switching scheme.

Observation of the waveform of current through resistive load of rectifier shows the value of current is more when the inverter is operated with the newly designed modified switching scheme. Here again the observation of RMS and peak values of current, voltage, the values of THDs and their waveforms shows the superiority of newly designed modified scheme over the PWM scheme under given operating conditions, as like to previous cases.

TABLE 4.2

SIMULATION RESULTS FOR NON - LINEAR LOAD (THREE-PHASE)

Load Type	Parameters	PWM	Modified Switching
Non - linear Load	Vrms	196.7	212
	Irms	11.12	11.45
	Vpeak	278.2	299.9
	Ipeak	15.73	16.2
	V THD	92.50%	59.14%
	I THD	4.02%	2.15%
	DC component in Voltage	5.832	0.5593
	DC component in Current	0.9474	0.0314

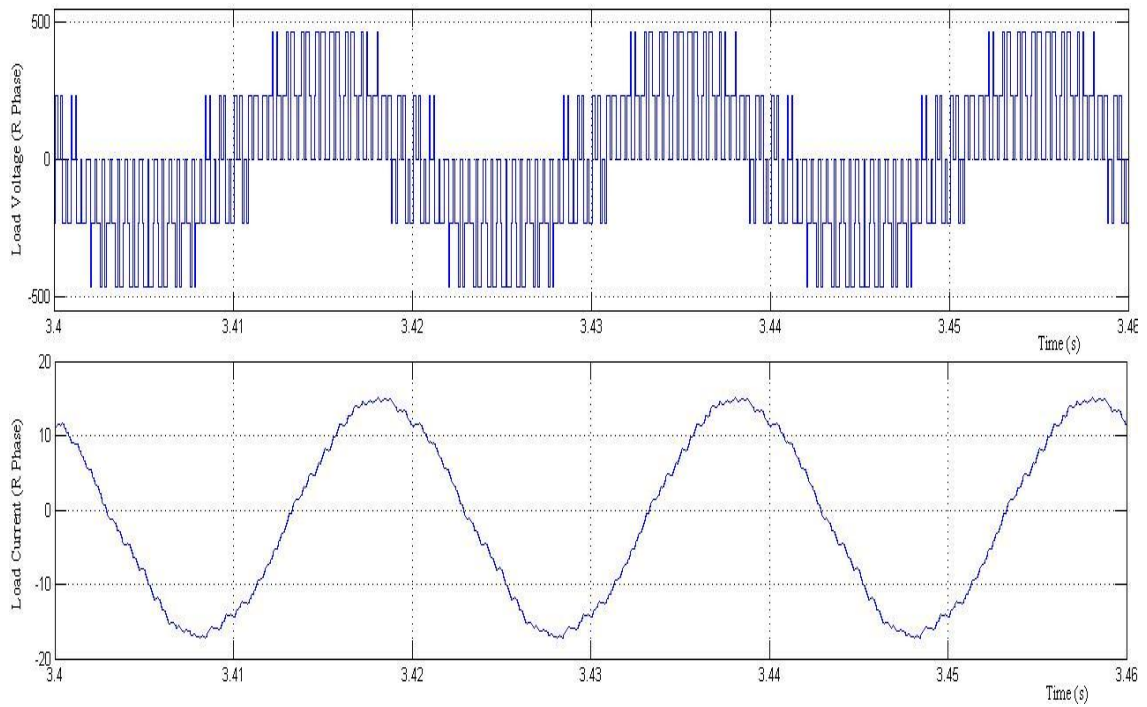


Figure 4.11 Three-phase VS DC-AC inverter output (load voltage and load current) waveform of R- Phase under non- linear loading using PWM scheme.

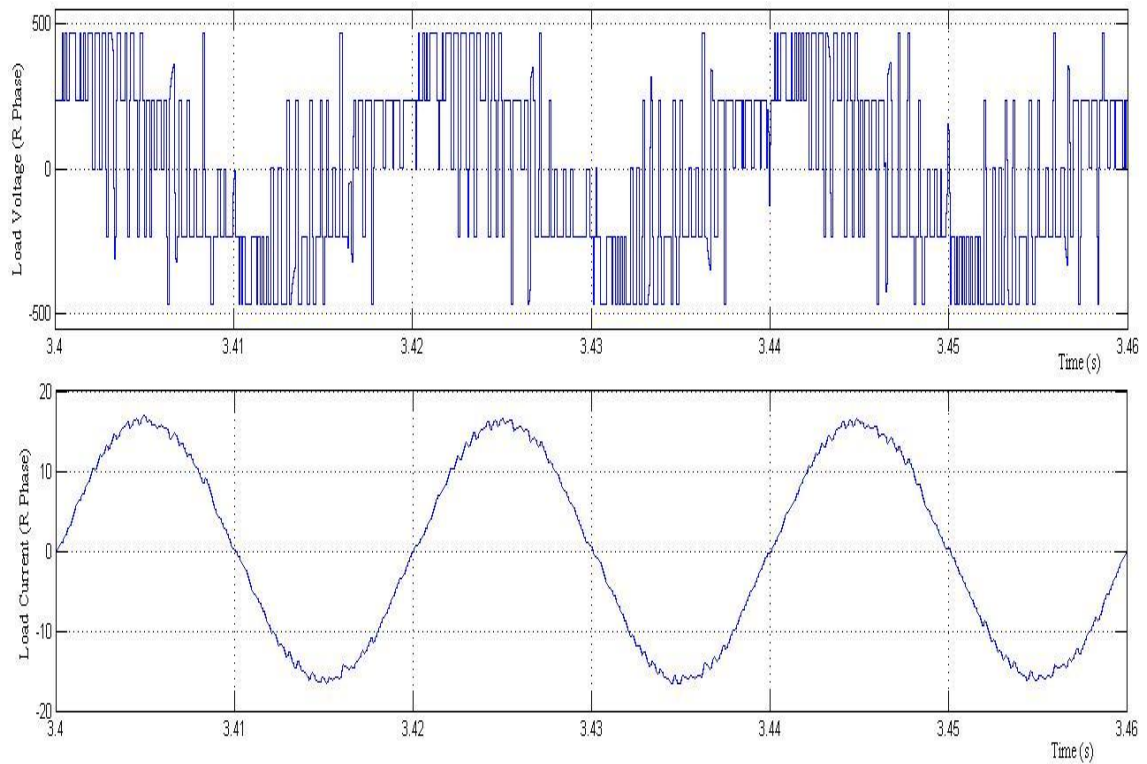
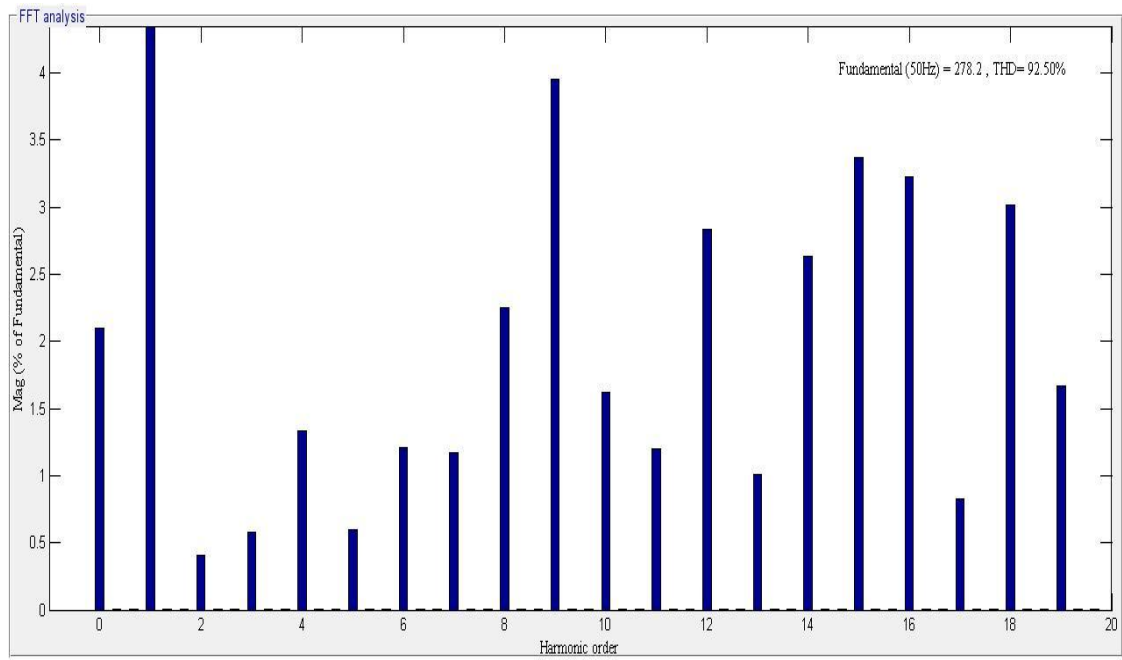
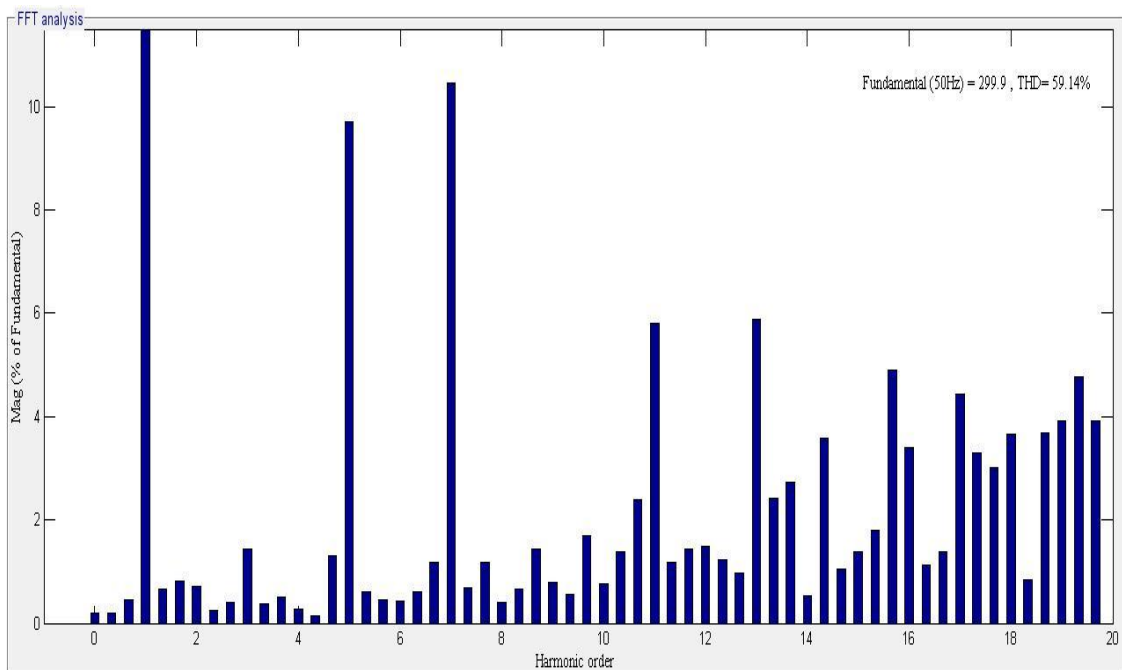


Figure 4.12 Three-phase VS DC-AC inverter output (load voltage and load current) waveform of R- Phase under non- linear loading using modified scheme.

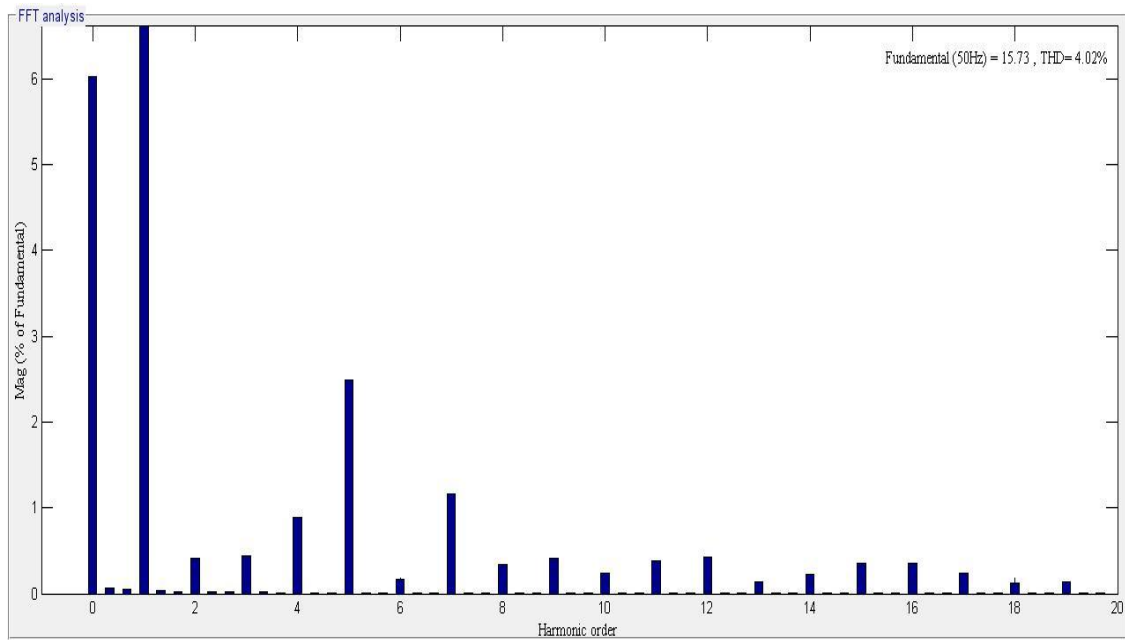


4.13 (a)

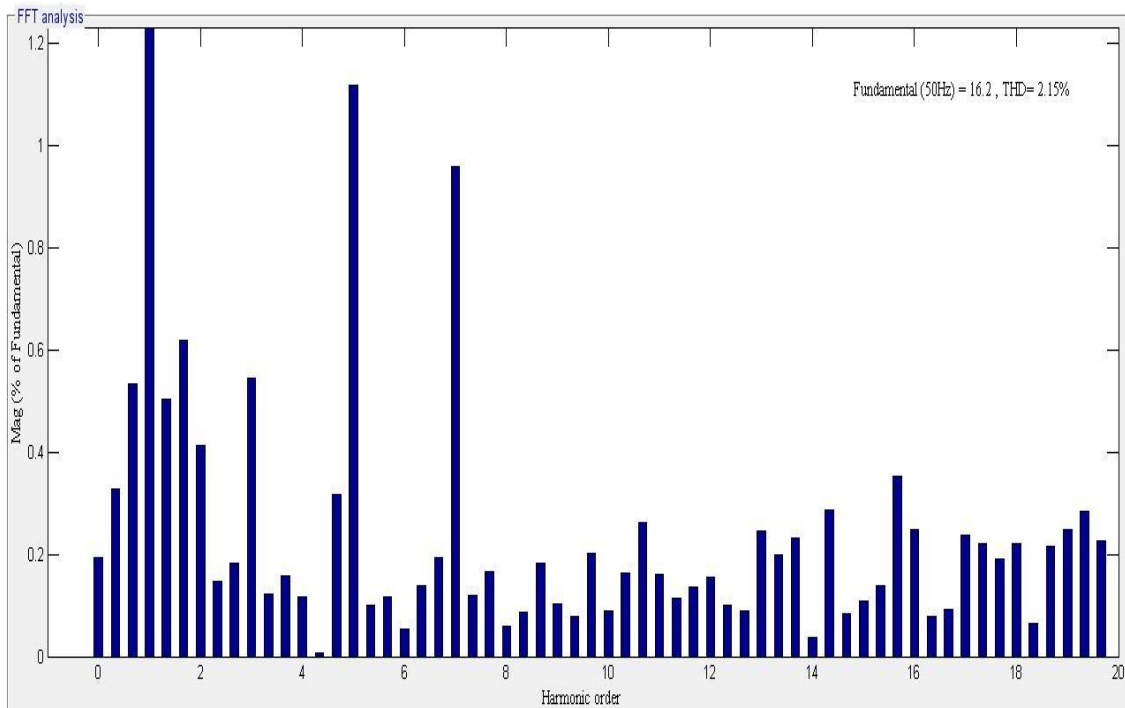


4.13 (b)

Figure 4.13 THD in load voltage waveforms of Three-phase VS DC-AC inverter with non-linear load (a) PWM (b) Modified switching scheme.

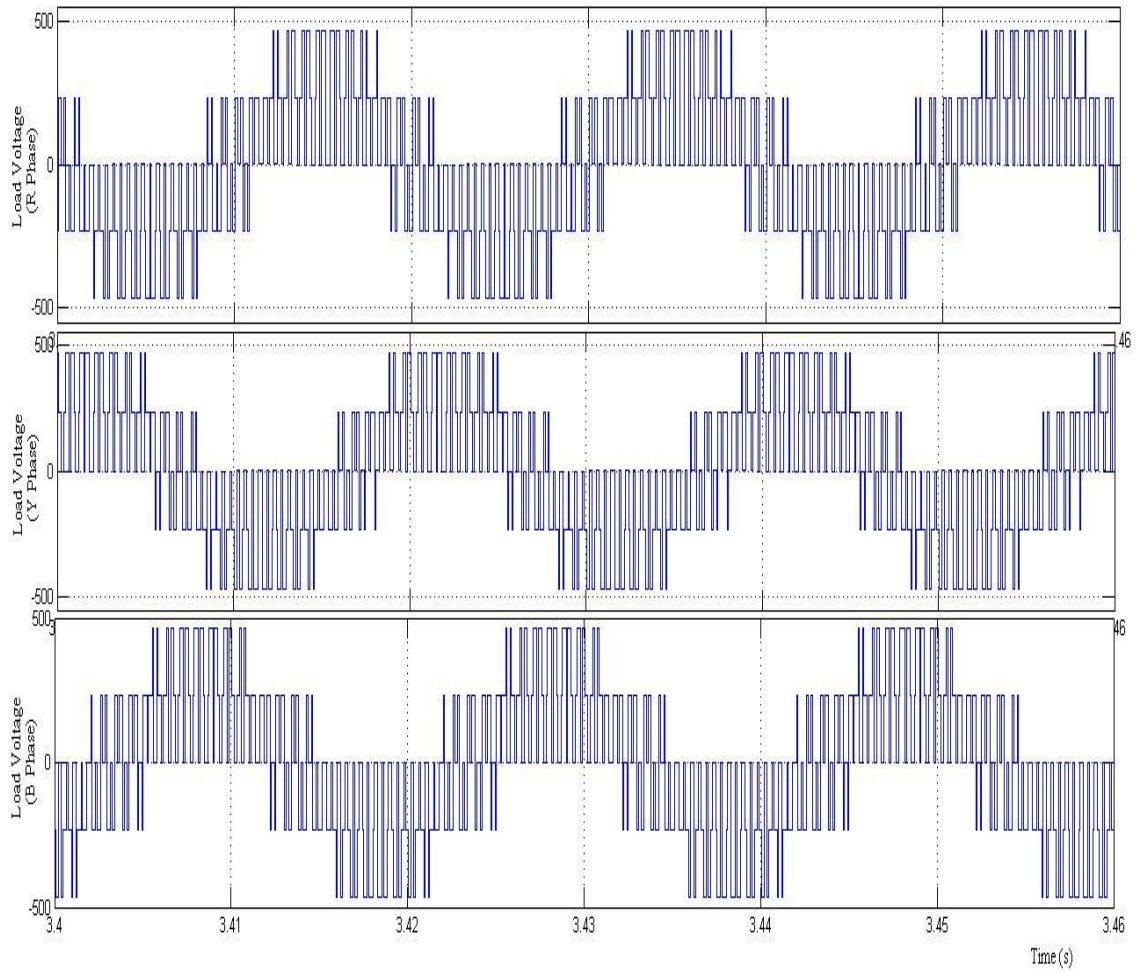


4.14 (a)

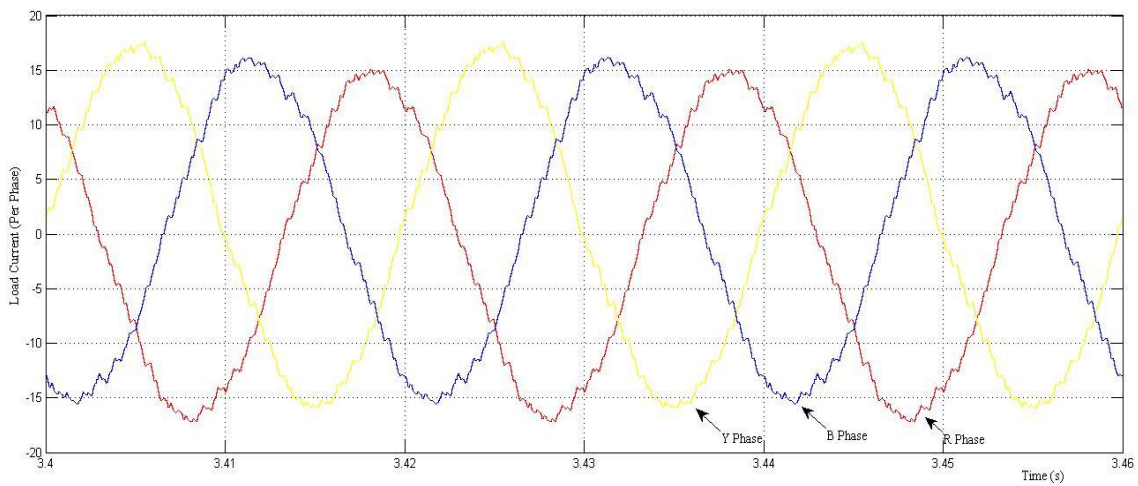


4.14 (b)

Figure 4.14 THD in load current waveforms of Three-phase VS DC–AC inverter with non- linear load (a) PWM (b) modified switching scheme.

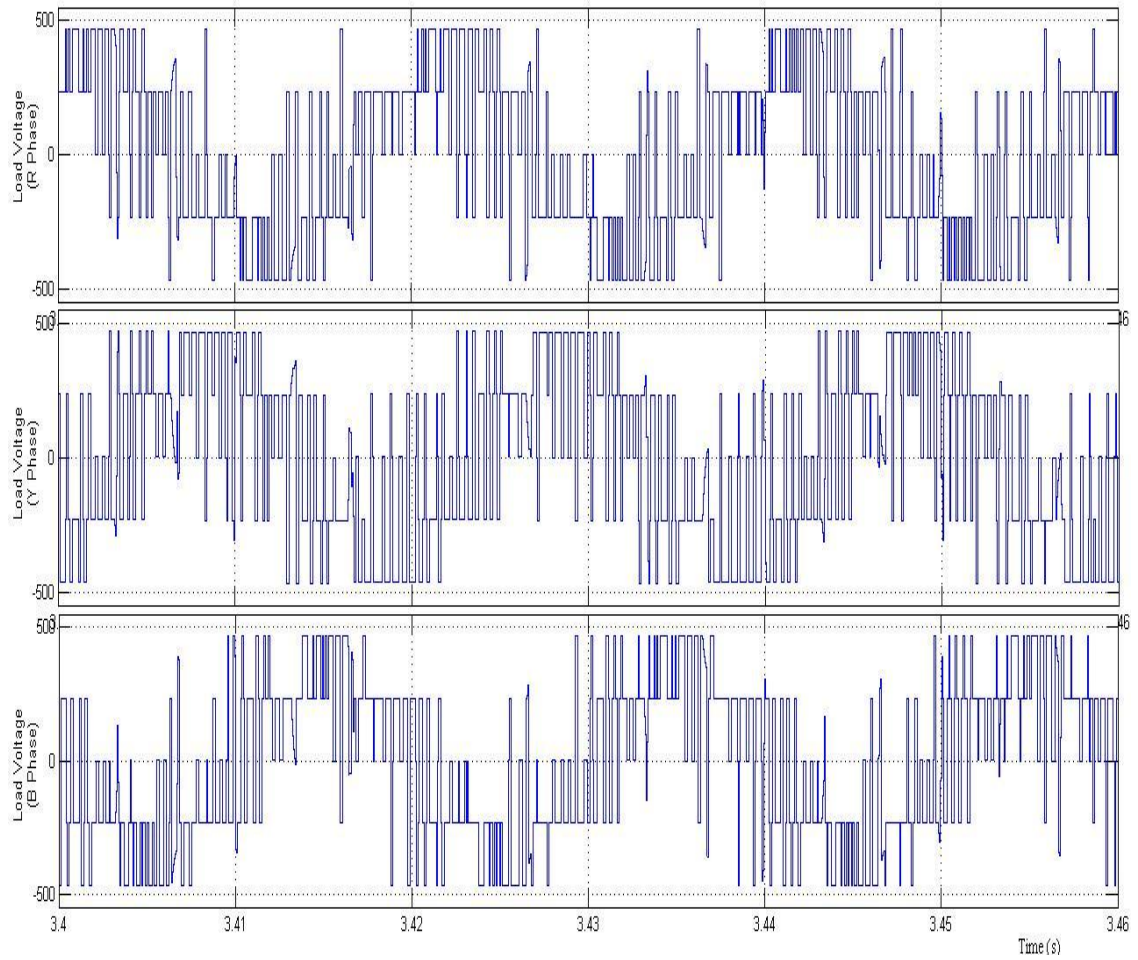


4.15 (a)

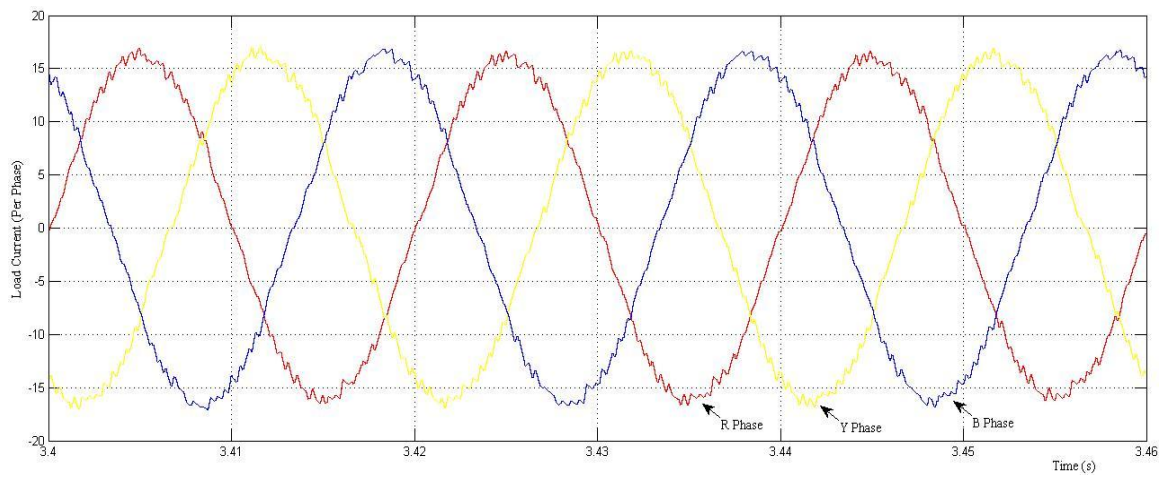


4.15 (b)

Figure 4.15 Three-phase VS DC–AC inverters output waveform under linear loading using PWM scheme. (a) Voltage of R, Y and B-phase (b) Current in R,Y and B-phase.



4.16 (a)



4.16 (b)

Figure 4.16 Three-phase VS DC-AC inverters output waveform under non-linear loading using modified scheme. (a) Voltage of R, Y and B-phase (b) current R,Y and B-phase.

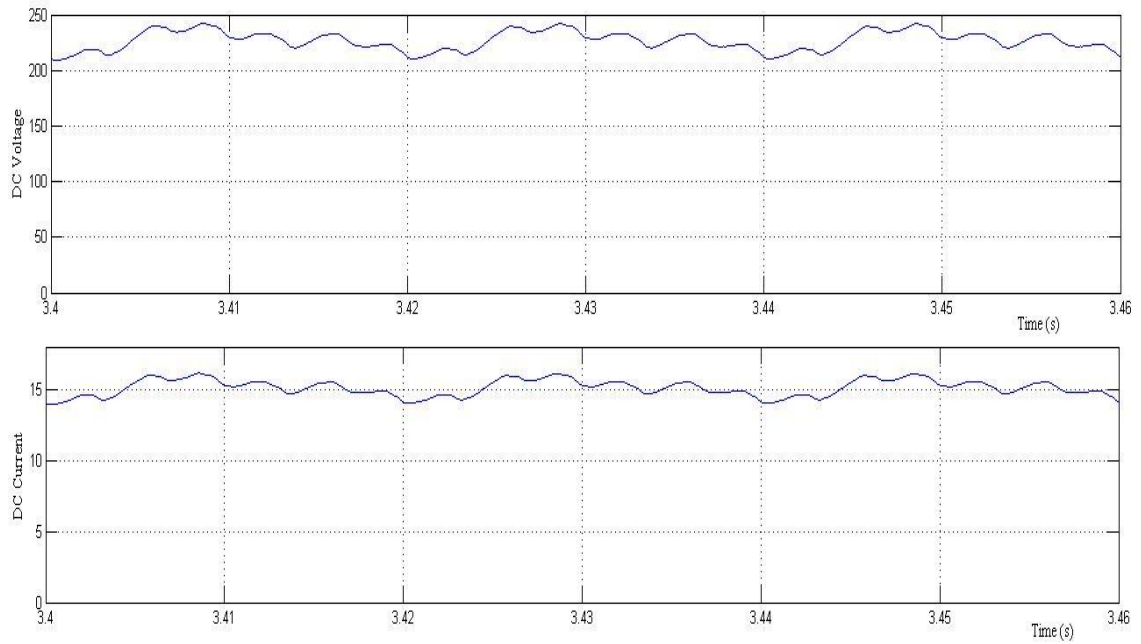


Figure 4.17 Load voltage and load current waveform for load resistance of rectifier when supplied from three-phase VS DC–AC inverter with PWM switching scheme.

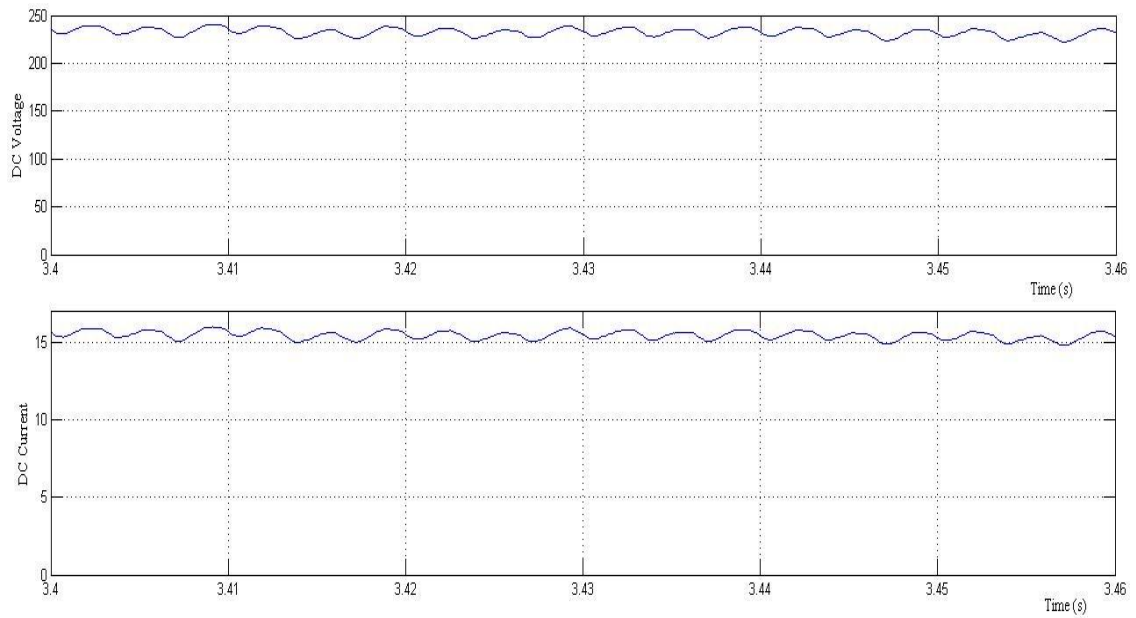


Figure 4.18 Load voltage and load current waveform for load resistance of rectifier when supplied from three-phase VS DC–AC inverter with modified switching scheme.

CHAPTER 5

WAVELET MODULATION FOR 1-PHASE INVERTER

CHAPTER 5

WAVELET MODULATION FOR 1-PHASE INVERTER

5.1 Modulation Overview

The wavelet modulation for DC-AC single-phase inverter is a process of sampling and reconstruction of signal. The various elements of modulation are discussed below.

5.1.1. Reference Signal

The output of DC-AC single-phase inverter is sinusoidal wave. In wavelet modulation, the focus is on generating samples of a sinusoidal reference signal and reconstructing the sinusoidal output from these samples. The reference signal (S_M) of frequency f_M can be written as:

$$S_M = \sin(2\pi f_M t) \quad (5.1)$$

$$f_M = \frac{1}{T_M} \quad (5.2)$$

Samples are generated from this reference signal over a time-period of T_M . Each two samples corresponds to one group of samples (i.e. each group of sample of have two samples) denoted by 's'. Thus 's' is the total number of group of samples over time-period T.

5.1.2. Output Waveform

The output current waveform of DC-AC single-phase voltage source inverter is desired to be sinusoidal wave. It has been observed in case of PWM, as shown in figure 5.1, that the rectangular output voltage pulses of inverter gives the sinusoidal current waveform and the quality of the output current waveform depends upon the width of rectangular output voltage pulses as well as their number. These output pulses are function of gate pulses resulting from the switching logic, which could be PWM, RPWM, SHE, square pulse or the one used in this paper i. e. wavelet modulation.

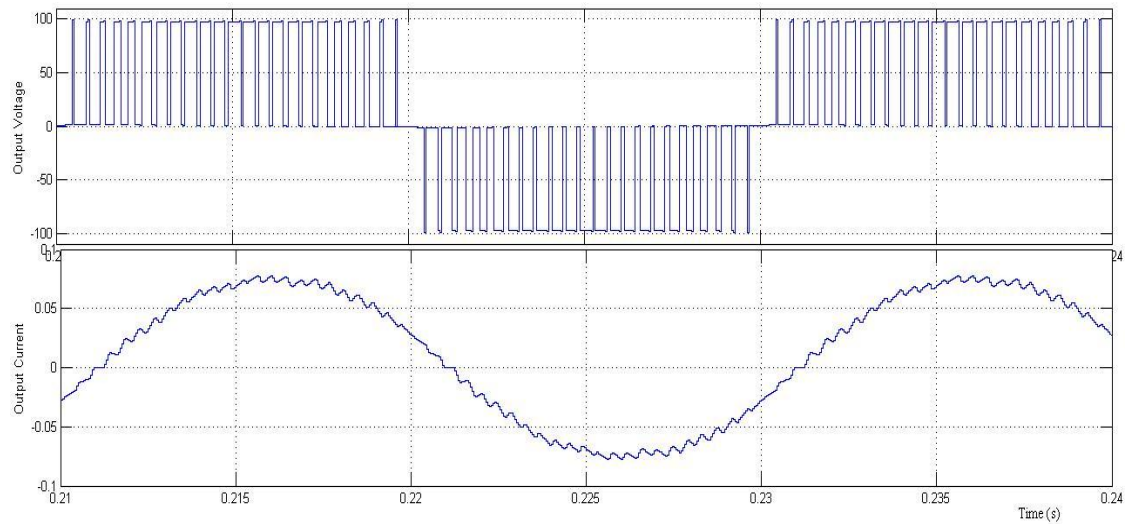


Figure 5.1 An example to view the relation of output voltage and current (in PWM method).

5.1.3. Sampling and Reconstruction

Sampling and Reconstruction is the link between the reference signal and the output waveform. As the nature of output waveform can be controlled by varying the width of rectangular pulses and so the sampling and reconstruction also needed to be non-uniform in nature. Thus only a non-uniform sampling can lead to sinusoidal output. The gate pulses of inverter are basically ON-OFF signal and the ON signal can be modeled from Haar scaling function. Duration and location of the pulses can be controlled by suitable scaling function.

5.1.1. Sampling

For single-phase DC – AC inverter the desired output should be as close as possible to the sinusoidal reference signal $S_M(t)$ frequency f_M which is defined as in (5.1) and (5.2)

This constraint on the output can be viewed as if each switching action is one stage in reconstructing the reference signal from its non-uniform samples. The groups of non-uniform recurrent samples formed over one cycle of the reference signal can be viewed as a set D as follows:-

$$D = \{d_0, d_1, d_2, \dots, d_{D-1}\} \quad (5.3)$$

Since, dyadic MRA can support only uniform sampling, we need to design a MRA that can support the non-uniform sampling theorem for switching the dc – ac inverter [28].

It is to be noted that, for the case of dc – ac inverter, the sampled signals are sinusoidal ones (with a period of T_m seconds) that have a quarter – cycle symmetry property. This property causes ' j ' to increase over the intervals $[0, (T_M/4)]$ and $[(T_M/2), (3T_M/4)]$ and to decrease over intervals $[(T_M/4), (T_M/2)]$ and $[(3T_M/4), T_M]$. As a result, the non-uniform recurrent sample groups will follow the scale j , as it changes over each cycle of $S_M(t)$.

5.1.2. Reconstruction

For reconstruction of the sinusoidal signal we need to define interpolation function as:

$$\lambda_{1j} = \frac{t \left[1 - \left(\frac{t}{2^{-j-1}} \right) \right] \left[1 - \left(\frac{t}{1-2^{-j-1}} \right) \right]}{\left[1 - \left(\frac{1}{2^{j+1}+1} \right) \right] [t - rT - td1]} \quad (5.4)$$

$$\lambda_{2j} = \frac{t \left[1 - \left(\frac{t}{2^{-j}-1} \right) \right] \left[1 - \left(\frac{t}{1-2^{-j}-1} \right) \right]}{[2-2^{j+1}][t-rT-td_2]} \quad (5.5)$$

Where td_1 and td_2 are defined as:

$$td_1 = d + 2^{-(j+1)} \quad (5.6)$$

$$td_2 = d + 1 - 2^{-(j+1)} \quad (5.7)$$

Where $d = 0, 1, 2, \dots, D-1$

The interpolation function λ_{1j} and λ_{2j} have their intervals of support such that $td_1 \leq t \leq td_2$, where the subscript d indicates that the interpolation is over the sample group of d of $X_c(t)$. These interpolation functions are used to activate the switching element of an inverter. It is to be noted that the properties of switching element used in inverter force their output to be rectangular pulses. The reconstruction of the reference-modulating signal $S_M(t)$ from its non-uniform recurrent samples is carried out by using dilated and shifted version of the synthesis scaling function. Each dilated and shifted version of synthesis scaling function has an interval of support that given by $[td_1 \ td_2]$.

5.1.4. Flowchart

Using the above concept and a detailed analysis, a flow chart of the complete process can be drawn as presented in figure 5.15. Using this flowchart, one can define the steps and strategy to get a modulated output from a single-phase inverter as we are doing in this project. Similar to single-phase the wavelet modulation can be implemented to three-phase inverters also [29]-[30]. The designing of switching scheme for voltage source inverter has performed on MATLAB using the S-function block of SIMULINK. The concept of programming and MATLAB are given in [31].

5.2 Wavelet Modulation

A wavelet modulation (wavelet transformation) starts with defining wavelet function ψ (mother wavelet) and scaling function ϕ (father wavelet) and using these functions a new scaling function can be derived as per requirement. The inverter gate pulses are basically ON-OFF pulses, so Haar's wavelet and scaling function can be used for deriving a scaling function which can be used further for switching of inverter.

The Haar wavelet function is defined as in (5.8).

$$\psi(t) = \begin{cases} 1, & 0 \leq t \leq \frac{1}{2} \\ -1, & \frac{1}{2} \leq t \leq 1 \\ 0, & \text{otherwise} \end{cases} \quad (5.8)$$

The Haar wavelet function can be represent as in figure 5.2

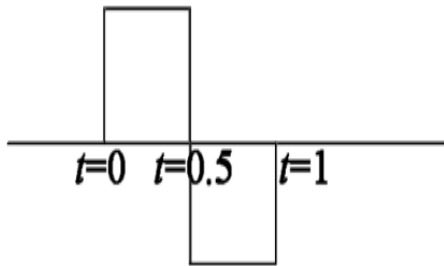


Figure 5.2 Haar wavelet function.

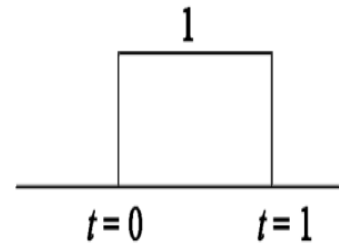


Figure 5.3 Haar scaling function.

Haar Scaling function is defined as in (5.9).

$$\phi(t) = \begin{cases} 1, & 0 \leq t \leq 1 \\ 0, & \text{otherwise} \end{cases} \quad (5.9)$$

Haar Scaling function can be represent as in figure 5.3.

Further the wavelet modulation involves multi-resolution analysis (MRA) which is analysis of the space $L^2(\mathbb{R})$ consist of a sequence of nested subspaces as in (5.10).

$$V_0 \subset V_1 \subset V_2 \subset V_3 \subset V_4 \dots \dots \dots \subset L^2(\mathbb{R}) \quad (5.10)$$

As discussed above using the Haar scaling function a new scaling function has been derived as in (5.11)

$$\phi_k(t) = \phi(a^{k+1}t) + \phi(a^{k+1}(t - 1 + a^{-(k+1)})) \quad (5.11)$$

Where $k = 1, 2, 3, \dots$ and the value of 'a' should be chosen according to the frequency of output signal.

The dual scaling function can be obtained by subtracting it from Haar scaling function. The other factors are ts1 and ts2 which can be defined as in (5.12) and (5.13).

$$T_{s1} = d * T_p + 2^{-j-1} \quad (5.12)$$

$$T_{s1} = d * T_p + T_p + 2^{-j-1} \quad (5.13)$$

where $s = 1, 2, 3, 4, \dots, S$

At time ts1, ON pulse start and at ts2, it stops. S is the number of samples in one cycle (i.e. time period T_m). T_p is the time of one sample and mathematically can be define as $T_p = 1/S$;

5.3 Modeling and Simulation

Simulation has been performed using SIMULINK facility of MATLAB R2011b, on the 1-ph 4-pulse H-bridge voltage source DC-AC inverter. The SIMULINK model of the circuit is shown in figure 5.4. The wavelet modulation has been implemented using S-function block of SIMULINK. Programming of S-function is done using C language. The inverter is based on four switch topology using the IGBT as the switches and controlled by gate signals.

The all four IGBT switches operate according to the gate pulses provided to them. When IGBT.1 and IGBT.2 both are conducting then they generates positive cycle of voltage and current across the load and similarly negative cycle of voltage and current gets generated by operating IGBT.3 and IGBT.4. Thus repeated operation of both the group one after another provides an alternating voltage and current across the load. The gate signal circuit block of figure 5.4 has the S-function Block inside, this S-Function block is link between the programmed file and the simulation model of inverter. The programmed file contains the logics required for generating GATE pulses according to the concept of wavelet modulation. This programmed file is initially written in C Language and then converted in MATLAB executable file using the command “mex filename”.

5.4 Results and Discussion

To analyze the wavelet modulation techniques designed above, simulation has been performed for various kinds of linear loads. Resistive load (R load) and resistive–inductive load (R–L load) are used for simulation and testing of new wavelet modulation technique. The simulation has also been performed for PWM and Square pulse techniques under same loading condition. Results of all the three techniques have been used for comparative analysis of performance. All the operating conditions are kept identical to all the schemes during the simulation process. The simulation tests are performed for current output of 50Hz. The loading conditions and other parameter used for simulation are as follows-

- I. Source voltage (V_s) = 50 V
- II. Source impedance (Z_s) = 0.1 Ω
- III. R Load = 25 Ω
- IV. R – L load = 15 + j12.566 Ω
- V. Modulation index for PWM = 0.8
- VI. Modulation frequency for PWM = 1.2 KHz

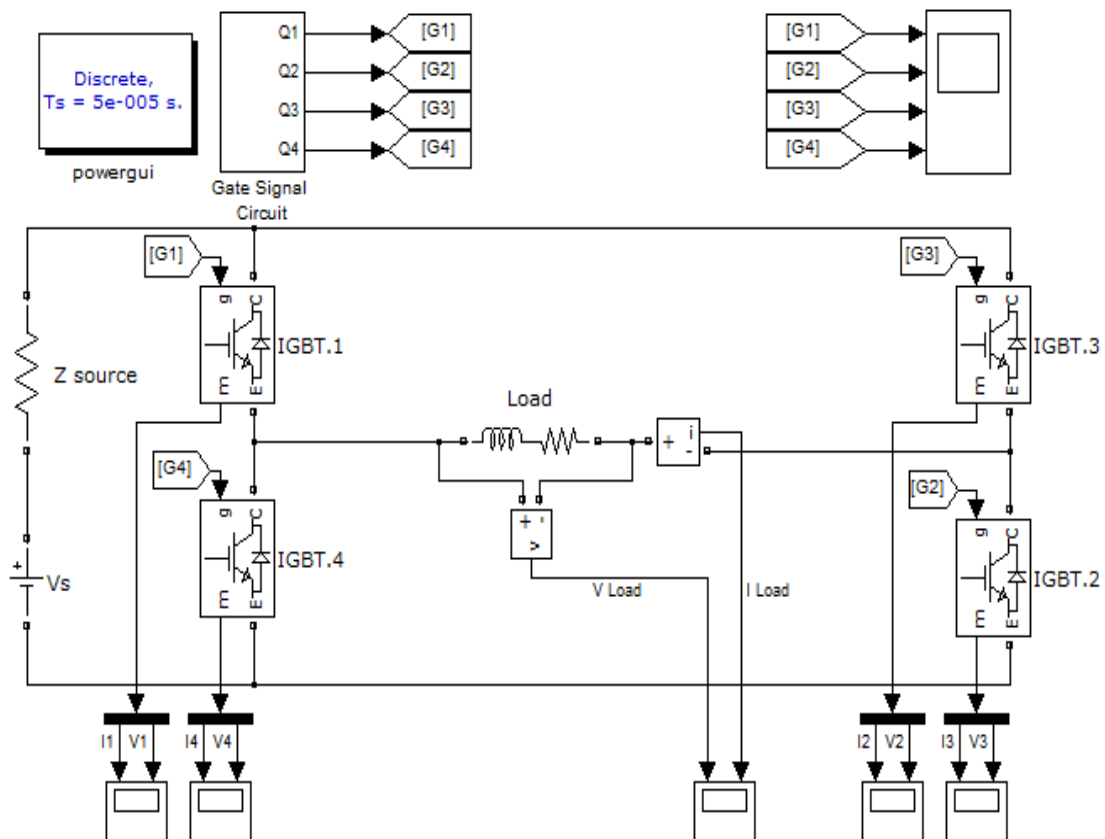


Figure 5.4 MATLAB model of single-phase H-bridge voltage source DC – AC inverter using IGBTs.

5.4.1. R – L Load

Simulation test is performed using resistive – inductive load of given value on the SIMULINK model of single-phase H-bridge voltage source DC-AC inverter shown in figure 5.4, using wavelet modulation by taking 12 groups of samples in each cycle. Similarly, simulation has been performed for PWM and square pulse methods.

The plots of the results obtained from simulation of single-phase H-bridge VS DC–AC inverter under R-L loading with PWM switching scheme is presented in figure 5.5, same with square pulse switching is shown in figure 5.6 and the figure 5.7 is simulation results for wavelet switching scheme under same condition. The THD (total harmonic distortion) in voltage waveform and current waveform are shown in figure 5.8 and 5.9 respectively for all the three switching schemes. A comparative result of performances of all the three methods is also presented in table 5.1.

The RMS value of voltage with PWM scheme is 30.11 V, and with square pulse switching is 44.83 V while with wavelet modulation scheme is 42.29 V. Similarly peak voltage with PWM scheme is 42.58 V, with square pulse scheme is 63.41 V and with wavelet modulation is 59.81 V. Also in terms of THD in voltage waveforms PWM schemes results with 70.47% THD, square pulse provides 48.50% THD and wavelet modulation results in 47.14% THD. Thus, we can observe that in terms of RMS and peak value of voltage wavelet modulation give much better results than that obtained from PWM scheme. Observation of THD in voltage shows that wavelet modulation provided results with significant improvement in level of THD with respect to PWM and square pulse scheme. With PWM scheme the RMS value of current is 1.539 A and same with square pulse and wavelet modulation scheme is 2.291 A and 2.161 A respectively. The peak value of current is 2.176 A, 3.24 A and 3.057 A respectively for PWM, square pulse and wavelet modulation schemes. In terms of THD in current PWM scheme provides results with 4.76% and square pulse and wavelet modulation schemes results in 17.73% and 16.93% THD respectively. Thus, we can observe the RMS and peak value of current obtained from wavelet scheme shows improvement over result obtained from PWM scheme similar to the case of voltage waveform. Current waveform obtained from wavelet schemes results in lesser THD than the same from square pulse scheme.

In the case of PWM, THD in load current is less than the same in the wavelet modulation in present case. However it is significant point to observe that the voltage THD and output voltage for wavelet modulation is better than PWM.

TABLE 5.1

SIMULATION RESULT FOR R-L LOAD (SINGLE-PHASE)

Load Type	Parameters	PWM	WM	Square Pulse
R – L load	Vrms	30.11	42.29	44.83
	Irms	1.539	2.161	2.291
	Vpeak	42.58	59.81	63.41
	Ipeak	2.176	3.057	3.24
	V THD	70.47%	47.14%	48.51%
	I THD	4.76%	16.93%	17.73%

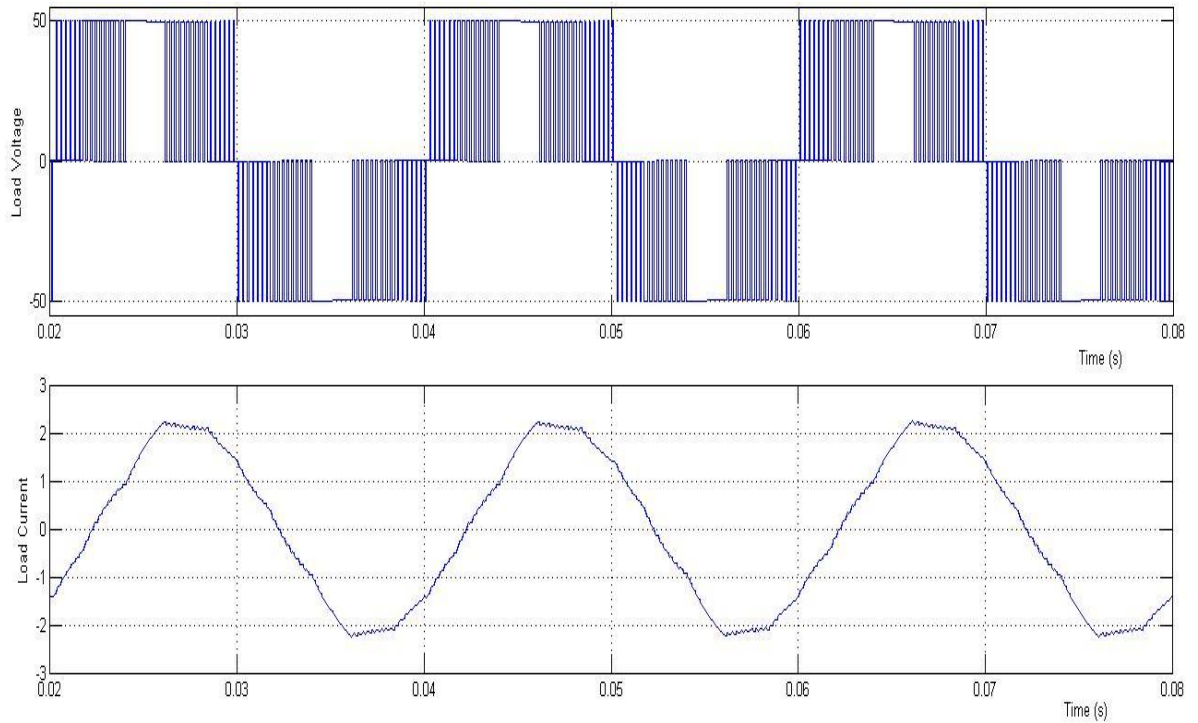


Figure 5.5 Single-phase H-bridge VS DC–AC inverter test result (load voltage and load current waveform) for R-L load using PWM switching scheme.

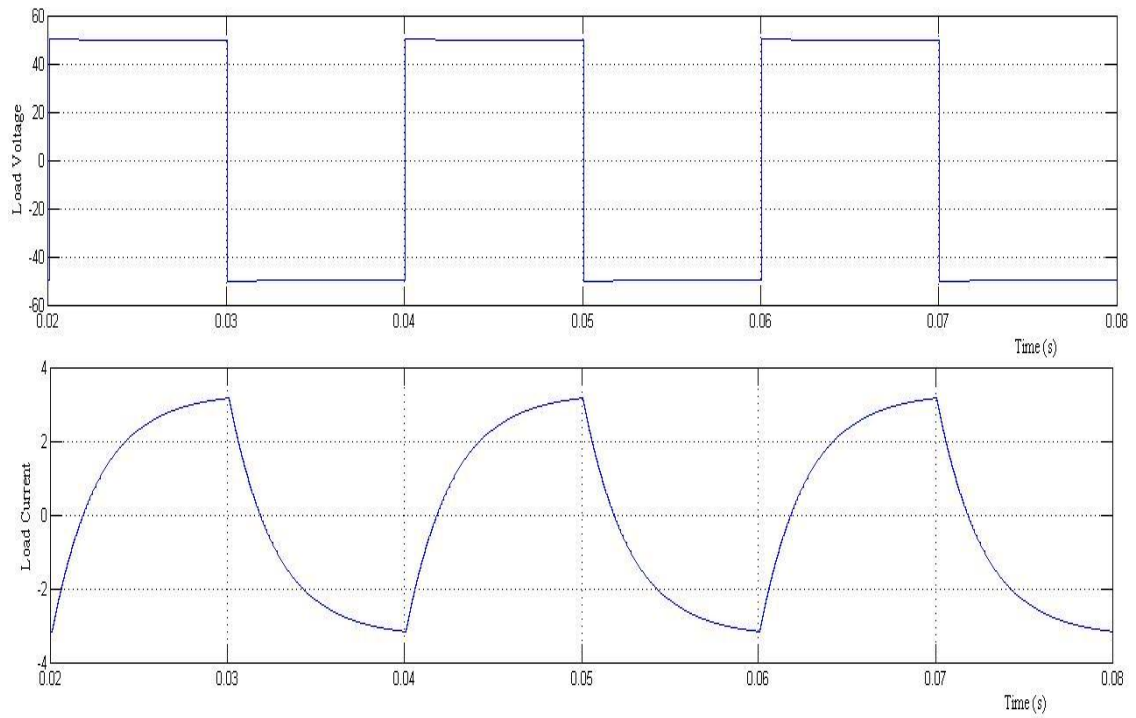


Figure 5.6 Single-phase H-bridge VS DC-AC inverter test result (load voltage and load current waveform) for R-L load using square pulse switching scheme.

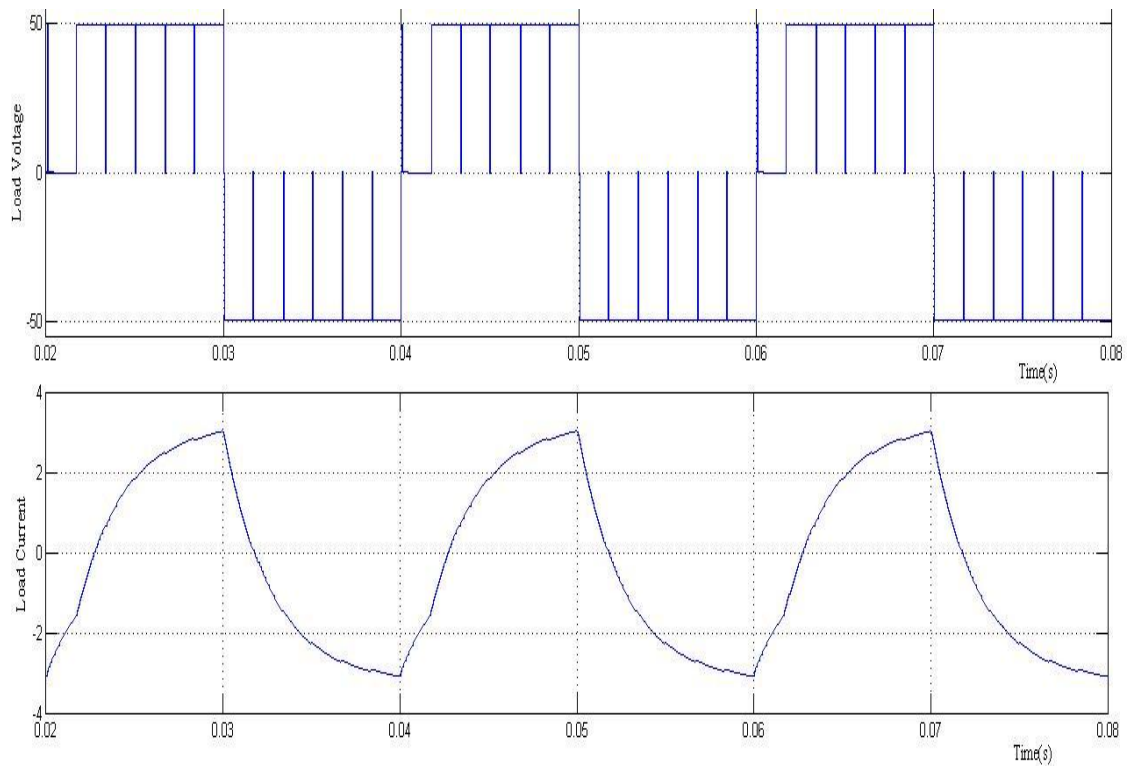
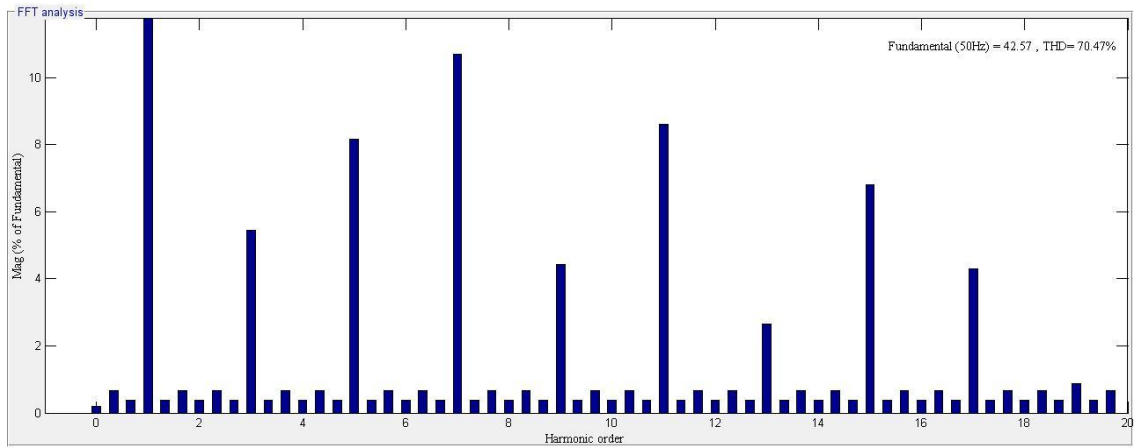
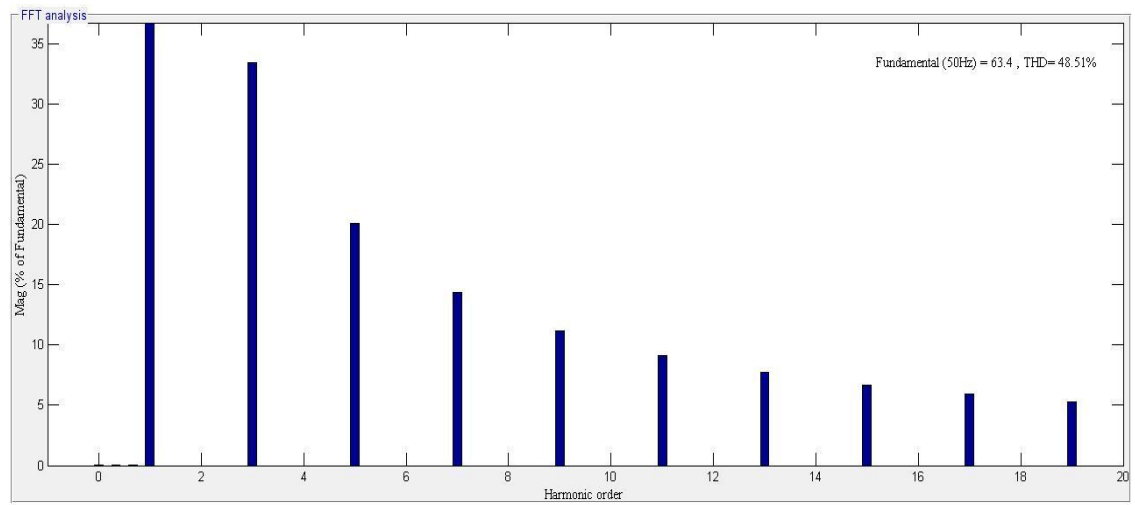


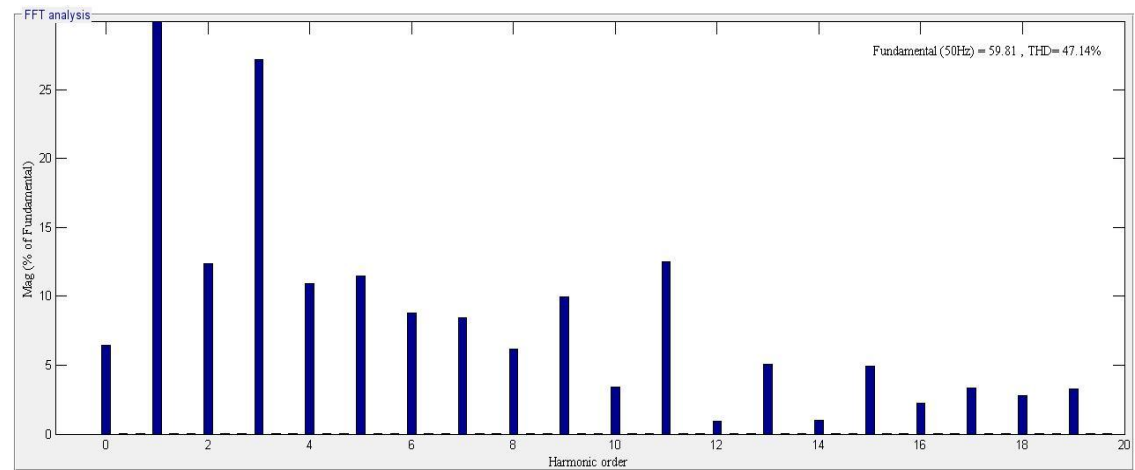
Figure 5.7 Single-phase H-bridge VS DC-AC inverter test result (load voltage and load current waveform) for R-L load using wavelet switching scheme.



5.8 (a)

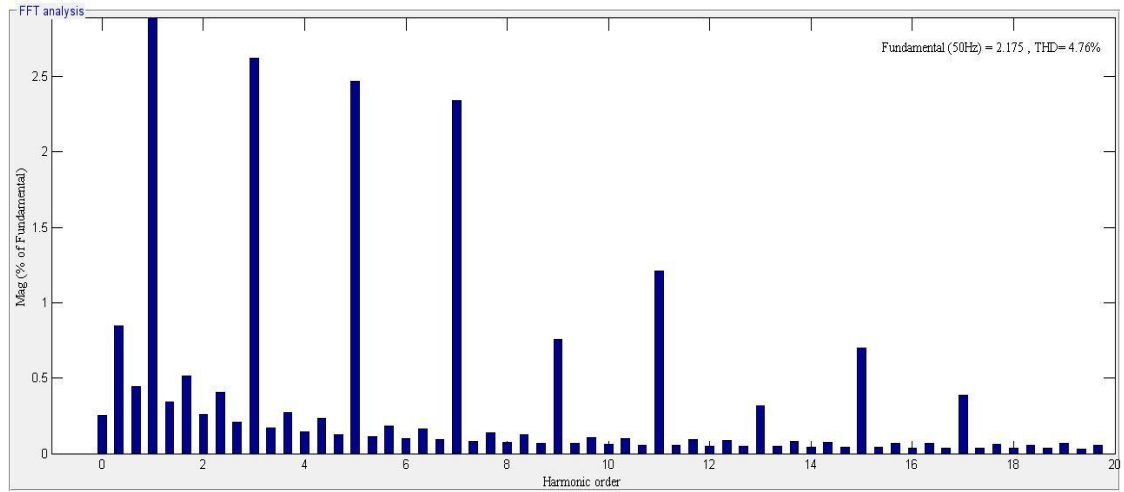


5.8 (b)

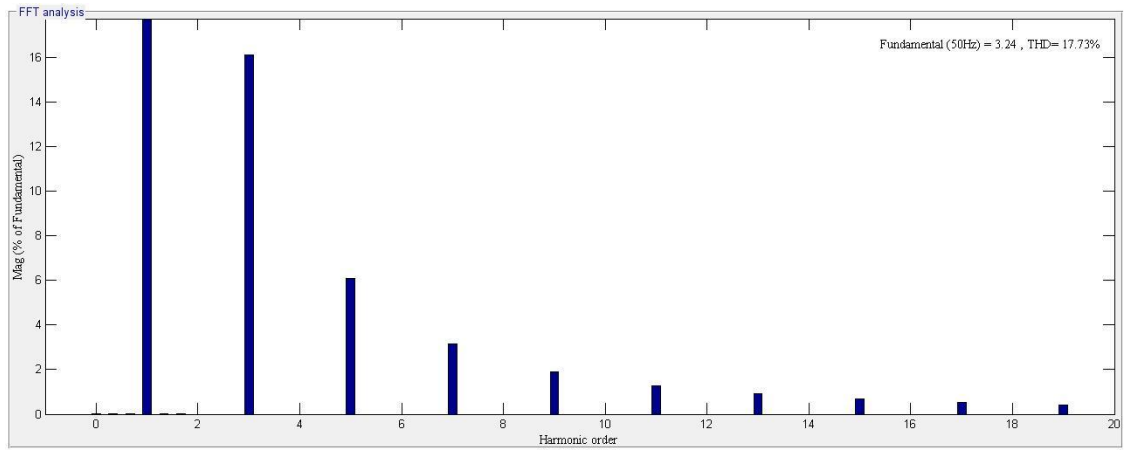


5.8 (c)

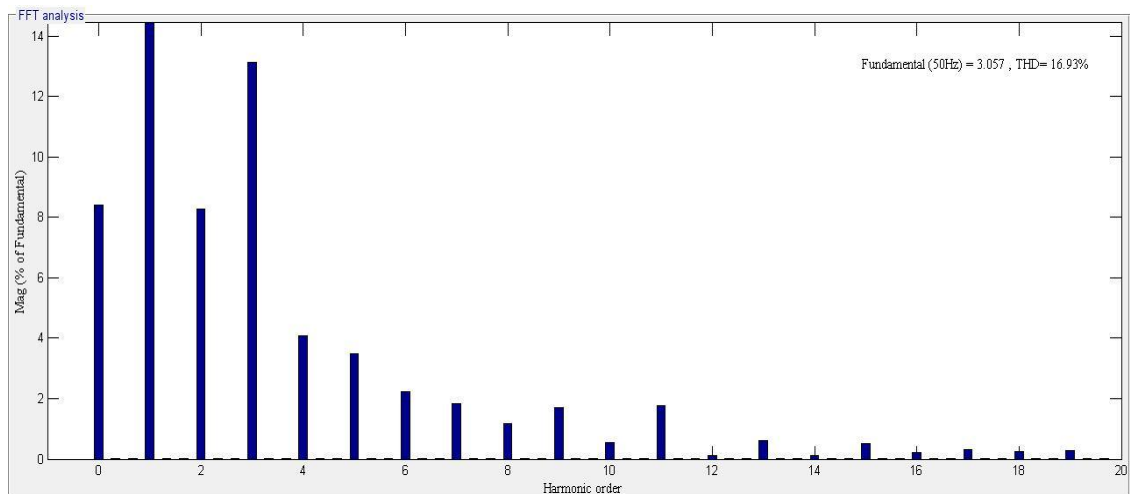
Figure 5.8 THD in load voltage waveform of single-phase H-bridge VS DC-AC with R-L load using (a) PWM (b) square pulse (c) wavelet switching scheme.



5.9 (a)



5.9 (b)



5.9 (c)

Figure 5.9 THD in load current waveform of single phase H-bridge VS DC-AC with R-L load using (a) PWM (b) square pulse (c) wavelet switching scheme.

5.4.2. R Load

Similar to R–L load, Simulation is also performed with pure resistive load using the SIMULINK model of single-phase H-bridge VS DC–AC inverter shown in figure 5.4. In this case, also simulations have been performed for all the three switching techniques, wavelet modulation, PWM and square pulse. Performance results of these simulation tests are shown in table 5.1. The waveform of voltage and current respectively are shown in figure 5.10 for PWM scheme, in figure 5.11 for square pulse scheme and in figure 5.12 for wavelet modulation scheme.

The RMS and peak value of voltage obtained from PWM scheme is 30.15 V and 42.62 V respectively. In case of square pulse the RMS value of voltage is 44.83 V, peak voltage is 63.4 V, and with wavelet modulation, RMS and peak value of voltage is 42.25 and 59.75 respectively. The THD obtained in voltage waveform is 69.85% for PWM scheme and same is 48.34% for square pulse scheme and 38.56% for wavelet modulation switching strategy. Thus, the value of THD in voltage waveform shows the significant improvement in case of wavelet modulation in comparison to PWM and square pulse switching schemes. Under resistive loading condition the PWM scheme results in 1.206 A and 1.705 A respectively as RMS and peak value of load current. 1.793 A and 1.69 A is the RMS value of current from square pulse and wavelet modulations strategy respectively. The peak value of current for square and wavelet modulation is 2.536 A and 2.39 A respectively. The value of THD in current waveform from PWM is 69.85% and same from square pulse and wavelet modulation is 48.34% and 33.74% respectively.

In comparison to PWM and Square wave, wavelet modulation has given much better result. The THD of current as well as of voltage are much lesser in case of wavelet modulation than that in PWM and square pulse switching scheme. The RMS and peak value of load current and voltage have higher value in case of wavelet modulation than that in case of PWM. Since the nature of load is pure resistive, we observe the identical value of THD in current and voltage waveform for any selected switching scheme.

TABLE 5.2

SIMULATION RESULT FOR R LOAD (SINGLE-PHASE)

Load Types	Parameters	PWM	WM	1 Pulse
R load	Vrms	30.15	42.25	44.83
	Irms	1.206	1.69	1.793
	Vpeak	42.62	59.75	63.4
	Ipeak	1.705	2.39	2.563
	V THD	69.85%	33.74%	48.34%
	I THD	69.85%	33.74%	48.34%

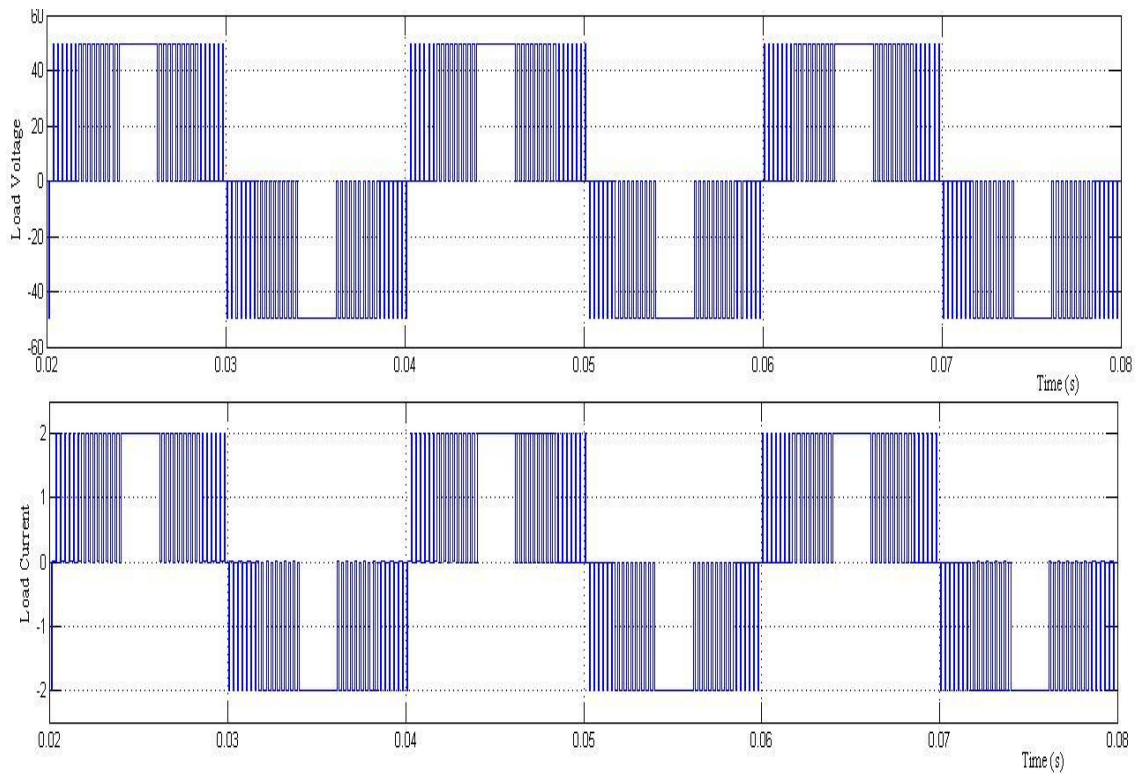


Figure 5.10 Single-phase H-bridge VS DC-AC inverter test result (load voltage and load current waveform) for R load using PWM switching scheme.

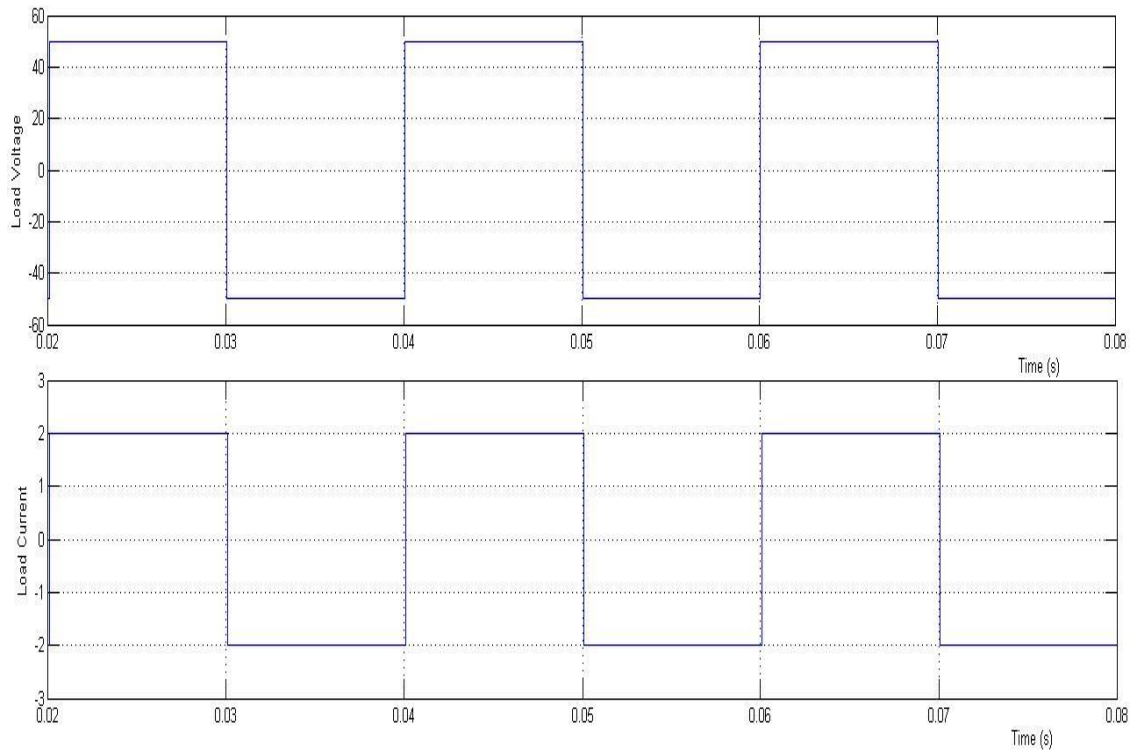


Figure 5.11 Single-phase H-bridge VS DC-AC inverter test result (load voltage and load current waveform) for R load using square pulse switching scheme.

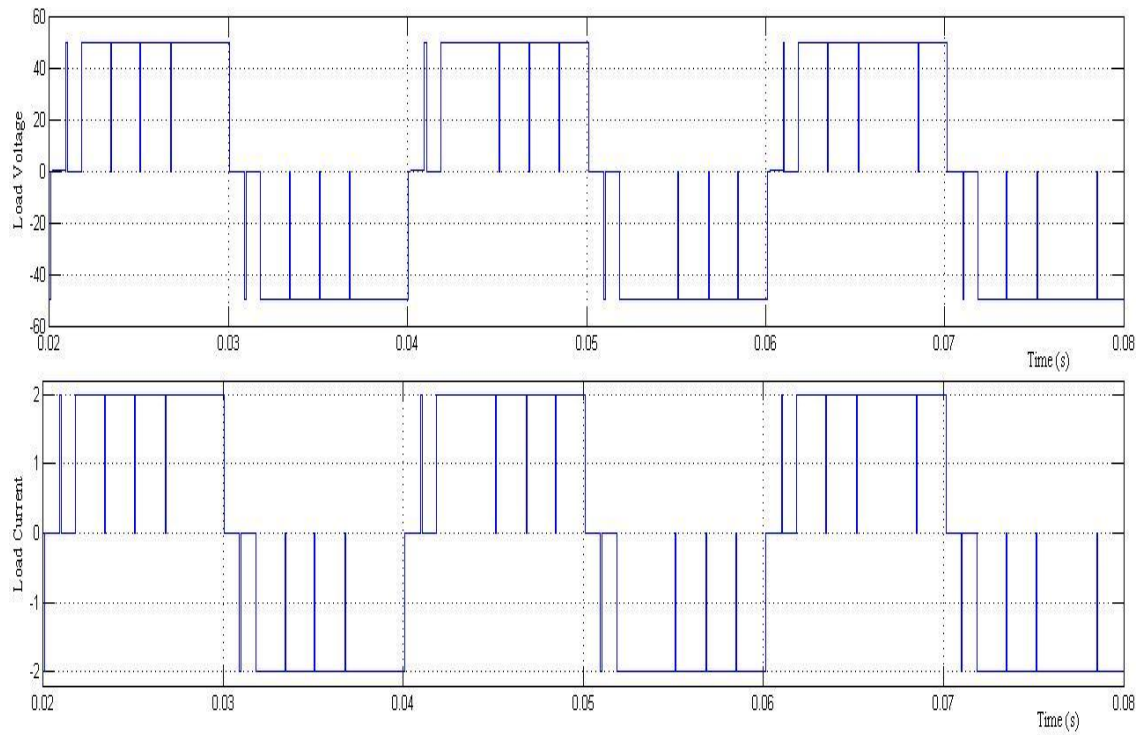
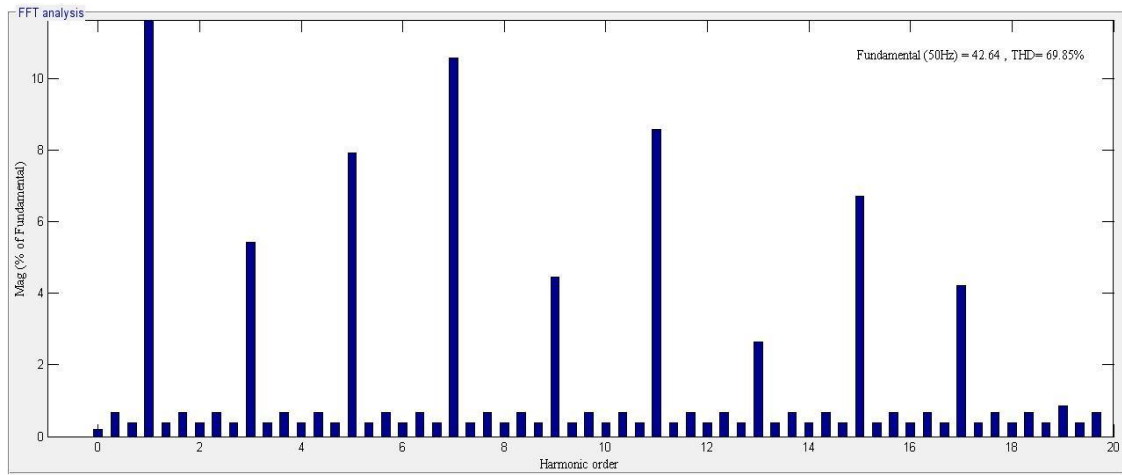
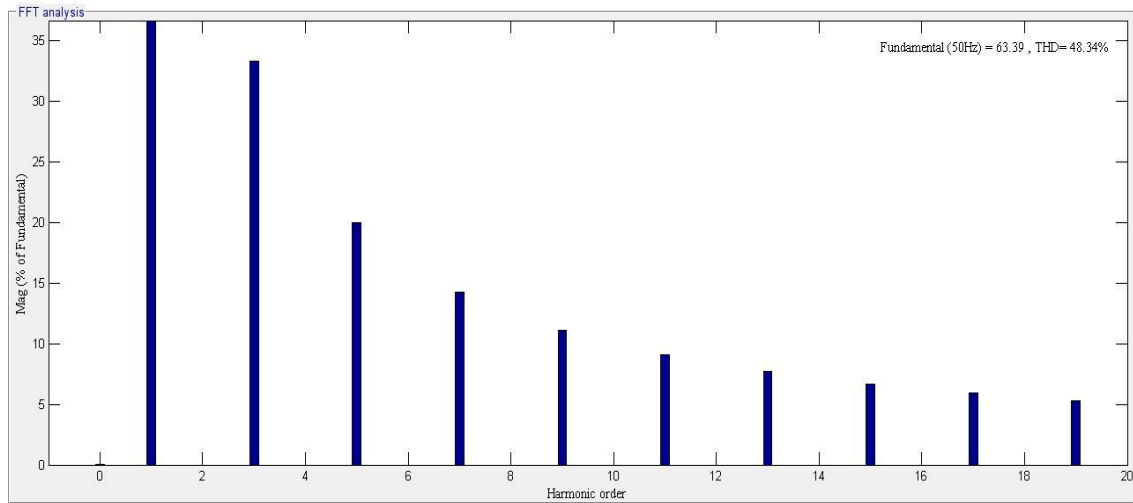


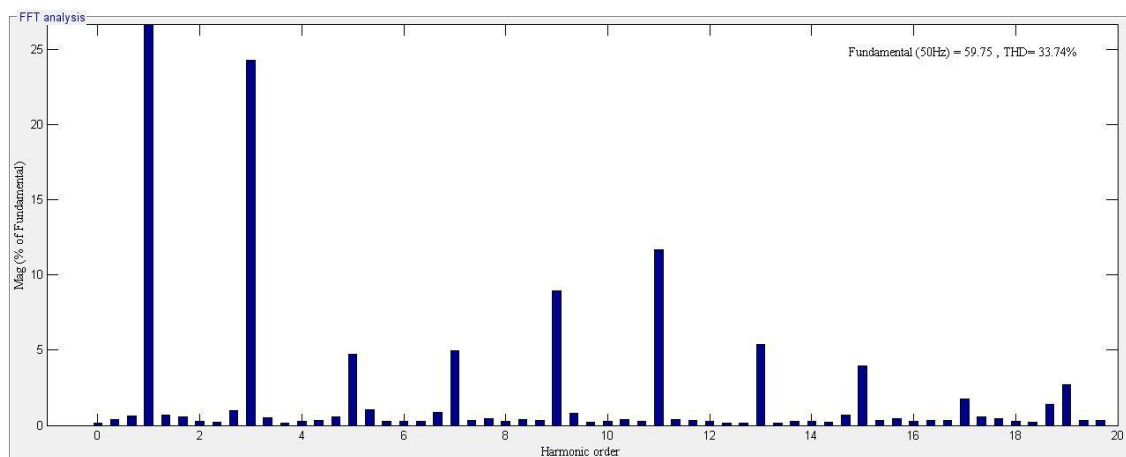
Figure 5.12 Single-phase H-bridge VS DC-AC inverter test result (load voltage and load current waveform) for R load using wavelet switching scheme.



5.13 (a)

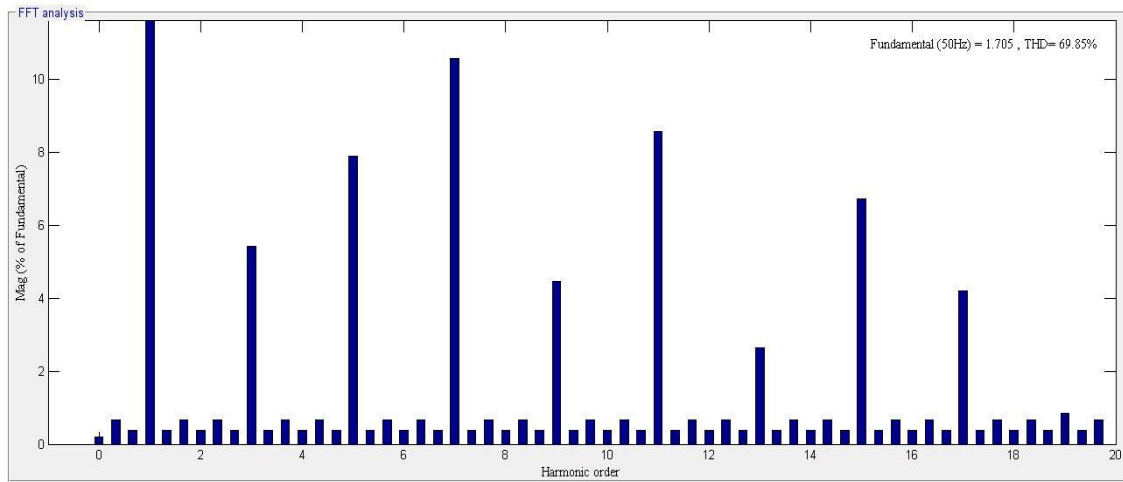


5.13 (b)

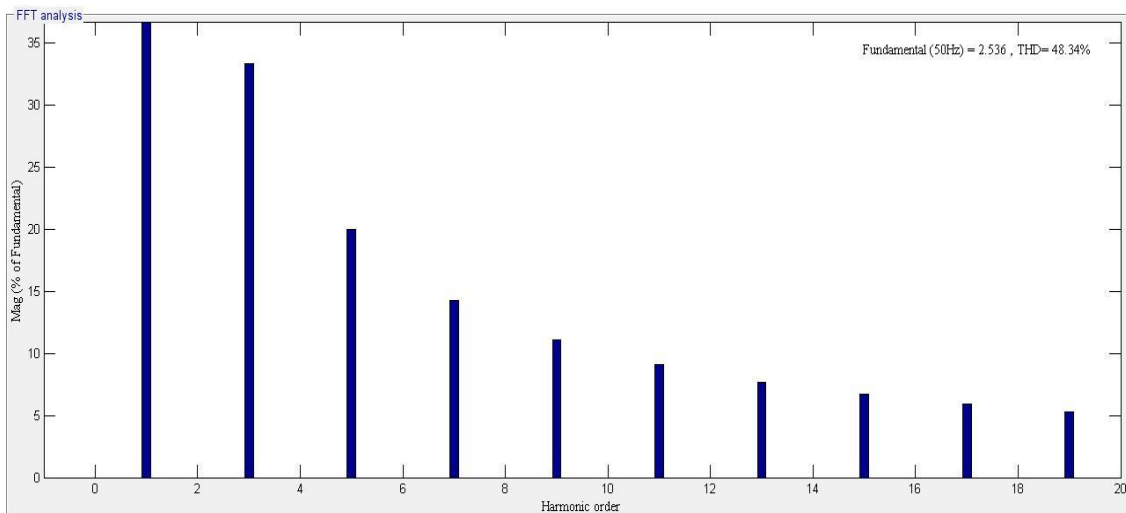


5.13 (c)

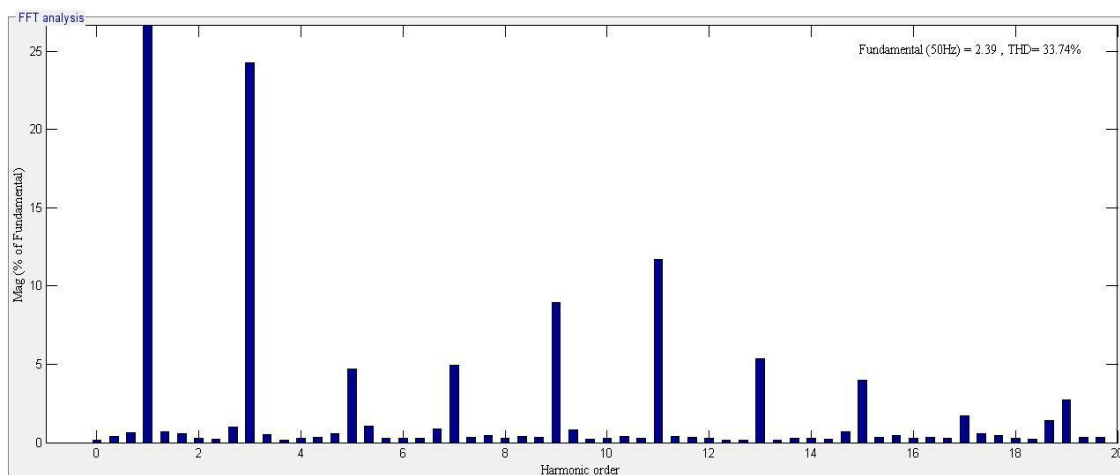
Figure 5.13 THD in load voltage waveform of single-phase H-bridge VS DC–AC with R load using (a) PWM (b) square pulse (c) wavelet switching scheme.



5.14 (a)



5.14 (b)



5.14 (c)

Figure 5.14 THD in load current waveform of single-phase H-bridge VS DC-AC with R load using (a) PWM (b) square pulse (c) wavelet switching scheme.

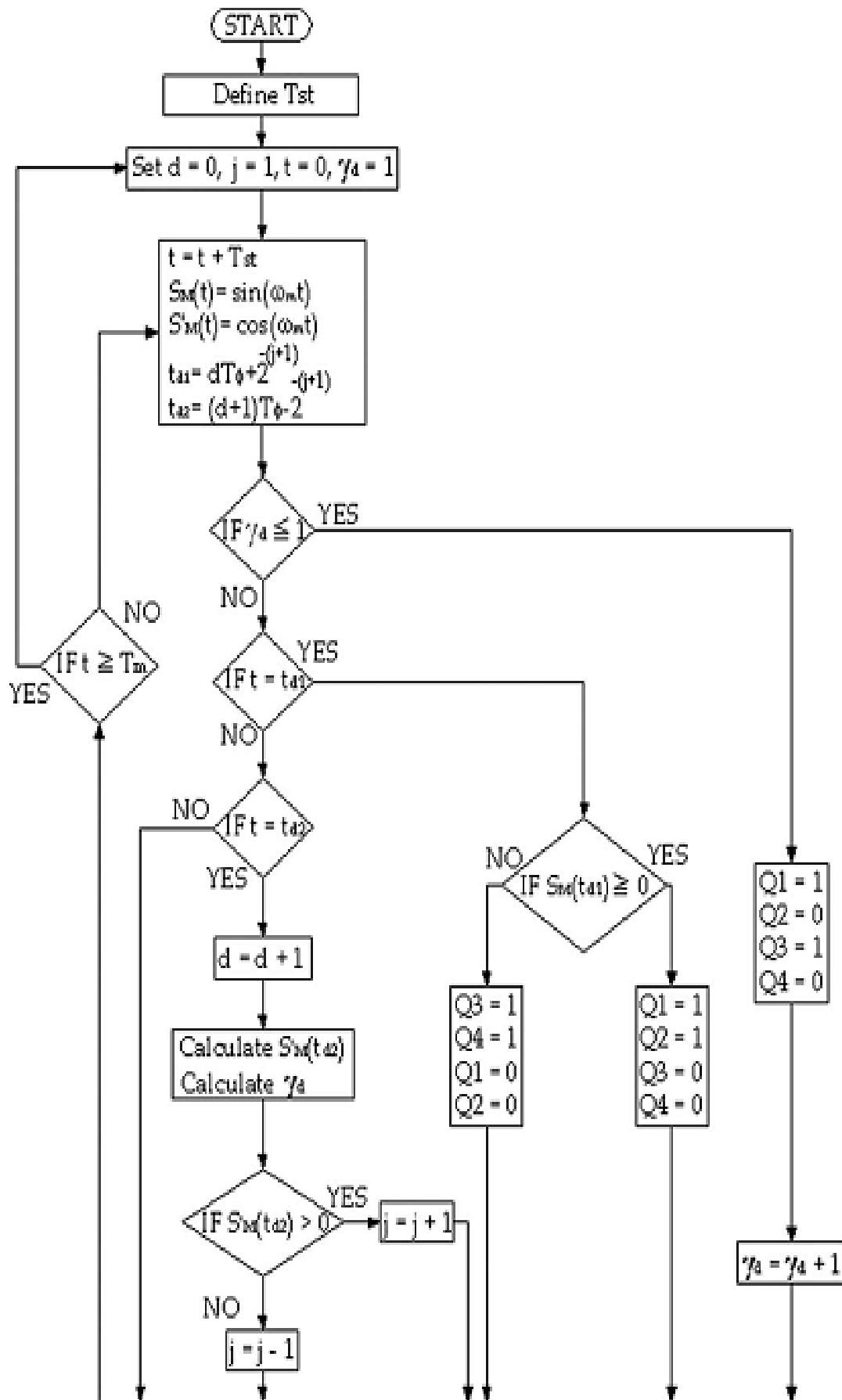


Figure 5.15 Flowchart of wavelet modulation for single-phase inverter.

CHAPTER 6

CONCLUSION

CHAPTER 6

CONCLUSION

In the beginning of this project, the purpose was to design new switching schemes for voltage source inverter that can perform better than the available switching schemes. The work was later focused mainly over designing of two new methods for switching of power electronic devices used in voltage source inverter. First one is modification of existing hysteresis band current control and second one is using the concept of wavelet modulation. The two switching schemes has been designed, simulated and tested using the new scheme has been implemented using SIMULINK facility of MATLAB. The modified hysteresis-switching scheme has given significantly improved results than the PWM scheme in every considered parameter while the wavelet based switching scheme has given better results in terms of few-selected parameters.

The modified hysteresis Switching Scheme has been designed for single-phase as well as for three-phase. In case of single-phase, the simulation has been performed with linear load as well as with dynamic load to analyze the performance of newly designed switching scheme. The result obtained from new scheme is compared with the result obtained from PWM scheme. The modified switching scheme has shown better results than the PWM scheme in terms of RMS value, peak value and THD for output current as well as for output voltage. In case of three-phase voltage source inverter simulation and testing includes the linear as well as nonlinear loading condition for both scheme i.e. PWM and modified scheme.

The wavelet modulation technique has been designed and modeled for the single phase voltage source DC-AC inverter. Simulation has been performed to analyze its performance for R and RL Load. Simulation results have been compared with square

pulse and PWM switching techniques under the identical load conditions. Wavelet modulation technique has given improved results over square pulse switching techniques and it has performed better in terms of Voltage harmonics and output but current harmonics are more compared to PWM.

Results obtained from both schemes have been compared in terms of RMS values, Peak values, THD and DC component for both voltage as well as current waveforms. Similar to the single-phase the new scheme has given better results than the PWM scheme for three-phase also. For linear loading, R-L load has been used and for non – linear loading has been realized by using the rectifier load. Few additional modifications can be made to further improve the performance. Also the schemes may be implemented in hardware for applying it in to power system.

CHAPTER 7

FUTURE SCOPE

CHAPTER 7

FUTURE SCOPE

As discussed, two new switching schemes have been designed in this project. Both the schemes have resulted in improved performance with respect to PWM scheme. Both switching schemes seem to have great future scope in field of switching of power electronics devices.

Wavelet based switching scheme has been designed and tested for single-phase voltage sources inverter. Further work can be done using concept of three-phase system. A new switching scheme using wavelet can be designed for three-phase voltage source inverters. As we have observed that the wavelet switching scheme is based on scaling function, so we can drive different scaling functions for much more improved results even for single-phase also. Along with single-phase and three-phase system the switching schemes using wavelet can be designed for multiphase inverter also. Modified hysteresis switching scheme has been designed for single as well a three-phase voltage source inverter.

For both the cases, very significant improvement has been observed over PWM scheme under given conditions. The similar approach can be use to design the switching schemes for various kind of multilevel inverter. These schemes can be tested with many more different kind of loading, even with grid connected system also. In this work we have considered only voltage source inverter; further current source inverters also can be considered.

REFERENCES

REFERENCES

- [1]. Ned Mohan, Tore M Undeland and William P. Robbins, “Power Electronics – Converters, Application and Design” 3rd ed. Wiley India, Noida:2012
- [2]. Dr. P. S. Bimbhra, “Power Electronics,” 4th ed. Khanna Publishers, Delhi:2009
- [3]. Jai P. Agrawal, “ Power electronic systems – Theory and Design,” 1st ed. Pearson Education Asia, Singapore:2001
- [4]. L. Umanand, “Power Electronics Essentials & Applications,” 1st ed. Wiley, Delhi:2010
- [5]. Pankaj H. Zope, Pravin G. Bhangale, Prashant Sonare and S. R. Suralkar, “Designing and Implementation of carrier based Sinusoidal PWM Inverter,” in International Journal of Advanced Research in Electrical, Electronics and Instrumentation Engineering, Vol. 1, Issue 4, October 2012, ISSN: 2278 – 8875.
- [6]. Weni Zhang, Yuye Wang, Weiming Tong, Huiming Xu, and Lemin Yang, “ Study of Voltage-Source PWM Inverter Based on State Combination Method,” in IEEE PES Transmission and Distribution Conference & Exhibition, Asia and Pacific Dalian, China, 2005.
- [7]. Wenyi Zhang and Wensheng Chan, “Research on Voltage-Source PWM Inverter Based on State Analysis Method,” in Proc. of IEEE International Conference on Mechantronics and Automation, China, August 9-12, 2009 .
- [8]. Firuz Zare and Jafar Adabi Firouzjee, “Hysteresis Band Current Control for Single Phase Z-Source Inverter with Symmetrical and Asymmetrical Z-Network,” in Power conversion Conference, Nagoya, 2007, PP.143-148.
- [9]. Yen-Shin Lai, Ye-Then Chang and Bo-Yuan Chen, “Novel Random-Switching PWM Technique With Constant Sampling Frequency and Constant Inductor Average Current for Digitally Controlled Converter,” in IEEE Transaction on Industrial Electronics, Vol. 60, No 8, August 2013.
- [10]. Ki-Seon kim, Young-Gook Jung and Young-Cheol Lim, “A New Hybrid Randaom PWM Scheme,” in IEEE Transaction on Power Electronics, Vol. 24, No. 1 January 2009.
- [11]. Yen-Shin Lai and Bo-Yuan Chen, “Two dimentional Random PWM Technique for Full-Bridge DC/DC Converter,” in 38th Annual Conference on IEEE industrial Electronics Society, IECON-2012, Canada, PP. 846-851.

- [12]. David Solomon George and M. R. Baiju, "Space Vector Based Hybrid Random Pulse Width Modulation Technique for 3-Level Inverter," in IEEE PEDS, Singapore, 5-8 December 2011.
- [13]. Phoivos D. Zigas, "The Delta Modulation Technique in Static PWM Inverters" in IEEE Trans. on Industrial Applications, vol.IA-17, No. 2, March/April 1981, pp. 199-204.
- [14]. M. Azizur Rahman, Jhon E. Quaicoe, and M. A. Choudhary, "Performance Analysis of Delta Modulated PWM Inverters," in IEEE Trans. on Power Electronics, Vol. PE-2, No. 3, July 1987, PP. 227 – 233.
- [15]. B. Vasantha Reddy and B. Chitti Babu, "Hysteresis Controller and Delta Modulator – Two Viable Scheme for Current Controlled Voltage Source Inverter," in IEEE International Conference on Technical Postgraduates 2009, 14-15/Dec/2009, Kuala Lumpur, Malaysia.
- [16]. Jonathan W. Kimball, Philip T. Krein and Yongxiang Chen, "Hysteresis and Delta Modulation Control of Converters Using Sensorless Current Mode," in IEEE Trans. on Power Electronics, Vol. 21, No. 4, July 2006.
- [17]. Yen-Shin Lai, Yong-Kai Lin and Chih-Wei Chen, " New Hybrid Pulse Width Modulation Technique to Reduce Current Distortion and Extend Current Reconstruction Range for a Three-Phase Inverter Using Only DC-link Sensor," IEEE Transaction on Power Electronics, Vol. 28, No. 3, March 2013.
- [18]. Prasopchok Hothongkham, Somkiat Kongkachat and Narongchai Thadsaporn, "Performance Comparison of PWM and Phase-Shifted PWM Inverter Fed High-Voltage High-Frequency Ozone Generator," in IEEE Region 10 Conference, TENCON 2011, PP. 976-980
- [19]. Wensheng Song, Xiaoyun Feng and Keyue Ma Smedley, "A Carrier-Based PWM Strategy With the Offset Voltage Injection for Single-Phase Three-Level Neutral-Point-Clamped Converters.
- [20]. P.T. Krien, Xing Geng and R. Balog, "High-Frequency Link Inverter Based on Multiple-Carrier PWM," in Applied Power Electronics Conference and Exposition, APEC 2002, vol.2, PP. 997-1003
- [21]. Istvan Nagy, "Novel Adaptive Tolerance Band Based PWM for Field-Oriented Control of Induction Machine," in IEEE Trans. on industrial Electronics, Vol.41, No. 4, August 1994.
- [22]. <http://en.wikipedia.org/wiki/Wavelet>

- [23]. Agostino Abbate, Casimer M. DeCusatis and Pankaj K. Das, “ Wavelet and Subbands Fundamental and Applications,” Birkhauser, Boston:2002.
- [24]. Stephane Mallat, “a Wavelet Tour of Signal Processing,” 2nd ed. Academic Press, London: 1999.
- [25]. S. A. Saleh, C. R. Moloney and M. A. Rahman, “Development and Testing of Wavelet Modulation for Single-Phase Inverters,” IEEE Trans. Ind. Electronics, vol. 56, no. 7, pp. 2588 – 2599, July 2009.
- [26]. http://en.wikipedia.org/wiki/Multiresolution_analysis
- [27]. S. A. Saleh, C. R. Moloney and M. A. Rahman, “Developing a Non – Dyadaic MRAS for Switching DC – AC inverters,” in Proc. IEEE 12th DSP Conf. , Jackson Lake Lodge, WY, Sep. 2006, pp. 544 – 549.
- [28]. S. A. Saleh, C. R. Moloney and M. A. Rahman, “Experimental Performance of the Single-Phase Wavelet-Modulated Inverter,” IEEE Trans. Power Electronics, vol. 26, no. 9, pp. 2650 – 2660, Sep. 2011.
- [29]. S. A. Saleh, “the Implementation and Performance Evaluation of 3 ϕ VS Wavelet Modulated AC – DC Converters,” IEEE Trans. Power Electronics, vol. 28, no. 3, pp. 1096 – 1106, March 2013.
- [30]. S. A. Saleh, C. R. Moloney and M. A. Rahman, “Analysis and Development of Wavelet Modulation for Three-Phase Voltage-Source Inverters,” in IEEE Trans. on Industrial Electronics, Vol. 58, No. 8, August 2011.
- [31]. Stephen J. Chapman, “MATLAB Programming for Engineers,” 3rd ed. Thomson Learning, Singapore: 2005.

PUBLICATIONS

Published

- [1] Ankit Yadav and M. M. Tripathi, "Novel switching scheme for single phase VS Inverter using value of output current as modulating signal," in International Journal of Science & Technology. ISSN (online): 2250-141X, Vol. 3 Issue 3, December 2013.

Communicated

- [1] Ankit Yadav and M. M. Tripathi, "A Novel Wavelet Modulation Scheme for Single Phase Inverter," in IEEE Power India Conference 2014
- [2] Ankit Yadav and M. M. Tripathi, "Modified Hysteresis Switching Scheme for 3-Phase Voltage Source Inverter" IEEE Power India Conference 2014

